

DESIGN, ANALYSIS AND DEVELOPMENT OF A NACELLE MAIN LOAD
FRAME FOR A 500KW WIND TURBINE

by

AHMET SELİM PEHLİVAN

Submitted to the Graduate School of Engineering and Natural Sciences
in partial fulfillment of
the requirements for the degree of
Master of Science

Sabanci University
August 2012

DESIGN, ANALYSIS AND DEVELOPMENT OF A NACELLE MAIN LOAD
FRAME FOR A 500KW WIND TURBINE

APPROVED BY:

Assoc. Prof. Dr. Mahmut F. Akşit
(Thesis Supervisor)

Assoc. Prof. Dr. Ali Koşar

Asst. Prof. Dr. Güllü Kızıлтаş Şendur

Asst. Prof. Dr. Murat Makaracı

Asst. Prof. Dr. İlyas Kandemir

DATE OF APPROVAL: 06.08.2012

© AHMET SELİM PEHLİVAN 2012

ALL RIGHTS RESERVED

DESIGN, ANALYSIS AND DEVELOPMENT OF A NACELLE MAIN LOAD
FRAME FOR A 500KW WIND TURBINE

Ahmet Selim PEHLIVAN

Mechatronics Engineering, M.Sc. Thesis, 2012

Thesis Supervisor: Assoc. Prof. Dr. Mahmut F. AKŞİT

Keywords: Nacelle, bedplate, finite element analysis, static stress and deflection, fatigue, topology optimization, joint design, modal analysis.

ABSTRACT

Wind energy is gaining increasing momentum over the last two decades. Wind energy business is one of the most attractive in renewable energy sectors. While several wind turbine designs are available in the industry, developing a wind turbine for continuous commercial electricity production is one of the challenging engineering problems in today's world. This work involves design, analysis and development of a nacelle main load frame for a 500kw wind turbine as part of the national wind turbine development project (MILRES) of Turkey. Starting from conceptual design stage complete static and dynamic analyses were conducted including the crane loads on the nacelle bedplate. Conceptual and detail design work were conducted using commercially available 3D solid modeling code SOLIDWORKS. Structural analyses such as stress and strain calculations and modal analyses of the main load frame were performed using the finite element method. A hybrid (cast iron main base and weld formed steel extension) structure has been developed to improve stiffness while controlling overall weight. A bolted joint assembly was designed for cast base and steel extension interface. Analytical joint and bolting calculations were confirmed by finite element simulations of the assembled bedplate structure. An iterative design approach has been used. Design

and analysis iterations were carried out to improve functionality, weight, and stress levels. For an optimum stress and weight design solution, topology optimization methods were applied to the structure in order to minimize weight while maintaining design safety limits and stiffness of the structure. Topology optimization stage was conducted by commercially available codes OPTISTRUCT and ANSYS shape optimization module. The optimization work resulted in 30% reduction of weight. The analysis results for optimized geometry indicated sufficiently high design safety margins for all design load combinations. Overall, an optimum Nacelle bedplate design has been developed achieving high safety factors with minimum weight.

500 KW RÜZGAR TÜRBİNLERİ İÇİN ANA TAŞIYICI İSKELET TASARIM EVRELERİ VE DAYANIM ANALİZ YÖNTEMLERİ

Ahmet Selim PEHLİVAN

Mekatronik mühendisliği , Yüksek lisans tezi, 2012

Tez Danışmanı: Doç. Dr. Mahmut F. AKŞİT

Anahtar Kelimeler: Nasel, taşıyıcı iskelet, sonlu elemanlar analizi, static gerilme ve esneme, yorulma, topoloji optimizasyonu, eklem tasarımı, titreşim analizi.

ÖZET

Rüzgâr enerjisi son dönemlerde önemini artıran ve kendini geliştiren son derece ilgi gören bir iş koludur. Çeşitli rüzgâr türbin tasarımları piyasada mevcuttur ve enerji sektöründe kullanılmaktadır. Kullanılabilir elektrik enerjisi üretebilmek için rüzgâr türbini tasarımı geliştirebilmek günümüz mühendislik dünyasındaki en ilgi çekici problemlerden biridir. Bu yüksek lisans tez çalışmasında, Türkiye'nin ilk yerli orta sınıf rüzgâr türbini tasarımı projesi (MILRES) içeriği olarak ana taşıyıcı iskelet tasarımına odaklanılmıştır. Tez çalışmasının gayret gerektiren ve yenilikçi bölümü, kavramsal tasarımlardan başlayarak taşıyıcı iskeletin statik ve dinamik analizlerinin orta sınıf rüzgâr türbinlerinde bulunmayan bütünleşmiş iç vinç yüklerinin de eklenerek tamamlanması olarak belirlenmiştir. Kavramsal ve detaylı tasarım çalışmaları ticari bilgisayar destekli tasarım programı olan SOLIDWORKS ortamında yürütülmüştür. Yapısal analizlerden gerilme ve esneme hesapları ve titreşim analizleri sonlu elemanlar modelleri ile kurgulanmıştır. Hibrit yapı (döküm parça ve profil uzantıları ile) sistemin dayanıklılığını ağırlığını kontrol ederek tasarlanmıştır. Döküm şase ve çelik uzantısı için civatalı bir eklem tasarlanmıştır. Analitik olarak yapılan eklem ve civata hesapları monte edilmiş ana taşıyıcı iskeletin sonlu elemanlar modelleri ile doğrulanmıştır. Tasarım ve analiz evreleri sistemin işlev, ağırlık ve gerilme seviyelerini geliştirebilmek için tamamlanmıştır. En iyileştirilmiş gerilme ve ağırlık tasarım problemi, sistemin güvenlik katsayılarını ve gerilme seviyelerini sabit tutarak, ağırlığının azaltılması için topoloji en iyileştirme yöntemi uygulanmıştır. Topoloji en iyileştirme evresi ticari olarak kullanılan OPTISTRUCT ve ANSYS yapı modülleri kullanılarak tamamlanmıştır. En iyileştirme metodu sayesinde sistemin ağırlığında yüzde otuz

azalma sađlanmıřtır. En iyileřtirilmiř geometri iin analiz sonularının da gsterdiđi gibi sistemin yeterince yksek tasarımı gvenlik marjini oluřabilecek tm ykler karřısında mevcuttur. Sonu olarak en iyileřtirilmiř tařıyıcı iskelet tasarımı yksek gvenlik katsayıları ve en hafif ađırlıkla elde edilerek tasarlanmıřtır.

To greatest grandfather ever who gave me all the means...

ACKNOWLEDGEMENT

I would like to give my sincere and deep gratitude to my thesis advisor Assoc. Dr. Mahmut F. Akřit for his continuous support and practical guidance during the course of the thesis. I would also like to express my sincere thanks to my instructor Asst. Dr. Gll Kızıltaş for her continuous advice and support during optimization and finite element stages of the work. I am also grateful to my committee members Assoc. Dr. Ali Kořar, Asst. Dr. İlyas Kandemir and Asst. Dr. Murat Makaracı for their interpretation on the dissertation. I am also thankful to my beloved girlfriend Merve Aydan Kılıç for her continuous supports and means for my life. I would like to thank to my closest friends Mustafa Bulut Cořkun, Osman Yavuz Perk, Trker İzci, Alihan Kaya, Ahmet Fatih Tabak, Elif Hocaođlu, Glnihal evik, Tarık Kurt and Eren nl for their friendship. Finally, I would like to express my best gratitude to my family members for their never ending love and continuous support from the beginning of my life.

TABLE OF CONTENTS

CHAPTER 1	19
INTRODUCTION AND PROBLEM STATEMENT	19
1.1. OVERVIEW ON WIND TURBINES	19
1.1.1. Turbines (Blades).....	20
1.1.2. Power Conveying Equipment.....	21
1.1.2.1. Hub.....	22
1.1.2.2. Low speed shaft	23
1.1.2.3. Gear box (Gear train type turbines).....	24
1.1.3. Generator and Power Electronics Equipment	24
1.2. PROBLEM DEFINITION	25
CHAPTER 2	27
BACKGROUND AND LITERATURE SURVEY	27
2.1. LITERATURE SURVEY ON WIND TURBINES, BEDPLATE DESIGN AND MATERIALS	27
2.2. LITERATURE SURVEY ON STRESS-WEIGHT TOPOLOGY OPTIMIZATION	29
CHAPTER 3	32
CONCEPTUAL DESIGN AND ANALYSIS	32
3.1. MATERIAL SELECTION	32
3.1.1. Casting Part Material Selection Process.....	33
3.1.2. Material Selection for Welded Profiles	38
3.1.3. Bolt Material Selection Process	40
3.2. ITERATIVE DESIGN APPROACH	41
3.2.1. Design Constraints	43
3.2.2. Design and Analysis Constraints	48
3.3. FINITE ELEMENT MODEL AND PRELIMINARY ANALYSES	50
3.3.1. Codes and Solver Capabilities	51
3.4. BOUNDARY CONDITIONS DURING CONCEPTUAL DESIGN STAGE 56	
3.4.1. Estimated load values	57
3.4.2. Calculated boundary conditions	58
3.5. PRELIMINARY STRESS ANALYSIS	61
CHAPTER 4	63
OPTIMIZATION STUDIES	63

4.1.	TOPOLOGY OPTIMIZATION.....	63
4.1.1.	SIMP Models	64
4.2.	WEIGHT AND STRESS OPTIMIZATION (Main Optimization Stage).....	65
4.2.1.	Pre-Design	65
4.2.2.	Design constraints	67
4.2.3.	Post-Design	67
4.3.	SHAPE OPTIMIZATION (Refined Optimization Stage)	71
4.3.1.	The Casted Part with Final Shape.....	71
CHAPTER 5	74	
DETAILED DESIGN AND ANALYSIS OF MAIN LOAD FRAME	74	
5.1.	STATIC ANALYSIS.....	74
5.1.1.	Boundary conditions for detailed analysis.....	78
5.1.2.	Static analysis results	80
5.1.3.	Crane and maintenance loads analysis.....	86
5.2.	HIGH CYCLE FATIGUE ANALYSIS OF THE BEDPLATE.....	91
5.2.1.	Strategy for the problem.....	92
5.2.2.	S-N Curve and number of cycles	99
5.3.	Mesh Refinement and Convergence Issues.....	100
5.4.	FE DISCONTINUITY	102
5.5.	MODAL ANALYSIS	108
5.5.1.	System working frequency definitions.....	109
5.5.2.	FE results and system loads	110
5.5.2.1.	FE results for operational loads	110
5.5.2.2.	FE results under gravity load.....	111
5.6.	BOLTED JOINT DESIGN AND ITERATIONS.....	112
5.6.1.	Joint force calculations.....	113
5.6.2.	Joint calculations using FEM	115
CHAPTER 6.....	119	
CONCLUSION	119	
REFERENCES.....	121	
APPENDIX A.....	124	
AUXILLARY DESIGN AND CAD INTEGRATION.....	124	

1.1.	YAW BEARING FORCE CALCULATIONS AND BEARING SELECTIONS.....	124
APPENDIX B		128
1.2.	CAD INTEGRATION AND FINAL ASSEMBLY.....	128
1.3.	YAW MOTOR TORQUE AND POWER CALCULATIONS	131

LIST OF FIGURES

Figure 1.1: Typical gear train wind turbine structure (1).....	19
Figure 1.2: Rotor swept area and blade illustration (2).....	20
Figure 1.3: Energy extraction tube for a wind turbine (3).	21
Figure 1.4: Standard gear train power conveying equipment (4).....	22
Figure 1.5: Isometric view for a wind turbine hub (5).....	23
Figure 1.6: The low speed shaft for a wind turbine (6).....	23
Figure 1.7: Standard 3 stage gear box for a middle class wind turbine (7).....	24
Figure 2.1: Meshed model of sample bedplate (8).....	29
Figure 3.1: General view for wind turbine with gearbox (38).	33
Figure 3.2: Different wind turbine components with ductile iron configurations (9).....	34
Figure 3.3: Charpy impact energy consequences on carbon rated ductile iron (9).....	35
Figure 3.4: Final shape of the casted part design.	37
Figure 3.5: Several Parts for St 52.	39
Figure 3.6: Final iteration of generator support part design.....	40
Figure 3.7: A conceptual design from initial iterations.....	42
Figure 3.8: First conceptual bedplate design independent of other groups.....	43
Figure 3.9: Two main supported system design.....	44
Figure 3.10: 3 main point support system design.....	44
Figure 3.11: Different corner structure and flat space for housing.	45
Figure 3.12: First system integration and general design problems.....	46
Figure 3.13: Ramped profile design.....	46
Figure 3. 14: 5 degree horizontal inclination has been introduced to avoid blade-tower contact under heavy wind loads.....	47
Figure 3. 15: Blade to tower distance.....	48
Figure 3.16: Square shape profile for torsion.....	49
Figure 3.17: Final I-profile design.	50
Figure 3.18: Diverged solution from COMSOL with nonlinear problem.....	53
Figure 3. 19: Fixed and roller supported beam schematic.	59
Figure 3. 20 : Fixed constraint for the analyses.	60
Figure 3. 21 : COMSOL results with estimated boundary conditions.	61
Figure 3. 22 : More detailed analysis using COMSOL including representative preloads.....	62
Figure 4.1: Topology optimization samples (17).....	64
Figure 4.2 : The bulky model before the optimization applied.	66
Figure 4.3 : Stress results before optimization applied.	66
Figure 4.4: OPTISTRUCT solution providing guidance for optimization and material removal areas.	68
Figure 4.5: Cast part after main stage of optimization.....	68

Figure 4.6: High bending stress region.	69
Figure 4.7: Secondary region without removal (4).	69
Figure 4.8: Final shape of the bedplate after topology optimization.....	70
Figure 4.9: Additional material to the casted part.	71
Figure 4.10: Removal suggestions by ANSYS optimization solution.	72
Figure 4.11: Final shape of the bedplate.	72
Figure 4.12: Analysis results after the refinement optimization stage.	73
Figure 5. 1: Bolted joints and frictional contacts between the surfaces.	75
Figure 5. 2: Meshed model of the bedplate.	75
Figure 5. 3: Reaction 1 force illustration with 2 loads steps.	76
Figure 5. 4: Load steps application in ANSYS.	76
Figure 5. 5: Bolt pretension manifestation.	77
Figure 5. 6: Load steps for bolts with lock option.	77
Figure 5. 7: Full static loading illustration under ANSYS.	78
Figure 5. 8: First iteration without crane loads.	79
Figure 5. 9: Final design analysis results.	80
Figure 5. 10: Static stress values for casted part of the bedplate.....	81
Figure 5. 11: Discontinuity region under the main frame.	82
Figure 5. 12: Safety factor calculations with ANSYS.	83
Figure 5. 13: Profile part stress values.	83
Figure 5. 14: Total deformation values under full static loading case.	84
Figure 5. 15: Frictional stresses on the contact surfaces.	85
Figure 5. 16: Shear stress values for bolts safety.	85
Figure 5. 17: Crane analysis load illustration.....	87
Figure 5. 18: A trial design for crane attachment to bedplate.	87
Figure 5. 19: Three point supported crane configuration (Orientation 1).	88
Figure 5. 20: Crane orientation 2.	89
Figure 5. 21: Stress results for crane orientation 2.	89
Figure 5. 22: Crane orientation 3.	90
Figure 5. 23: Stress locations for crane orientation 3.....	91
Figure 5. 24: ANSYS fatigue layout.	92
Figure 5. 25: Static results under full wind load.	93
Figure 5. 26: High stress at discontinuity region.	94
Figure 5. 27: Static value with only gravity loads.....	94
Figure 5. 28: Discontinuity region for fatigue analysis.....	95
Figure 5. 29: Stress oscillation applied on the cast part.	96
Figure 5. 30: Profile part under dynamic wind loads.	97
Figure 5. 31: Analysis results for the fatigue life calculations.	98
Figure 5. 32: Stress oscillations for the profile part.	98
Figure 5. 33: S-N curve example for casted material (16).	99
Figure 5. 34: Coarse meshed structural analysis.	100
Figure 5. 35: Stress analysis with the coarse mesh.	101
Figure 5. 36: Convergence of stress value around 524 MPa.....	102

Figure 5. 37: Sharp transitional region.....	103
Figure 5. 38: 90 degrees sharp mesh nodes for the model.	103
Figure 5. 39: Stress results for the chase without radius for the discontinuous region.	104
Figure 5. 40: Regional fillet for casted part.	105
Figure 5. 41: Discontinuous region after filleting.	105
Figure 5. 42: New cad design for proof.	106
Figure 5. 43: 20 MPa for the critical regions.	107
Figure 5. 44: Meshed model for discontinuous region.....	107
Figure 5. 45: The most corrected analysis results with smaller discontinuity.	108
Figure 5. 46: First six frequencies of the bedplate.	110
Figure 5. 47: First and second modes respectively.	110
Figure 5. 48: Third and fourth mode shapes respectively.	111
Figure 5. 49: Bedplate under gravity load.....	111
Figure 5. 50: Joint design with fillet and chamfer.....	112
Figure 5. 51: Friction force illustration.	113
Figure 5. 52: M24 bolt with 2 nuts supported.	115
Figure 5. 53: Class 8.8 bolt results.	116
Figure 5. 54: 90% reduction ratio bolt analysis.	116
Figure 5. 55: Stress value for 90% preload ratio.....	117
Figure 5. 56: Bolt analysis for 12.9 class.	118
Figure 0. 1:Example places for turntables.....	125
Figure 0. 2: Static loading condition for the main bearing.....	125
Figure 0. 3:Illustration of the main bearing that is chosen for the project (18).....	126
Figure 0. 4:Cad design of the yaw bearing.	127
Figure 0. 5:Cross section view of the bearing (19)	127
Figure 0. 6:Static loading curve for the yaw bearing (17).	128
Figure 0. 7:Frontal view of the wind turbine.	129
Figure 0. 8:Isometric view of the complete wind turbine.	130
Figure 0. 9:Internal view of the national wind turbine.....	131
Figure 0. 10: Complete system with a convenient coordinate system.	132
Figure 0. 11:Mass - Inertia matrix of the system.	132
Figure 0. 12:Yaw motors integrated to the system.....	133

LIST OF TABLES

Table 3.1: Common chemical composition of wind turbine cast iron.	35
Table 3.2: Chemical Composition of EN-GJS Series Materials.	36
Table 3.3: Mechanical properties different EN series materials.	36
Table 3.4: Technical Properties of EN series materials (10).....	37
Table 3.5: Chemical Composition of St52.	38
Table 3.6: Mechanical Properties of St 52 (11).	39
Table 3.7: Chemical composition of steels (12).....	41
Table 3.8: Mechanical properties of candidate materials (12).	41
Table 3. 9 : Estimated load values.	57
Table 3. 10: Calculated load values.	58
Table 5. 1: Boundary conditions for detailed analysis.	78
Table 5. 2: Mesh refinement and converged stress values.	101
Table 5. 3: Operational frequencies.	109
Table 0. 1: Mechanical Properties for materials (12).....	125

NOMENCLATURE

P_d : Power delivered by turbine

C_p : Power coefficient

A : Rotor swept area

U : Wind Speed

L : Length of bedplate

W : Width of bedplate

H : Height of bedplate

M : Mass of bedplate

P : Mechanical power

T : Torque

ω_i : Angular speed

F : Force

R_1 : Reaction force 1

R_2 : Reaction force 2

n_{static} : Static safety factor

S_e : Modified endurance limit

C_{load} : Load factor

C_{size} : Size factor

C_{surf} : Surface factor

C_{temp} : Temperature factor

C_{rel} : Reliability factor

S_e' : Endurance limit

S_{ut} : Ultimate limit

$n_{dynamic}$: Dynamic safety

F_f : Friction coefficient

F_i : Initial bolt force

S_p : Proof strength

A_t : Tensile Area

D_3 : Root diameter

D_2 : Pitch diameter

M_{bending} : Bending moment

I : Moment of inertia

F_a : Axial force

d : Distance between the supports of components

Greek Symbols

ρ : Density of air

σ_{yield} : Yield stress

σ_{max} : Maximum stress

σ_{min} : Minimum stress

$\Delta\sigma$: Stress alternation

σ_m : Mean stress

μ : Friction coefficient

Ω : Design space

ρ_d : Discrete section field

α : Angular acceleration

CHAPTER 1

INTRODUCTION AND PROBLEM STATEMENT

1.1. OVERVIEW ON WIND TURBINES

Wind turbines are in fact mechatronic systems that convert aeromechanical power to electrical power with different technologies. Kinetic energy of the air is extracted from wind flow by the blades, and conveyed through other internal systems up to generator of the wind turbine. Modern wind turbines have two classifications as direct drive and geared systems both of which are commonly used in the wind industry. The main difference between direct drive and geared turbines is the high speed shaft in geared systems. This thesis deals with nacelle bedplate design for a geared wind turbine system. Recently large power output wind turbines are generally designed as direct drive systems, and do not have a gear box between the generator and main rotor. Typical gear trained wind turbine systems have a similar structure to produce electricity. Based on functionality, systems in a common geared turbine can be grouped in three main subsystems: turbine blades, power train mechanisms and electrical systems.

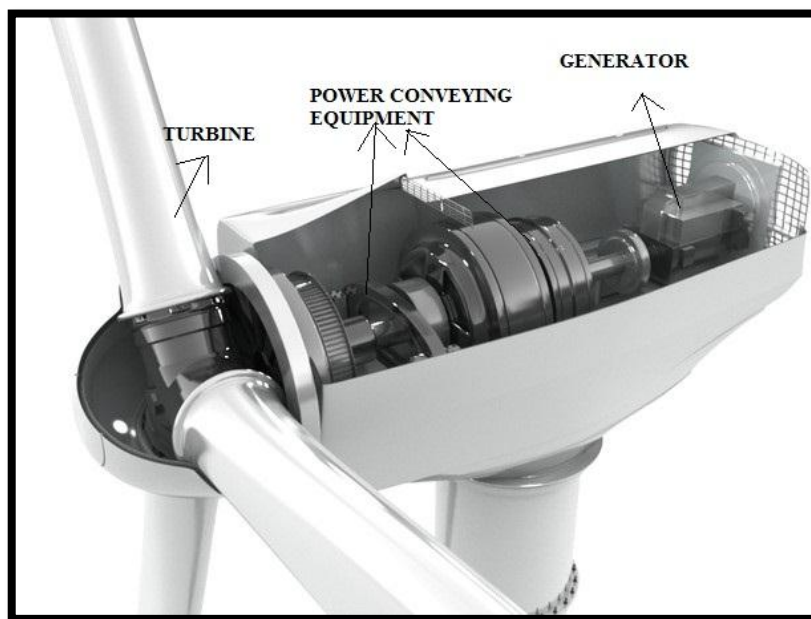


Figure 1.1: Typical gear train wind turbine structure (1).

1.1.1. Turbines (Blades)

Blades for the wind turbines are one of the most fundamental components of the wind turbine which behave like the turbine blades in other power producing turbines. The blade length that dictates the rotor swept area is one of the most significant design parameter in wind turbine engineering that directly affects the power output of the whole structure. The blades convert the aeromechanical energy to rotational mechanical power which is conveyed through the gear train up to generator. The blades for wind turbines have complex structure and varying cross sectional areas resulting in a twisted body. The structure is made of composite material that makes blades flexible. Standard geared wind turbines have 3 blades.

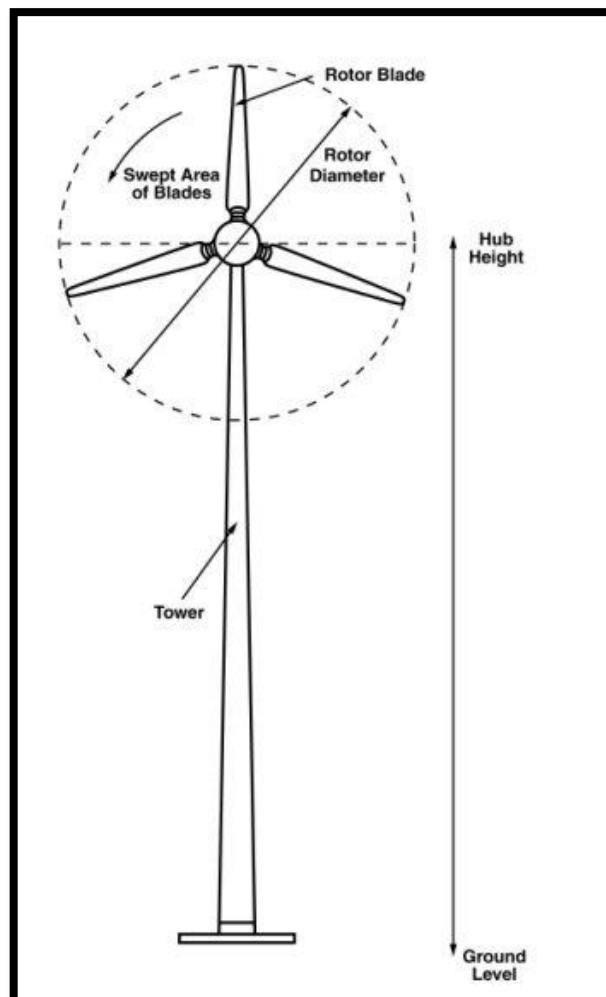


Figure 1.2: Rotor swept area and blade illustration (2).

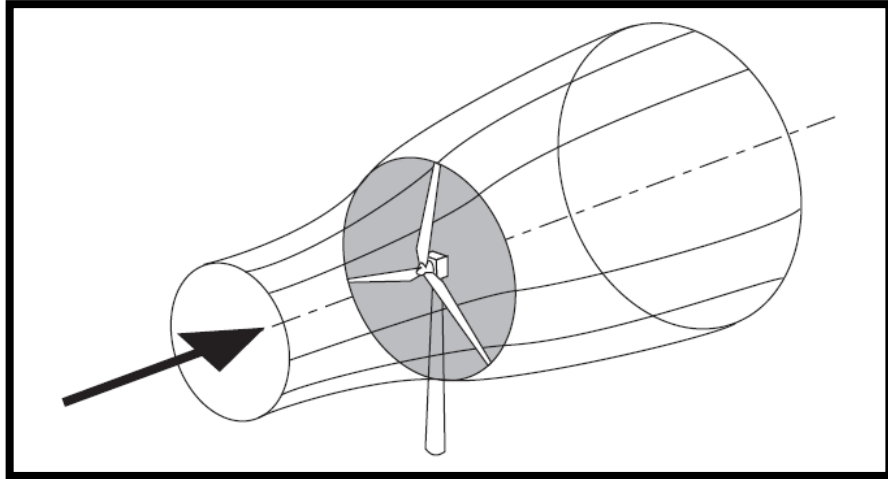


Figure 1.3: Energy extraction tube for a wind turbine (3).

The power output for the turbine is calculated by the formula given in (1.1) that is dependent on the rotor swept area.

$$P_d = \frac{1}{2} * C_p * \rho * A * U^3 \quad (1.1)$$

where A is the rotor swept area as shown in Figure 1.3 (3) which is directly related to blades length. Therefore, blade length is very important in wind turbine. The term U represents the linear wind speed, and C_p is the power coefficient for turbine. Power coefficient is defined as a fraction that power in the wind may be converted into mechanical work. It has a theoretical maximum value as 0.593, and lower coefficients may be obtained for different operations (3).

1.1.2. Power Conveying Equipment

After the aeromechanical power is converted to mechanical rotation, mechanical power is conveyed through several mechanisms on standard geared wind turbines. All of the components have different efficiencies according to their design. Therefore, there are significant losses during power transfer from blades to the generator.

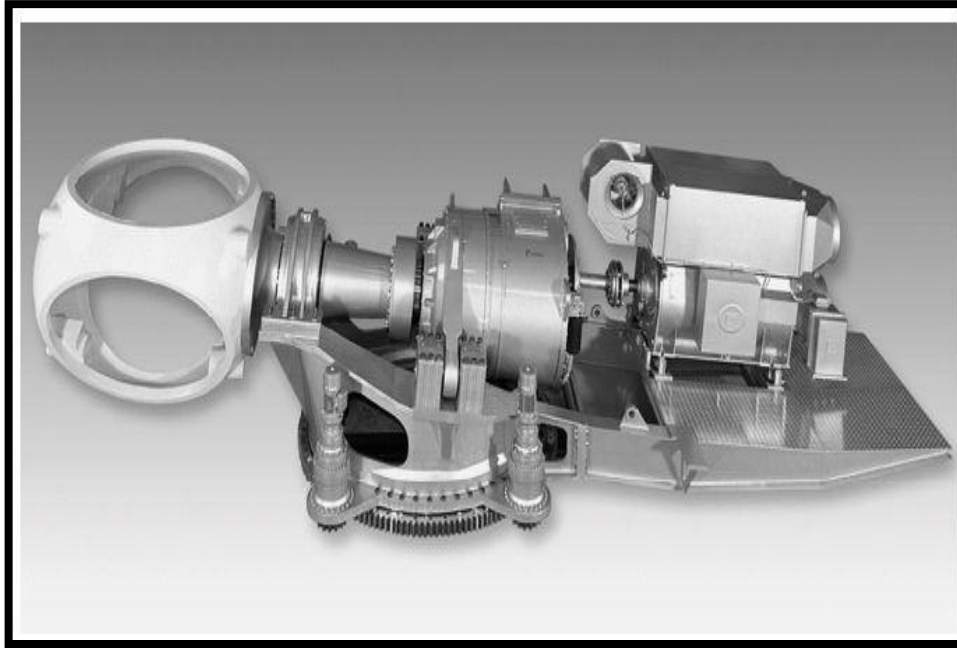


Figure 1.4: Standard gear train power conveying equipment (4).

As shown in the Figure 1.4 (4), power conveying system consists of hub, main rotor, gear box, and generator. The power flows from the starting point of hub to generator where the mechanical power is converted to electricity. All of the components and mechanisms shown in the Figure 1.4 should be designed very carefully in order to have a complete operation of a wind turbine.

1.1.2.1. Hub

The mechanical power produced by the blades is conveyed from hub. The system should be well analyzed to ensure that hub has sufficient strength to carry peak torque values. Hub is component where the blades are integrated, and they are generally spherical shaped structures.

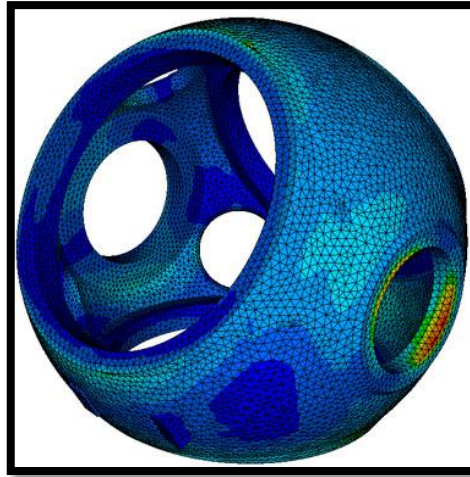


Figure 1.5: Isometric view for a wind turbine hub (5).

1.1.2.2. Low speed shaft

Main rotor is the component for a wind turbine that connects the blade rotation to the gear box. Low speed shaft is connected to the hub with a suitable flange. Therefore, all torsional loads of the turbine flows from the main rotor to the gear box. The system works under highly dynamic loads. Therefore, fatigue life calculations should be carefully conducted. The low speed shaft can be generally cylindrical or conical in shape according to load designs.



Figure 1.6: The low speed shaft for a wind turbine (6).

1.1.2.3. Gear box (Gear train type turbines)

Gear box system is one of the most crucial components of a gear trained wind turbine. The inlet of the gear box is the low speed shaft. The gear system boosts up the rotational speed with a desired ratio. The gear ratio is determined with respect to the nominal working speed of the main shaft and the nominal working speed of the generator. A standard gear box for a typical wind turbine has 3 different stages that consist of two planetary and single helical gear stages. The planetary gear stages are the first two stages, and final stage is arranged as a helical one. The gear box is one of the heaviest components of a wind turbine which weighs up to 6500 kg for a 500 kW turbine.



Figure 1.7: Standard 3 stage gear box for a middle class wind turbine (7).

1.1.3. Generator and Power Electronics Equipment

The outlet of the gear box is connected to the generator via high speed shaft where a variable frequency AC signal is produced. At generators mechanical torque is converted to AC current via electromagnetic waves.

The system also has power electronic equipment that includes several electronic converters to feed the grid with a continuous and fixed electric signal. Typically converters have a variable frequency AC to DC converter as a first stage. Then, most

generally, this DC signal is conditioned with a DC to DC converter to 220 V. Last stage of the converter is an inverter that inverts the DC signal to 50 Hz AC signal.

1.2. PROBLEM DEFINITION

All of the components of the wind turbine that are mentioned above should be carried by a main load frame that is called bedplate in the wind turbine terminology. The topic of the thesis study is to design and develop a main load frame for a 500 kW wind turbine which will carry all the static and dynamic loads of the components explained above.

The main load frame of the nacelle should be designed strong enough to handle both static and fatigue loads that are exerted by wind and other components. There are three different design approaches in nacelle bedplate design; fully cast, welded steel frames, and hybrid designs that combine both. In this thesis, the hybrid design approach is utilized for an optimum structure. A cast base is used to support main bearing and gear box, and a welded steel extension is used to carry generator. While cast base provides high stiffness around bearing and heavy dynamic loads section, welded structure reduces overall weight where loads are relatively low.

Nacelle bedplate transfers all of the loads to the yaw bearing, and provides mountings for the main wind turbine components. With a hybrid approach, the structure has cast and profile parts attached with the aid of bolts.

In this thesis study, middle power class wind turbines are studied. The middle class wind turbines that have a power range from 100kW to 700 kW generally do not have any integrated full load crane in the nacelle. Typically, they have very small cranes with capacities in a couple of hundred kilograms payload. These cranes are provided to handle light weight repair equipment or to lift maintenance oil bins. They are not sufficient for major repairs that may require gear box or generator replacement. In this work, a self-sufficient turbine system is designed for remote areas. To enable major repairs or replacements without any need for external cranes, a heavy duty internal crane system is designed and attached to nacelle bedplate. Therefore, unlike typical turbine designs that require static and dynamic analysis for wind loads, this work also

considers internal crane loadings which may involve offset loads around 10 tons. The crane that weighs more than 4 tons –by it self- is designed to handle gear box or generator overhaul that may involve more than 5 tons of load each. Furthermore, to keep overall weight at a minimum while maintaining a safe design margin for all the loads topology optimization has been applied.

CHAPTER 2

BACKGROUND AND LITERATURE SURVEY

2.1. LITERATURE SURVEY ON WIND TURBINES, BEDPLATE DESIGN AND MATERIALS

Wind turbines bedplate design relies on the computer aided engineering. Therefore, the thesis study is also based on CAE. Both static and dynamic analyses were performed with sufficient safety factors via finite element method. Aside from the design methods, material selection has to be carefully conducted for the bedplate designs because the strength is dependent on material selection. The loading cases should be arranged carefully and plausible maximum loadings should be determined for the analyses.

Nacelle bedplate is a significant part of wind turbine, which not only supports the rotor, gearbox, generator and other large components but also connects them to the tower through the yaw system. As also stated in reference (8) aerodynamic thrust and nacelle wind resistance loads the main shaft bearing which then transfer the load to the bedplate. Moreover, reference (3) explains the importance of the nacelle bedplate as the main coupler part in which the external loads on all wind turbine components flow through the bedplate to the main yaw bearing and the tower respectively. As mentioned previously, loads on the bedplate should be determined carefully especially for the fatigue life. Hau (31) states the importance of the static, dynamic and vibrational effects of the loads as three different aspects. First, the load components should be determined for extreme load conditions under both static and dynamic case. Second, the fatigue life of the wind turbine components must be guaranteed for their service life which is typically 20 or 30 years. Moreover, Hau (31) states that the fatigue life is virtually the key issue for wind turbines. Third, the components of the wind turbine must be

sufficiently stiff, so that all kind of vibrational modes for the system are beyond operating excitation frequency range.

Another aspect is the material selection process which has crucial impact on stress analyses of the bedplate. As will be mentioned in detail in the following chapters, the bedplate consists of two separate sections that are cast base and welded profile structures. For both parts material selection processes should be conducted carefully. Literature survey has provided significant insight during the material selection process. Ductile iron and structural steel were selected for the both parts respectively. Northon (14) states that ductile iron family is suitable for mass fabrication, and has low cost. In this work, for the cast base section of the nacelle design EN-GJS-400-18-LT material has been selected which is nodular cast iron. Northon (14) states that, nodular cast iron has the highest tensile strength of cast irons. Moreover, ductile irons have higher elastic modulus than gray cast irons. They are tougher, stronger, and exhibit linear stress-strain curves.

The majority of wind turbine parts are made out of ductile iron grade EN-GJS-400-18-LT. This grade of ductile iron features the properties necessary to withstand the wind loads, and long-term exposure to harsh environment without failure. Moreover, the cast parts must exhibit relatively high-impact strength at low temperatures, as wind turbines should safely operate at -10 to -20 C. For wind power to become competitive compared to other sources of energy, larger, more efficient, and less expensive wind turbines have to be developed. Cast components make up much of the weight of the wind turbine. To develop larger and more powerful wind turbines, lighter cast components are required (24).

Moreover, generally casting parts are heavy components. Therefore, the material selection process for the bedplate is extremely important from the weight to strength perspective. Roedter et al. (9) address this problem by suggesting ductile iron which offers 10% weight reduction compared to steel. Therefore, it is considered by designers for many other components as well. Selected material should also be suitable for easy casting. Roedter et al. (9) states that EN-GJS-400-18 material is quite suitable for both casting and machining which is typically required after casting. Moreover, the microstructure and chemical composition of the ductile cast iron is also very important for the mechanical strength of the material. Roedter et al. (9) suggests that if nodular

cast iron is cast with the nodule count of 200 nodules/mm², this results in excessively high impact strength. In addition, 95% level of nodularity is critical for impact rooted micro crack initiation. Northon (14) states that nodular cast iron is a preference for fatigue loaded parts. All the indicated features of nodular cast iron make it a suitable candidate for wind turbine nacelle castings. Therefore, as in most other wind turbines EN-GJS-400-18 material has been selected for the nacelle bedplate being designed as part of this thesis.

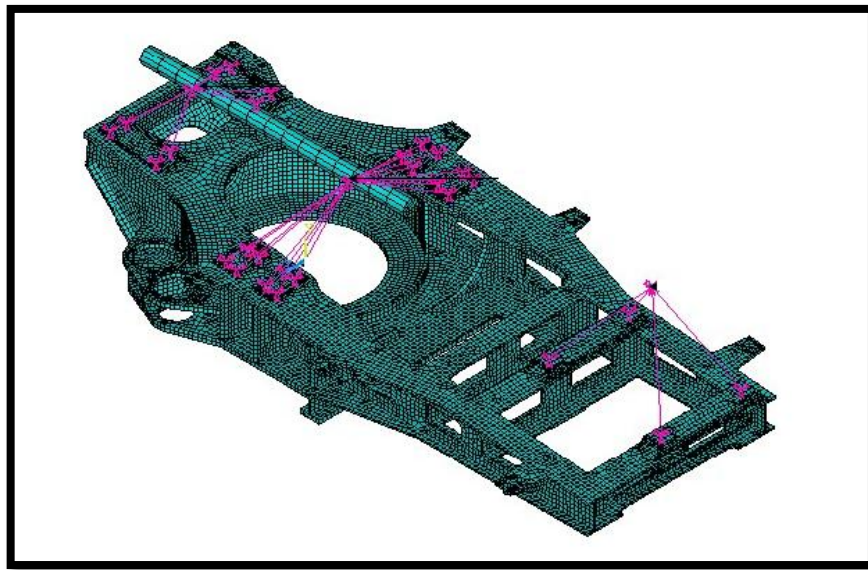


Figure 2.1: Meshed model of sample bedplate (8).

2.2. LITERATURE SURVEY ON STRESS-WEIGHT TOPOLOGY OPTIMIZATION

During the analysis phase of the design, finite element models are used to handle the 3D complex structural analysis. The model should have a fine mesh in order to achieve more realistic simulations to better determine the stress levels of the bedplate. The meshed model allows evaluation of element level parameters like stress, deflection, strain and so on. Peng et al. (8) state that static analysis is often used to simulate displacement and stress response to check if nacelle would withstand the extreme loadings. Maximum strain, stress and displacement values under different load combinations are obtained to decide on the stress worthiness of the designed structure.

Once the FEA models are established and verified, an optimization work is needed to minimize weight of the structure while keeping the stress levels in acceptable range.

Optimization of the bedplate is another important part of this thesis work. The literature survey on the optimization techniques including topology optimization yielded enlightening guidelines for the optimization stage of this work. Papalambros (3) states that analysis models are developed to increase the understandings of how system works. A design is also a system, typically defined by its geometric configuration, the materials used and the task it performs. In order to model a design one must be able to mathematically define it by assigning values to each quantity involved with the critical values satisfying mathematical relations representing the performance of the needed design task. Papalambros and Wilde (3) state that frequently the natural development of the design model will indicate more than one objective function. For the shaft example, we would really desire minimum weight and maximum stiffness. These objectives may be competing. For example, decreasing the weight will decrease the stiffness and vice versa. Therefore, some trade-off is needed.

Among the optimization techniques shape and topology optimizations were selected for structural optimization. Thomas (15) states that the purpose of the shape and topology optimization is to find the ideal structure where weight has been minimized and strength has been maximized. This goal is achieved by iterating on the shape and topology of a structure until the model converges to the optimum arrangement. The four popular methods for topology optimization can be listed as homogenization method, SIMP method, evolutionary structural optimization (ESO) and level set method. The first method introduces a porous structure where the optimization is simplified by increasing or decreasing the size of the pores. The method is effective for deleting holes only. SIMP and ESO methods are advanced tools, which start with initial finite element model. Based on specific objective function, the elements with the least contribution are removed. This method is very effective in obtaining a locally optimized structure, but may not achieve a globally optimized structure. Rong et al. (20) show that evolutionary structural optimization has been developed based on the simple concept that by systematically removing the unwanted material, the residual shape of the structural evolves towards an optimum. For ESO method, various types of optimality constraints occur like stress, displacement, frequency, and buckling. ESO has

wide coverage of optimality criteria. It is demonstrated that it is capable of solving all kinds of structural optimization problems in practical engineering.

Bendsoe and Sigmund (29) state that direct method of topology design using the material distribution method is based on the numerical calculation of the globally optimal distribution of material density which is the design variable. In order to achieve the optimal topology of a structure, designer should construct a suitable finite element mesh for the ground structure. This mesh should be fine enough to be able to capture realistic values. The mesh should also make it possible to apply fixed design variables to such areas of the model. Finite element method, then calculates the minimum compliance of the structure iteratively. When only marginal compliance changes occur, iterations stop indicating that optimality is satisfied. Then, density variable is updated. In this stage, program searches for the value of Lagrange multiplier λ for the volume constraint.

Finally, Navarrina et al. (21) elaborate on the traditional minimum compliance formulations. They indicate that these formulations offer some obvious advantages, yet avoid dealing with a large number of highly nonlinear constraints. However, one can argue that these models may have some drawbacks like obtaining unfeasible results for practical applications. Therefore, the minimum compliance problem is said to be ill-posed. The SIMP formulation is the most widely used minimum compliance approach so far. In this formulation, one introduces a non-dimensional design variable per element which may have values ranging from 0 to 1. The objective of the method is to compute the design variables in such a way that a highly non-linear objective function is minimized while the single linear constraint is satisfied.

CHAPTER 3

CONCEPTUAL DESIGN AND ANALYSIS

The main purpose of this thesis study is to design a nacelle bed plate for a 500 kW wind turbine. To achieve an optimum design, a hybrid (two part) bedplate design has been developed. Throughout the process of design, several iteration stages have been undertaken. Each design iteration of the system was conducted in line with the improvements of dependent design groups in the national wind turbine project. All of the design iterations are arranged with the new developments, and all design constraints are included. The bedplate is one of the most crucial elements of a wind turbine which should have highest stiffness and robustness. Bedplate design also has an influential effect on the turbine, since all other mechanical parts are integrated on the bedplate. Apart from typical wind turbines in the order of 100 - 700 kW, in this study the turbine bedplate is exposed to heavy crane load. Therefore, static and dynamic analyses of the wind turbine bedplate are conducted with the crane loads. Due to its significance in the overall system, bedplate material selection process is also critical. The system is capable of carrying full static and dynamic load while providing infinite life. In this chapter both 3D CAD design iterations, as well as static, dynamic and modal analyses of nacelle main load frame are examined.

3.1. MATERIAL SELECTION

As mentioned above, the material selection process has to be conducted quite cautiously for the system because of the main frames' working conditions. The system is exposed to heavy static and dynamic loads. Therefore, material strength should be high enough to accomplish all requirements per international standards. After the literature search, it has been decided that the system will be designed with a hybrid 2-segmented bedplate that is made of both cast and welded profile parts. In addition to strength, domestic

availability of the materials is set as another criterion in selection process. Yet another requirement for the casted part of the load frame is that the material must be suitable for the extra-large size castings

3.1.1. Casting Part Material Selection Process

Main load frames of the bedplates are usually casted parts. It is needed because of the requirement of stiffness values for the nacelle. The stiffness values of general cast materials are more robust than the other manufacturing techniques like extrusion or turning or milling. Bending stiffness of the structure is extremely important for the front part of the bedplate, since it is generally exposed to extreme bending stress for common wind turbines which will be explained in the following chapters. Throughout the literature, many examples and vast experience with cast main load frames can be seen. Therefore, cast load frame is selected for the main bedplate.

The material selection of the bedplate was made based on both mechanical properties and compatibility of production. Due to national nature of the project, as much as the importance of mechanical properties domestic availability of the both cast and the welded parts for the bedplate was also design criteria. According to both literature and the experience of the casting engineers, there are some common materials for wind turbine components such as hub, low speed shaft and main bedplate in which they are all manufactured by casting.

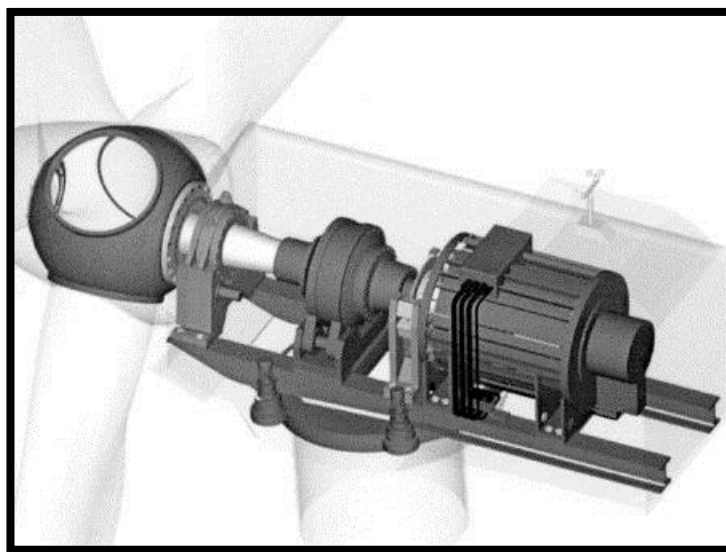


Figure 3.1: General view for wind turbine with gearbox (38).

Both rotor hub and nacelle bedplates are exposed to high bending stresses in nominal working conditions of a turbine. Therefore, the first requirement for the material is to have relatively high yield strength, and suitable chemical composition. Bedplate may have impact loading cases throughout the operating life of the turbine such as emergency braking and so on. Therefore, resistance to impact loading should be taken into consideration as a material characteristic requirement.

Cast irons form a family of materials. Their main advantages are relatively low cost and ease of fabrication. Cast iron family may have different tension and compression strengths, but generally their tension durability is weak compared to steel family. The most common means of fabrication is sand casting with subsequent machining operations.

Ductile iron and its different chemical configurations are used widely for wind turbine industry due to the mechanical requirements for both hub and main load frames. Nodular (ductile) cast irons have the highest tensile strength of cast irons. Their tensile strength range varies from 480 MPa to 930 MPa. The atomic structure of a ductile cast iron is spheroidal shape. Therefore, its name is nodular. Ductile cast irons generally have higher modulus of elasticity than the gray and white cast irons in which the value is about 170 GPa. Moreover, ductile cast irons follow linear stress –strain curve unlike the most general cast irons. Nodular cast iron is the most preferable one among all cast irons due its strength and durability against fatigue load (14).

Ductile iron has a perfect reliability on a wide temperature range from -20°C to 70°C . It has low density for specific configurations, so it is mostly preferred by wind turbine equipment producers.



Figure 3.2: Different wind turbine components with ductile iron configurations (9).

The chemical composition has significant effects on the materials mechanical properties. Especially Carbon and Silicon ratios are quite crucial. Generally, wind turbine ductile iron components should have 3.3% Carbon and 2.2 % Silicon and avoid high Phosphorus content.

Table 3.1: Common chemical composition of wind turbine cast iron.

Element	W _t %
C	3.3-3.5
S	0.008-0.012
Si	1.9-2.2
P	<0.030
Mn	<0.15
Mg	0.04

Amount of Carbon and Silicon are the critical parameters in the composition of a ductile iron. Our selected material has a very similar Carbon composition as given in the table.

Even though the bedplate may not be exposed to impact loading, some other parts may have impact loads on their operation lives. Therefore, carbon rate is quite important in the composition, because it has an important effect on toughness of material.

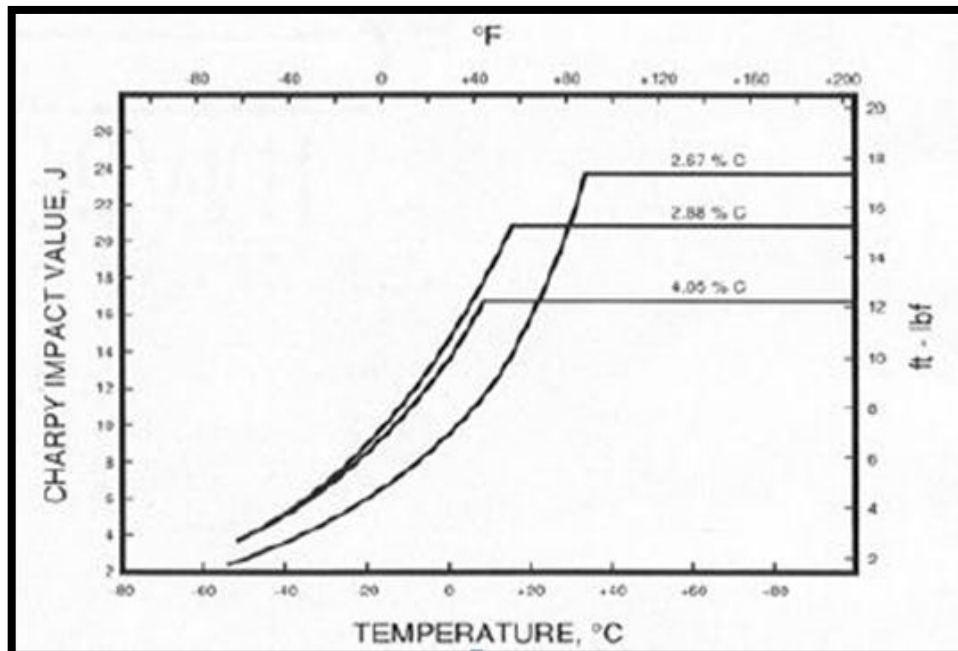


Figure 3.3: Charpy impact energy consequences on carbon rated ductile iron (9).

V –Notched Charpy test results can be seen from the Figure 3.3 which illustrates the effect of carbon rate in the composition on impact resistance. Charpy test is direct

information for toughness which is required when designing a structure for impact loading cases. As shown in the plot, when carbon rate increases, amount of energy absorbed by the material decreases when fracture occurs. This is an important criterion for selecting material composition of ductile iron.

Among the ductile iron family, EN-GJS series materials (from DIN standards) are highly suitable for wind turbine and other power industry applications due to their spheroidal cast iron structure and high stiffness properties. Especially, EN-GJS 400-18-LT is quite commonly used for the wind turbine industry, because of its compatible chemical composition that yields desirable impact toughness and bending stiffness. Moreover, this material can be easily supplied domestically, and quite preferable for sand casting.

Table 3.2: Chemical Composition of EN-GJS Series Materials.

Chemical Composition		EN-GJS -350-22-LT	EN-GJS-400-18-LT	EN-GJS-400-15	EN-GJS-450-10
	C	3.5-3.7 %	3.5-3.7 %	3.5-3.7 %	3.5-3.7 %
	Si	1.8-2 %	2.3-2.6 %	2.3-2.6 %	2.8-3.30 %
	Mn	max 0.2	max 0.25	max 0.25	max 0.4
	Mo	-	-	-	-
	Ni	-	-	-	-

The Carbon rate of EN-GJS-400-18-LT is quite similar to the previously mentioned most preferable composition of ductile iron material rates. One of the main reasons for the selection of EN-GJS-400-18-LT is its carbon rate, and relatively good impact test toughness.

Table 3.3: Mechanical properties different EN series materials.

Mechanical Properties	EN-GJS -350-22-LT	EN-GJS-400-18-LT	EN-GJS-400-15	EN-GJS-450-10
Tensile Strength	350 Mpa	400 Mpa	400 Mpa	450 Mpa
Yield Stress	220 Mpa	250 Mpa	250 Mpa	310 Mpa
Breaking Elongation	30%	22%	27%	20%
Elastic Modulus	1.2e11 Pa	1.2e11 Pa	1.2e11 Pa	1.2e11 Pa
Notched Impact Test	17J	14J	-	-
Brinell Hardness	110	120	135	160
Reversed Bending Stress	180 Mpa	200 Mpa	200 Mpa	220 Mpa
Alternating Tens-Comp Stress	120 Mpa	140 Mpa	140 Mpa	140 Mpa

The Charpy test results for EN-GJS-400-18-LT for -20 ° C is 12 J. This is why the material is referred to as -LT. In addition to good impact properties, mechanical properties of EN-GJS-400-18-LT are also suitable for the main load frame of the nacelle due to its high yield stress. Stress levels for fatigue analyses were also critical in selecting this material.

Before casting, material has to be heat treated to provide highest performance of strength for both static and dynamical loading. There are several ways for EN series heat treatments such as tempering, normalization, surface hardening and so on. However, normalization method of heat processing should be applied to EN-GJS-400-18-LT, because tensile and yield stress of the material gets maximized after this treatment.

Table 3.4: Technical Properties of EN series materials (10).

Technical Properties	EN-GJS -350-22-LT	EN-GJS-400-18-LT	EN-GJS-400-15	EN-GJS-450-10
Machinability	Very good	Very good	Very good	Good
Wear Resistance	Low	Low	Low	Low
Nitride Hardening	Good	Good	Good	Good
Flame Hardening	Low	Low	Low	Low
Weldability	Low	Low	Low	Low

Machinability of the material was another significant criteria since bedplate has a complex shape that resulted from topology optimization. As there will be machining process after casting good machinability was another reason for the selection of EN-GJS-400-18-LT.

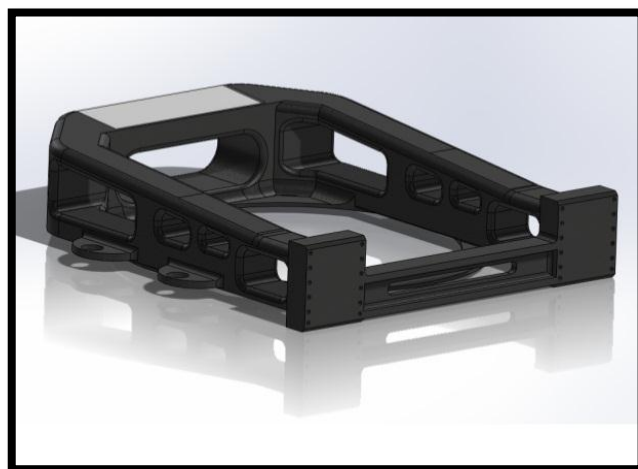


Figure 3.4: Final shape of the casted part design.

3.1.2. Material Selection for Welded Profiles

Structural steel part is designed to reduce weight, since casting of the entire nacelle structure as a whole would lead to extreme weight, cost and fragility. The steel part has to be light and strong enough to support generator and power electronics equipment weights, and generator torsional load. The material should be sufficiently strong for static as well as the fatigue loadings due to the dynamic torsional loads from generators.

The steel section that supports generator is constructed through welding of the sheet metal plates. The material selection process was similar to the previous section. As a very first step, various wind turbine sheet metal parts were examined. Even though some sheet metal profiles can be easily obtained domestically, some large profiles were not easily available. Considering the industrial experience, EN-AW-5182 (DIN standards) was chosen as the material for welded section to support the generator. This material is very frequently used in domestic shipping and construction industry, and well known by domestic suppliers. This steel contains Mg and Mn. The material is commonly known as St52. The material is also known as Al Mg4.5Mn0.4 in ISO standards, and has the following chemical composition, which makes it light and strong.

Table 3.5: Chemical Composition of St52.

EN_AW_5182	Mn	Mg	Fe	Si	Cu	Zn	Others
	4.0-5.0%	0.2-0.5%	<0.35%	<0.5%	<0.15	<0.25	<0.05

EN-AW-5182 material is one of the most preferable aluminized steel alloys due to its good corrosion resistance, high weld ability and formability. All of these properties are desired properties for the part that will be produced. The part will be welded from 30 mm thick sheet metals.

Apart from the reasons mentioned above, mechanical properties of the material are crucial for the selection process. The properties should be suitable and provide high strength for worst case loads. The desirable properties of relatively high yield strength, and the low density are quite significant for the selection process. Therefore, EN_AW_5182 aluminized steel has been selected for the welded section of the nacelle that will support generator.

Table 3.6: Mechanical Properties of St 52 (11).

EN_AW_5182		
Elastic Modulus		6.96e 10 Pa
Poisson Ratio		0.33
Shear Modulus		26000Mpa
Density		2650 kg/m3
Tensile Strength		380 Mpa
Yield Strength		320 Mpa

As can be seen from the table, material density is quite light in comparison to casting materials while the mechanical strength values are sufficiently high as observed in stress and deflection analyses. Moreover, it is commonly used in many different industries including wind turbines. Different examples of EN_AW_5182 products can be seen in the Figure below.



Figure 3.5: Several Parts for St 52.

As a consequence, EN_AW_5182 has been selected. This material is suitable for the design case, because of the formability and weldability reasons as well. Moreover, mechanical property values are also attractive reason for the generator support structure. Vast industrial experience and availability by domestic providers are also quite significant for the selection process.

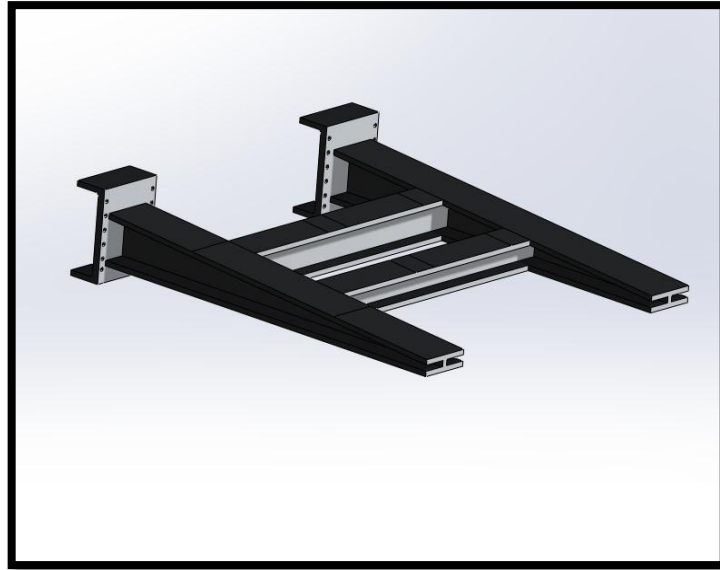


Figure 3.6: Final iteration of generator support part design.

3.1.3. Bolt Material Selection Process

Bolt material selection is also a significant part of the whole material selection process. The bolts that are used for joining casting and welded parts of the nacelle are the most critical throughout bedplate components. The material selection process is based on industrial experience and mechanical properties as well as extensive calculations.

As previously mentioned, the system should have a bolted joint in order to assemble cast and welded parts. The joint design should have acceptable factor of safety with sufficient bolt preload levels. Based on the standards of screws and nuts, structural steel was preferred as it is most commonly used for almost all types of bolted joints.

Material selection of the bolts is affected by the evolving design of the turbine. As stress levels change following the turbine design iterations, repeated bolt load calculations and FE analyses have been conducted. High yield strength requirement was the decisive among other material parameters. Among the structural steels AISI 1000, 4000 series and 5000 series were investigated.

AISI 4135, 4137, 5135, 5140 were all similar and quite suitable materials for bolting of the nacelle structures due to their favorable mechanical properties. AISI 4135 steel has been selected among them, because of its common acceptance and wide use in

the industry. The steel is also known as 34CrMo4 in ISO standards, and very commonly known as 12.9 or 8.8 quality steel in the market.

Table 3.7: Chemical composition of steels (12).

	Fe	C	Cr	Mn	Mo	P	Si	S
AISI 1035	99.09 %	0.38 %	-	0.9 %	-	0.04 %	-	0.05 %
AISI 4135	97.87 %	0.38 %	1.1 %	0.9 %	0.25%	0.035 %	0.35 %	0.04 %
AISI 4137	97.85 %	0.4 %	1.1%	0.9 %	0.25 %	0.035 %	0.35 %	0.04 %
AISI 5135	98.17 %	0.38 %	1%	0.8 %	-	0.035 %	0.3 %	0.04 %

Table 3.8: Mechanical properties of candidate materials (12).

	Density	Hardness	Tensile	Yield	Elasticity	Poisson Ratio	Elongation (Break)	Shear Modulus
AISI 1035	207 Br	7870 kg/m ³	710 Mpa	615 Mpa	200Gpa	0.29	16%	80 Gpa
AISI 4135	229 Br	7850 kg/m ³	1200 Mpa	1080 Mpa	205Gpa	0.29	-	80Gpa
AISI 4137	229 Br	7850 kg/m ³	1200 Mpa	1080 Mpa	205Gpa	0.29	-	80Gpa
AISI 5135	217 Br	7850 kg/m ³	1000 Mpa	800 Mpa	205 Gpa	0.29	-	80Gpa

As shown above, the selected AISI 4135 bolt material has high strength with some chemical and heat treatment processes like quenching and tempering. This steel is also as galvanized. AISI 4135 is the most suitable bolt material for the nacelle joint design because of the high yield strength and domestic availability.

3.2. ITERATIVE DESIGN APPROACH

At the very first stage of the project, only known information about the nacelle was rough set of enveloping dimensions which were only predictions based on experience. As the design process continued and design gets evolved, precise dimensioning and

knowledge of externally supplied prescribed boundary conditions were necessary. Because the project has multiple design team groups responsible for different subsystems, bedplate design is dependent on the design of other subsystems which are designed by other groups. The design iterations were arranged with both fundamental mechanical design needs and other subsystem design team demands. Design iterations have been started as a rough conceptual design without any knowledge from the dependent working groups. The illustration of the first design iteration can be seen in Figure 3.7 below.

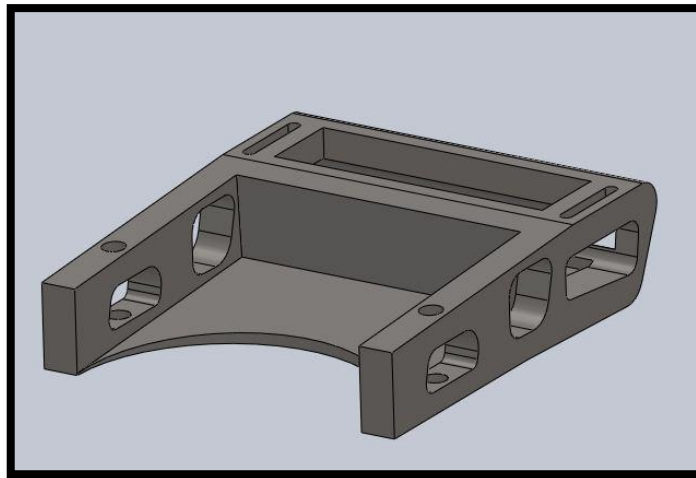


Figure 3.7: A conceptual design from initial iterations.

As the project progressed design criteria occurred due to the other groups needs such as blade deflection problems, or fundamental design approach changes from 2 to 3 point suspension turbine system. The design iterations determined whole turbine design including all nacelle structures such as gear box, main shaft, housing supports, generator and so on.

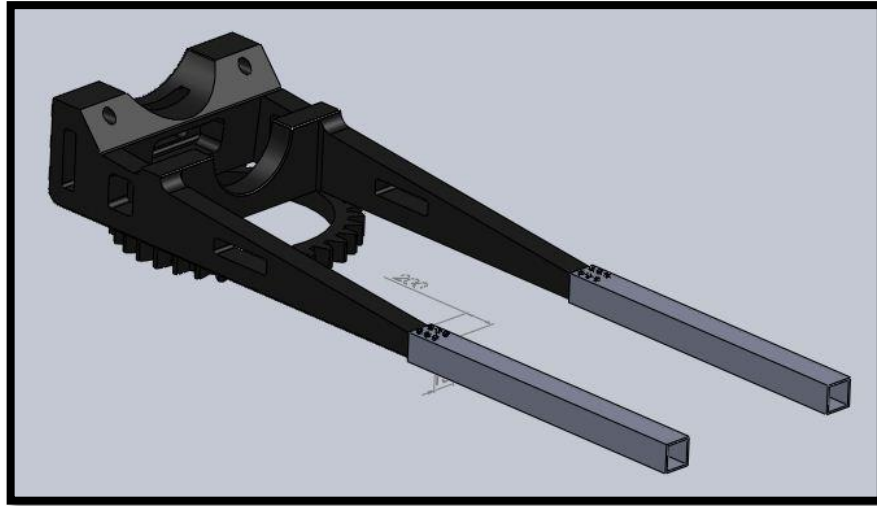


Figure 3.8: First conceptual bedplate design independent of other groups.

3.2.1. Design Constraints

As conceptual designs for all subsystems from other groups developed, final design of the bedplate has been reached iteratively. The progress caused some fundamental changes from the very first conceptual iteration like main shaft axis angle and overall shape of the structure. At the very first iteration, turbine design strategy was based on 2 main bearing supports on the low speed shaft. As the design evolved, turbine design became such that main shaft is supported at 3 points. The supports consist of single shaft bearing and two gear box supports which are called "bull's eye" in wind turbine terminology.

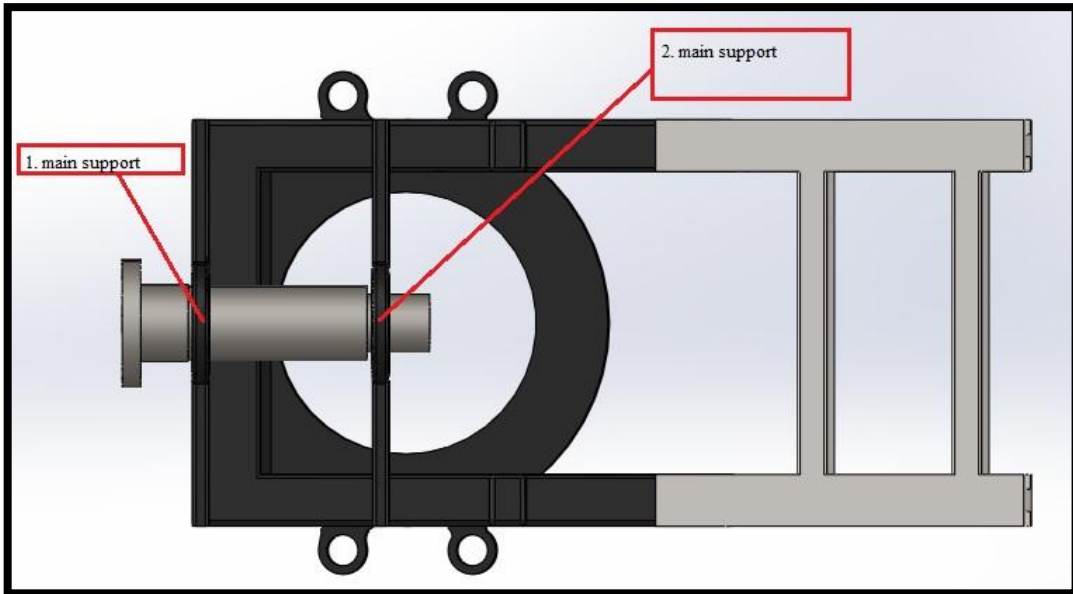


Figure 3.9: Two main supported system design.

As shown in Figure 3.9, in 2 point shaft suspension system design 2 main bearing houses are integrated to the cast nacelle bedplate. There are also 2 support points for the gear box. System working principle and strength analysis were different than the 3 point shaft suspension system design. Therefore, design iterations had to be consistent with other dependent groups' works.

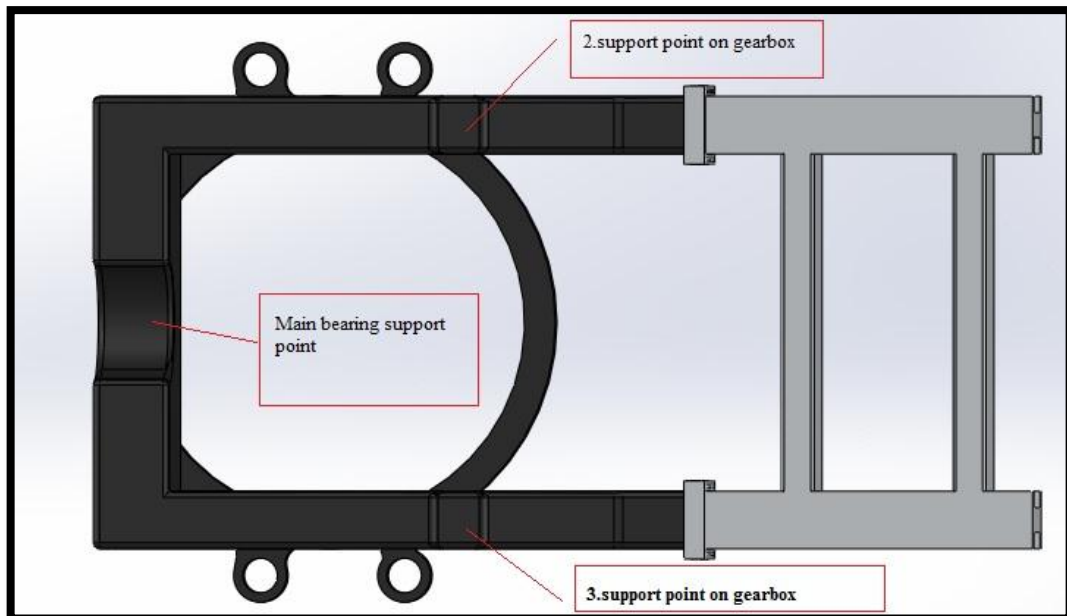


Figure 3.10: 3 main point support system design.

As seen in Figure 3.10, 3 point shaft suspension system works with one main shaft bearing and two gearbox support points. For this iteration, a semi-circle housing is designed for the main shaft bearing housing, and 2 explicit gearbox joint attachments were designed. At this stage of design, cast nacelle had square edges which make on tower hub assembly difficult. Nacelle corners have been trimmed at later design stages.

As other working groups progressed, their technical and geometric requirements from the bedplate altered. Therefore, there were many other iterations due to changing design constraints. Skipping minor design iterations, major design stages and iterations of the nacelle bedplate design are discussed below.

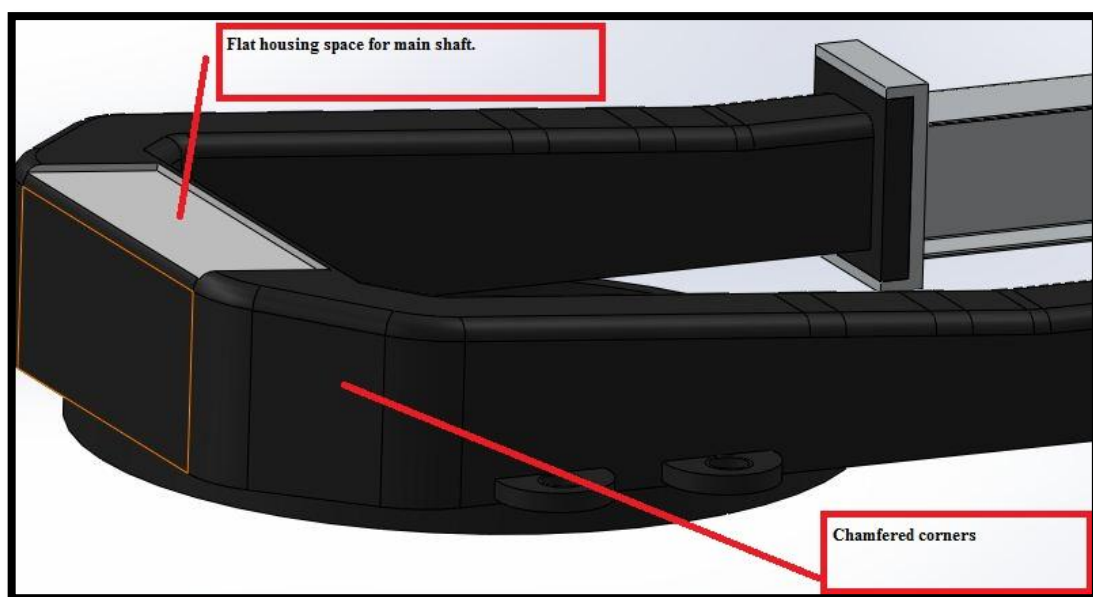


Figure 3.11: Different corner structure and flat space for housing.

Figure 3.11 illustrates a middle stage during design evolution. At this iteration, low speed shaft group did complete their design and preferred a housing that has a flat assembly surface. After some progress, main bearing space has been rearranged with an increased mounting area that led to reduction of static and dynamic stresses. Moreover, chamfered surfaces at nacelle corners have been designed in order to provide better access to assembly crew during bolting of hub to main shaft. Similar designs are also found in some other working wind turbines.

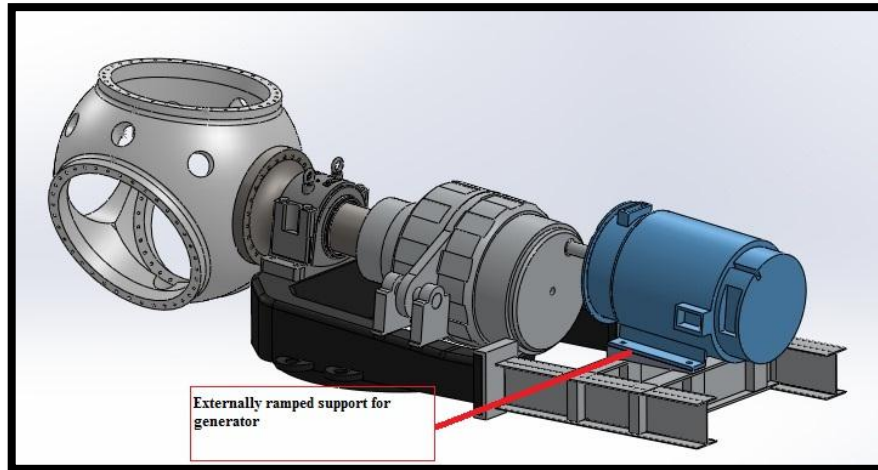


Figure 3.12: First system integration and general design problems.

During later stages of the design, other system component designs started to shape up. This stage of the design is shown in Figure 3.12. The welded frame part has been designed flat to get some benefits in system assembly, but it had some drawbacks. The high speed shaft at the third stage of the gear box has been positioned as free. This meant that welded frame part positioning was directly related to the position of high speed shaft.

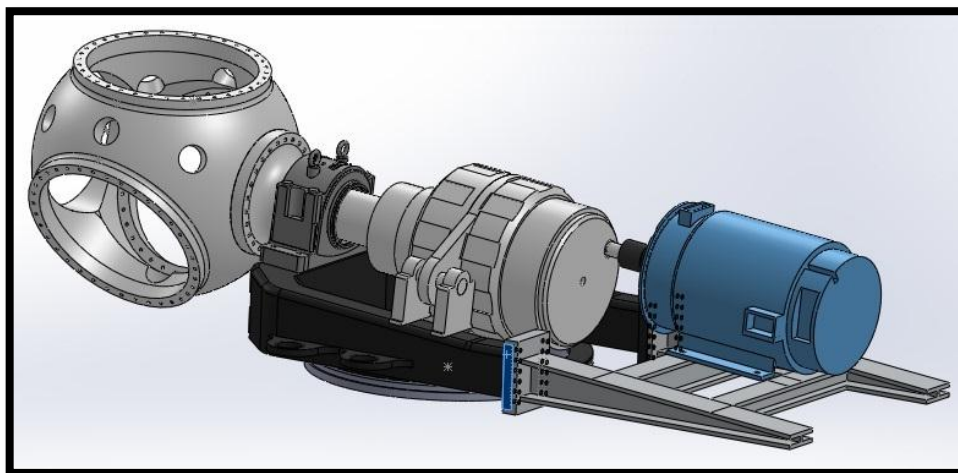


Figure 3.13: Ramped profile design.

Later, a change in turbine blades required more changes in the system. Blades are made up of some composite and aluminum materials. The blades may experience very large deflections under heavy wind loading. The maximum blade deflection dictates the distance/positioning of the blades with respect to the tower. In order to prevent any kind of blade-tower contact under wind loading, both tilt and blade mount cone angles are

calculated for both bedplate and hub respectively. Therefore, bedplate design has been rearranged so that main shaft axis has 5° angles with horizontal. The value for the turbine axis tilt angle has been selected based on the data in the literature, and the CAD integration performed on the whole system. Blade to tower distance has been measured and indicated safe clearance with the tower for 5° . The bedplate was flat and main shaft axis were horizontal during early iterations. After rotor-tower clearance calculations, the whole structure has been designed to have a 5 degree angle with horizontal. Figure 3.13 presents the nacelle design with 5° shaft axis.

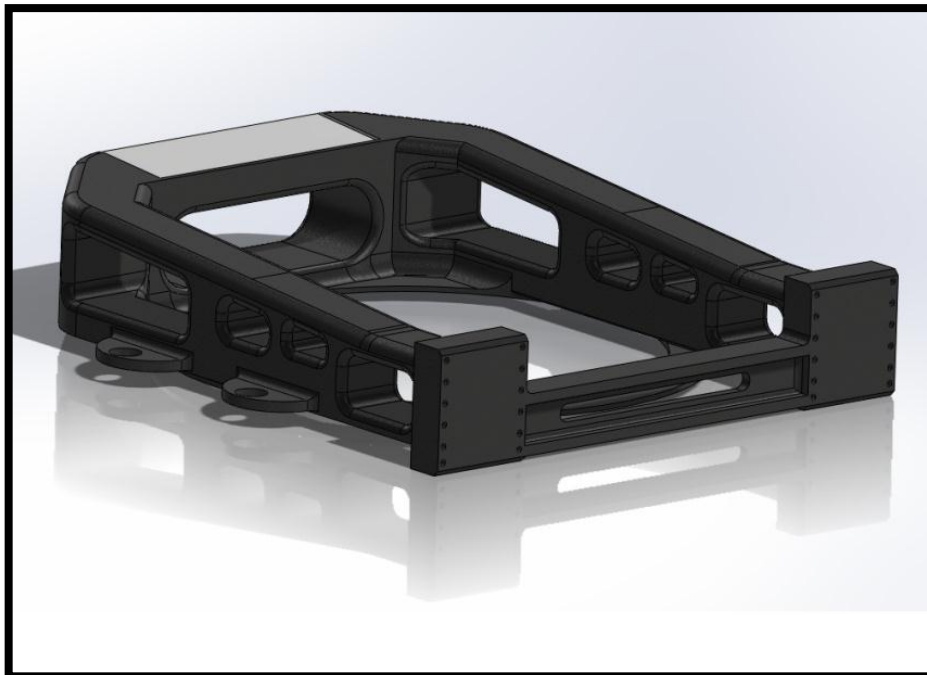


Figure 3. 14: 5 degree horizontal inclination has been introduced to avoid blade-tower contact under heavy wind loads.

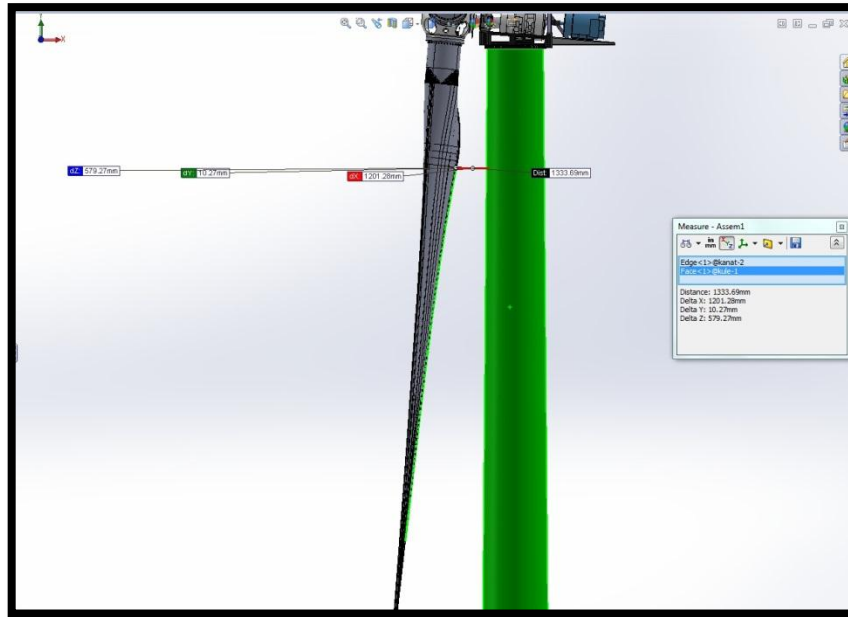


Figure 3. 15:Blade to tower distance.

Once the design iteration with inclined shaft axis has been completed, entire system has been assembled to check blade to tower clearance. As shown in Figure 3.14, after design iterations blade tip to tower distance has measured around 3200 mm.

For the welded portion of the nacelle that was designed as flat in the earlier design, an external ramp support part for the generator was needed. In addition, the space left for the power electronics inverters was too small. Therefore, another iteration has been conducted in order to get rid of both external ramp and small space problem. In the following design iteration, the space on left side of the generator has been designated for the power electronics equipment. Therefore, the exit positioning of the high speed shaft became very important. Welded part has been designed with a top surface with a 5° horizontal angle in order to be consistent with cast frame. Figure 3.15 presents the final nacelle structure design with 5° main shaft axis angle.

3.2.2. Design and Analysis Constraints

Apart from the geometric and system dictated limitations, there were some other design constraints due to the load capabilities of components. For the welded frame part, sheet metal plates are welded to form the structure. During early design iterations, there were some uncertainties about design strategy and the construction of the structure. First, a

non-hybrid and fully cast bedplate was decided to be used. However, due to possible extreme weight and extraordinary dimensions this approach has been discarded. Then, a two part hybrid design has been developed with cast main base and welded frame extension as in some similar literature work. During the second design iteration square cross section standard profiles were used due to some uncertainties in loadings. Square shaped extruded profiles are commonly available off the shelf, and they are better to resist torsional loads than I-Beams.

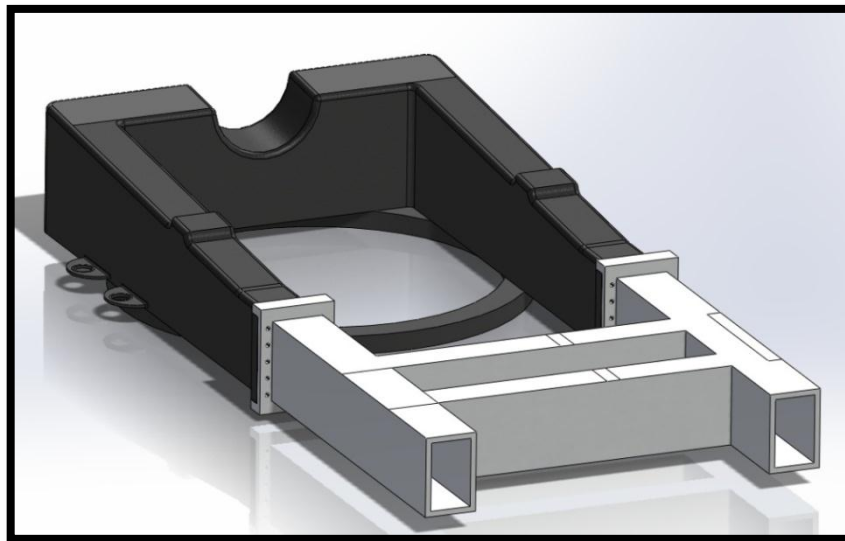


Figure 3.16: Square shape profile for torsion.

This iteration was aimed for increased torsional load resistance. At early phases of the design, generator operational load was applied as torsional. Later, analyses were conducted using force couples. I-cross section profile parts are more common than other cross sectional profiles. I-profiles are also easier to procure, and they are frequently used in almost all construction types due to its highly capacity for both axial and bending stresses. As mentioned above, the analyses have been conducted with force couples.

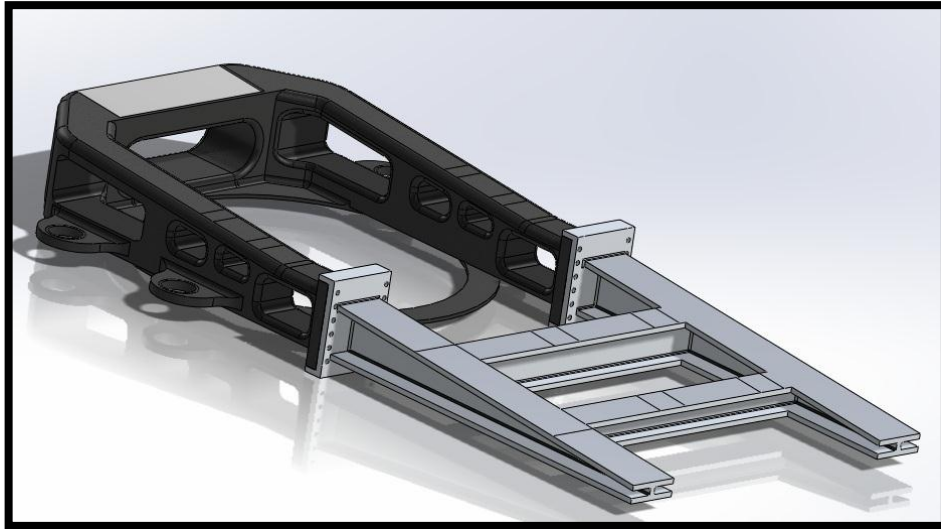


Figure 3.17: Final I-profile design.

After design and analysis iterations are completed, the final dimensions of the bedplate are as follows:

- L (length): 4900mm
- W (width): 2030 mm (2430 mm with motors' places)
- H (height): 421 mm
- M (weight): 4950 kg

The overall dimensions determine the weight and static loading of the system. System natural frequencies are also dictated by geometry and dimensions. The final bedplate dimensions resemble to those of other similar turbines around 500 kW power range.

3.3. FINITE ELEMENT MODEL AND PRELIMINARY ANALYSES

Throughout the project and the thesis study, finite element method has been widely used. It is a great advantage to use such powerful solution techniques for complex systems. The finite element method has been used for both stress analyses and the optimization stages of the thesis work. The analyses have been conducted in three dimensional space with multi variable loads, and variable material properties which make the problem very complex to solve analytically. Therefore, numerical methods are needed in order to complete all analyses, and to conduct optimization of the nacelle

bedplate. Throughout the process, static and dynamic fatigue analyses have been conducted using FE method. Moreover, natural frequency analysis and verification of bolts have been also performed using FE analyses. Finally, topology optimization has been accomplished using finite element approach as well. Details of the finite element analyses are explained in the following sections.

3.3.1. Codes and Solver Capabilities

Throughout the thesis study, several computer aided engineering codes were used. Especially the FE analysis and the topology optimization process are directly dependent on the strength of the solvers of the related codes. Finite element method is a numerical method; therefore, the efficiency of solvers has significant effect on solution time. Accuracy of the simulations is also related to solver's coding capability and suitability. When dealing with high number of meshed models, the computational time and numerical error can be optimized if the most suited solver is used for specific cases. From this point of view, the suitability of software and solver alternatives have been evaluated for the required static and dynamic analyses.

In early analysis iterations for static loading cases, COMSOL 4.2.a has been used. Although, the code was effective in linear analyses, it became inefficient with progressive needs such as nonlinear contact problems and bolt pre-stress analyses. During the early three quarter portion of the thesis work, COMSOL 4.2.a code has been used with a direct solver instead of iterative. At such earlier analysis stages the models did not have large number of degrees of freedom (nodes). COMSOL has three different solvers which are called SPOOLES, PARDISO and MUMPS for structural mechanics module. They are well written codes which are applicable for almost all common structural problems. However, they have some drawbacks. MUMPS and PARDISO are used at the very beginning of the project, and they both behaved the same. They are both direct solvers, and should be used for linear structural problems.

COMSOL is capable of choosing suitable solver for the problem. However, this feature is not arranged well. In advanced stages of the analysis encountered in this work, automatic solver selection did not work well, and started to select MUMPS solver directly. To further elaborate about these solvers, MUMPS is the most commonly used

one that is also default. It is fast for most problems, and allows multi core usage during solution. PARDISO is also fast, multi core capable and robust enough for structural mechanics. SPOOLES is slower than the other two above mentioned solvers, but it uses the least memory. Even though, all servers worked well for linear problems, only PARDISO worked fairly for the nonlinear cases at the advanced analysis stage of this thesis work. The numerical background of the solvers is based on Newton-Raphson method which is one of the most powerful numerical techniques for root finding. When the global stiffness matrix is formed, solver uses LU decomposition method to solve for matrix and further deflection value (33).

Software has coupled physics capability, which is well formed and useful for several cases. The analyses have been performed with the fully coupled option of COMSOL which enabled to all types of information flow between the geometries and materials and so on. When the evolution stage of the design has been completed in the project, more advanced analyses were required. Even though, such advanced tools are not available in COMSOL like application of pre-stress or bolt pretension, the segregated solvers are recommended for nonlinear problems. However, the convergence was too slow and failed many times during the advanced analyses of this work. Segregated solvers are recommended frequently for nonlinear convergence issues. These solvers try to iterate between different solutions variables. Overall, COMSOL's nonlinear solver capability has appeared insufficient with highly nonlinear problems like frictional contacts between surfaces (33).

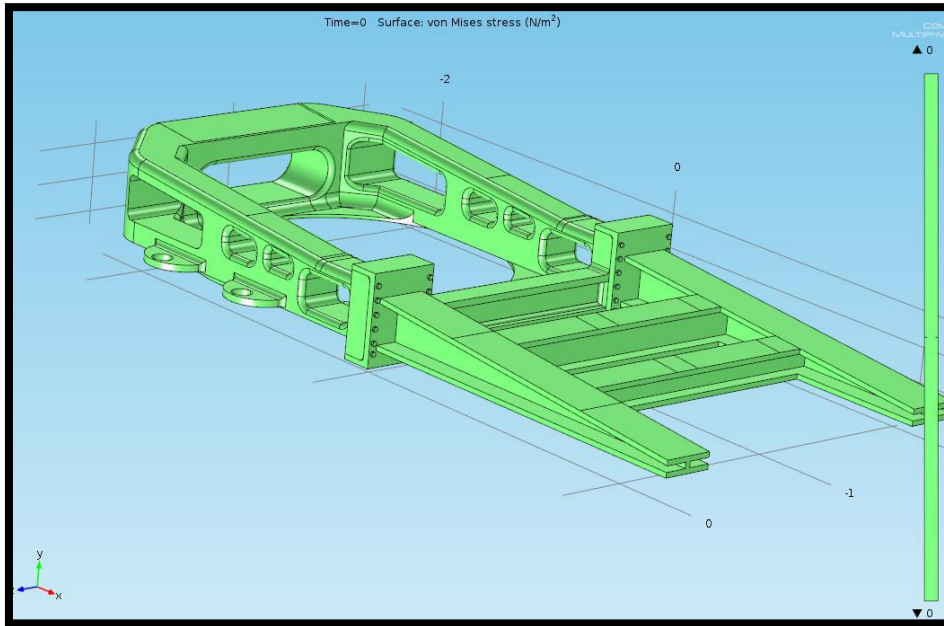


Figure 3.18: Diverged solution from COMSOL with nonlinear problem.

As illustrated in Figure 3.18, at later stages of the work with contact simulations, COMSOL could not converge after many trial iterations. Therefore, more advanced finite element codes were needed and solvers needed to be altered.

During course of this thesis work, SOLIDWORKS simulation toolbox which is designed for structural problems has been also used for the analyses of the bedplate. This code is a little more advanced than COMSOL in terms of functionality. It has different solvers as well, such as fatigue solver, frequency solver and quasi static solver and so on. Furthermore, this code has better contact capability and specific bolt and bearing forces and coupler. SOLIDWORKS is one of the well-known solid modeling and CAD programs, and it is very actively used. Throughout this thesis study, all computer aided design tasks have been accomplished with SOLIDWORKS 2012 including bedplate design and complete turbine assembly. Moreover, it has a simulation toolbox that is unfortunately not as well coded as CAD tool of the code. Simulation toolbox has three main solvers. However, there is no detailed information available about these solvers.

Simulation tool box offers an automatic solver that arranges the solver type while the model is being formed. The direct sparse solver and iterative solver in which SOLIDWORKS calls FFEplus solver are the two solvers that are used by

SOLIDWORKS simulation tool box. Both solvers are multi core capable, and a little faster than the COMSOL solvers. Both solvers have been tried and gave the same result if the same meshing is applied to the problem. The speed and performance varies with respect to size and type of the problem. The Sparse solver is convenient up to 300000 DOFs, and FFEplus solver is suitable over 300000 (28). SOLIDWORKS simulation toolbox has been used ensure the COMSOL results, and it worked well. The stress and deflection values were quite similar even though the meshing was different. Moreover, the calculated modal frequencies were approximately the same. However, background information about the solvers is not available. SOLIDWORKS simulation results have not been used to finalize the nacelle design.

A third code, ANSYS v.13, has been used as the main finite element software which has the most developed solver among all the programs that are used throughout this thesis study. ANSYS structural tool has been very effective in solving complex problems. It is one of the most frequently used software in the industry. Furthermore, ANSYS has good integration with SOLIDWORKS which has been an advantage to speed up the analysis process due to the fact that all cad designs has been constructed in SOLIDWORKS environment. ANSYS has advantage in analysis of advanced mechanical problems, because it has good diversity on solver types where detailed information is available. There are eight different solvers. They are all well written and capable of solving complex problems. Some solvers are well suited for nonlinear problems which are required for the advanced analysis of the bedplate. The list of solvers and information about their capabilities are listed below.

- 1) Sparse direct solver: This solver also includes Block Lanczos solver which is suitable for modal analyses. The solver is direct type solver and makes direct factorization of initial sparse matrix. Because the sparse direct solver is based on direct elimination, poorly conditioned matrices do not pose any difficulty in producing a solution. Direct factorization methods will always give an answer if the equation system is not singular. When the system is close to singular, the solver can usually give a solution (although the accuracy should be verified). (26). The solver is also the default one in structural module, and can be used for nonlinear problems.

- 2) The Pre Conditioned Conjugate Gradient (PCG) Solver: PCG solver is not used in the thesis but it is a well-designed solver for deflection and rotation problems. Instead of factoring the global matrix, the PCG solver assembles the full global stiffness matrix and calculates the DOF solution by iterating to convergence (starting with an initial guess solution for all DOFs). The PCG solver uses a proprietary pre-conditioner that is material property and element-dependent. (26).
- 3) The Jacobi Conjugate Gradient (JCG) Solver: JCG solver resembles PCG solver. It also assembles full stiffness matrix, and calculates solution to each DOF by iterative convergence. JCG is only oriented to static structural analyses.
- 4) The incomplete cholesky conjugate gradient solver (ICCG): This solver is more robust than the JCG solver. ICCG is tended to solve ill conditioned matrix problems. The approach of the solver is same as JCG.
- 5) The quasi minimal residual solver: The solver is only used for electromagnetic cases, and has not been used in the study.
- 6) The frontal solver: Frontal solver is a different solver than the others in a sense that, solver does not complete all global stiffness matrix and performs the assembly and the solution steps simultaneously as the solver continues with each elements (26).
- 7) The distributed direct sparse solver (DSPARSE): The solver is capable of dividing large stiffness matrices to smaller sub matrices and sends them to different processors. The solver is based on parallel processing and quite powerful for frictional contact problems.
- 8) The Automatic iterative solver: The solver is same as the iterative solvers like JCG, but it is faster than the others. The solver is generally used for difficult analyses where high iteration numbers are needed.

Among other codes that have been tried, ANSYS has been the best with most solver diversity. DSPARSE, Sparse, JCG and PCG solvers have been used for static cases. They have proven the same results under the same meshing. The default solver (Sparse) has been used for modal analysis. COMSOL MUMPS and PARDISO have

been used, but became insufficient for frictional contact problems. SOLIDWORKS tool box has been only used for ensuring the results from other codes (34).

While SOLIDWORKS 2012 alone has been used as the only code for CAD environment, and three different codes (COMSOL, ANSYS and SOLIDWORKS Simulation toll box) have been used for finite element analyses. Even though COMSOL has not been the best suited solver for advanced mechanical problems, it has some other benefits in CFD analyses where it allows the user to enter its own mathematical model as the weak forms of the model. ANSYS mechanical toolbox has excellent solver tools which have been used very frequently during advanced design stages of the thesis study. It has very developed fatigue and modal solvers. In addition, HYPERWORKS, OPTISTRUCT and ANSYS Shape optimization modules have been used for optimization of the nacelle's bedplate.

3.4. BOUNDARY CONDITIONS DURING CONCEPTUAL DESIGN STAGE

As mentioned previously, analyses of the main load frame has been conducted with the aid of finite element method. Boundary conditions for the analyses are quite significant in order to obtain realistic stress solutions. Loading conditions and fixed constraint definitions are the fundamental items for stress analysis of the structure. Boundary conditions for the worst case situation should be carefully defined in the finite element model that is used for the analysis. Therefore, load determination and other boundary conditions are crucial for the project.

National wind turbine project has several subgroups, therefore, determination of the boundary conditions depends on others work. Among the boundary conditions, some items were calculated, and others are taken directly from the related subgroups which are used for worst case analysis.

With the progress of the project, loading conditions have frequently changed. Therefore, preliminary analyses have been repeated for several iterations with different boundary conditions. In the earlier design stages, COMSOL has been used and several analysis iterations have been accomplished. The following sections clarify the boundary conditions for the static analyses. During the conceptual design phase first estimated

load conditions have been used. Later, boundary conditions based on preliminary calculations have been used.

3.4.1. Estimated load values

In the process of identifying boundary conditions, two different steps have been applied: estimated load values including several assumptions according to load cases, and calculated load values for convenient load scenarios. As previously mentioned, project has various design groups for certain turbine components. Therefore, during the conceptual design stage of the project, some loads have not been clearly determined due to incomplete subsystem designs.

Component weight parameters have been obtained from the relative design groups of the project. The load table provided below illustrates the boundary conditions taken into consideration for the earlier analyses. In the preliminary analyses, COMSOL software has been used.

Table 3. 9 : Estimated load values.

Wind	110000N
Generator	60000 N
Yaw Motors (Total)	7000N
Power Electronics	10000N

Table 3.9 presents the loads that have been applied for the conceptual design of the nacelles bedplate. Many iteration have been conducted under COMSOL as the force values altered frequently by the dependent work groups. These values were still estimated loads, because the component designs were under construction. Final boundary conditions included generator, yaw motors and power electronics equipment's weights as shown in the table 3.9. Moreover, bedplate joint design and bolt preloading values have not been completed at this stage. All of the values assumed during this analysis phase have changed during the later stages of the design process.

During the conceptual stage of the analysis, there was no integrated crane design. Later design phases include internal crane for maintenance of the nacelle. The detailed design and the analyses of the main load frame are explained in chapter 5 including crane loadings.

3.4.2. Calculated boundary conditions

Stress analyses have different load types which include gravitational loads and dynamic loads. Even though the project progressed well, during the conceptual design stage different information about the components of the turbine was missing such as the efficiency of the generator, frictional power loss for the gear box and so on. Therefore, calculated load values have been taken with the worst case assumptions which are explained later in the chapter.

Table 3. 10: Calculated load values.

R1 (main bearing)	300000 N
R2 (aft bearing/support)	80000N
Generator Torque	7296 N
Gear box frictional loss	6928N
Body loads	70000N
Bolt Preload	3553200N

As illustrated in the Table 3.10, reaction forces have been calculated in order to determine blades, hub and gearbox gravity loads and the related moments. Body loads refer to the weight of the main load frame which was 7000 kg. The main load frame was heavy and bulky, because at the preliminary design stage no optimization process has been applied. Bolts preloads could not be applied effectively, because COMSOL is not well suited to apply the pre tightening of bolts. Tension force was applied at the latest preliminary design stage. Later detailed analyses include well developed bolt pretension models which are presented at chapter 5.

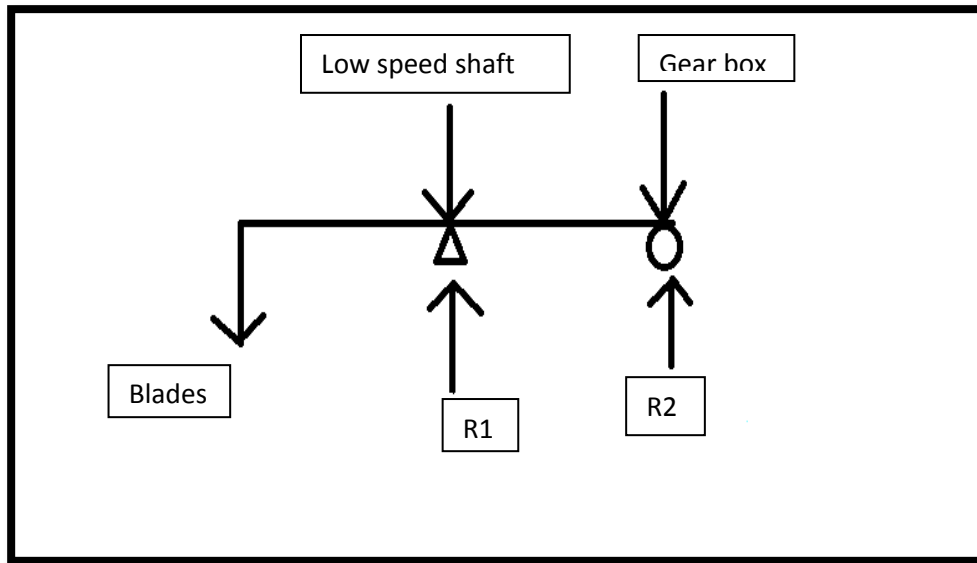


Figure 3. 19: Fixed and roller supported beam schematic.

Reaction forces are calculated as shown in Figure 3.19. weight of the blades, shaft and gearbox have been obtained and static force has been formed to calculate the reaction forces. These forces have been applied to the locations where housing of the shaft and the bull eyes of the gearbox are mounted on the bedplate. Therefore, reaction forces have allowed simplification of the analysis, and reduced the computational requirements since they are equivalent forces that replace several other loadings.

The efficiency of the generator was still not known by the relevant design group. Therefore, assumed worst case efficiency of 90% has been used. The output power of the generator is 500kW. Due to the losses through the generator the input power has been calculated as 550 kW. Speed of the high speed shaft has been taken as 800 rpm. Therefore, torque value from the generator has been calculated by the aid of the formula shown below,

$$P = T.W \quad (3.1)$$

$$F = T/d \quad (3.2)$$

The high speed shaft produces 550 kilowatt power at the generator inlet shaft. The bedplate is exposed to this generated mechanical power. The resulting torque value has been applied to the structure as a force couple. Generators regular working rotational speed has been taken as 800 rpm, and the torque value can be found from the formula given above.

$$550000 = T * 800 * 2 * \pi / 60$$

Therefore, torque, T, has been calculated as 6565 Nm. Moreover, generator support span has been given as 0.9 meters. Therefore, the force couple applied by generator on the nacelle support structure has been calculated as 7295 N. This force has been applied to the system as a force couple (two forces with opposite directions) at two different generator support surfaces.

Similarly, the torque loss due to generator losses has been also applied to the support system as a force couple. Maximum ten percent power losses estimated to occur at the gear which corresponds to 65kw power. The support forces due to generator losses are calculated with the same logic as

$$65000 = T * 22.4 * 2 * \pi / 60.$$

This yields 27710 Nm additional torque due to generator losses which has been applied to the bedplate as a force couple. Furthermore, the force value is applied on four different surfaces in the earlier design which also changed later in the project. Therefore the applied force couple value has been 6928 N.

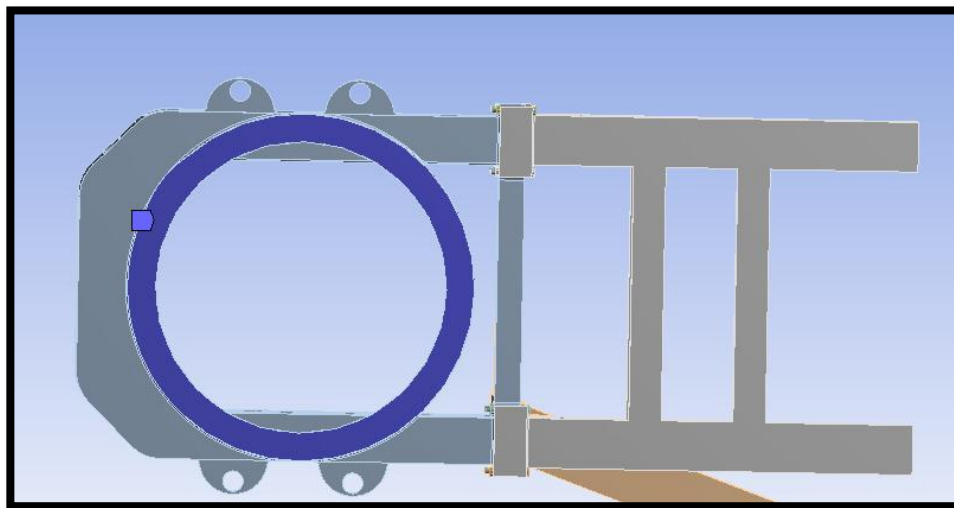


Figure 3. 20 : Fixed constraint for the analyses.

As boundary conditions, the ring that connects the yaw bearing to the bedplate has been chosen as a fixed constraint as illustrated in Figure 3.20. Fixing the surface below the ring (where ring is attached to the tower) provides six DOF restrictions. In the COMSOL analyses universal gravity has been added to the nacelle model in order to

compensate the gravity loads of the hybrid bedplate design. Any loads due to deflection of the tower are neglected in the both preliminary and detailed analyses.

3.5. PRELIMINARY STRESS ANALYSIS

After the boundary conditions have been set, analyses for the conceptual design stage have been accomplished using these boundary conditions explained above. The static loading analyses at the conceptual design stage have been conducted with COMSOL.

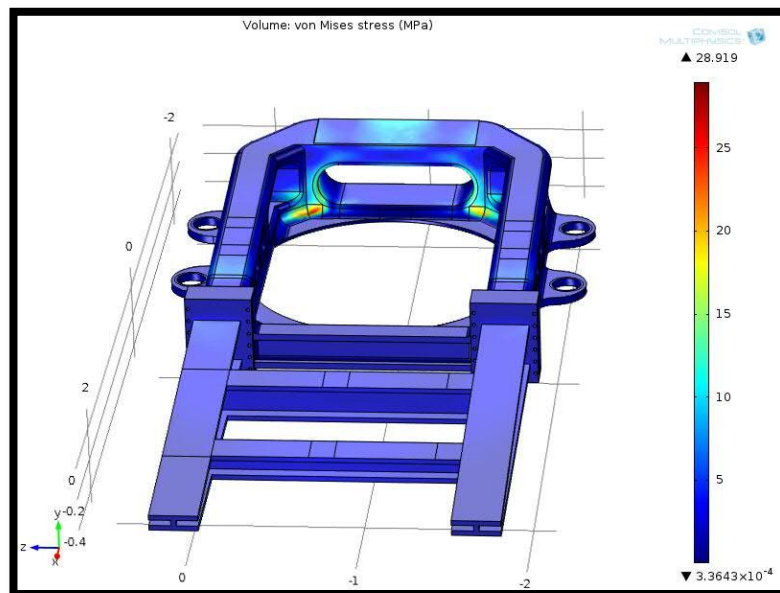


Figure 3. 21 : COMSOL results with estimated boundary conditions.

The Figure 3.21 shows the final design stage of the bedplate and preliminary static analysis results under COMSOL 4.2 a. The maximum von Mises stress value is around 30 MPa. However, this analysis does not fully reflect the actual load condition, because the crane loading has not been applied. Furthermore, at this preliminary analysis iteration the entire nacelle has been modeled as one part in COMSOL, even though there are two different parts made of two different materials, and joined through bolts. Therefore, this analysis omits the frictional contact between two bodies. Moreover, there should be bolt preloads in the system because of the bolted joint. COMSOL could not properly handle the bolt preload problems. Therefore, these early results from

COMSOL analyses were not sufficiently accurate due to the code's incapability of bolt pre-load effects, and its limitations with the modeling of nonlinear frictional contacts. As mentioned above, these results did not include crane loads either. Separate analyses have been conducted to simulate the maintenance situation with representative crane loads in order to capture any possible extreme stress levels when onboard crane works with heavy components.

A separate group of analyses have been conducted in order to see the preload effects on the system. Due to the limitations in COMSOL, a simplified representative preloaded analysis has been conducted. Total bolt preloads have been calculated and applied as part of boundary conditions as concentrated loads on the surfaces of both the profile part and the cast part. The analysis has been repeated with the simulated bolt preloads. The maximum stress location has shifted near bolts, and its magnitude has increased to 120 MPa.

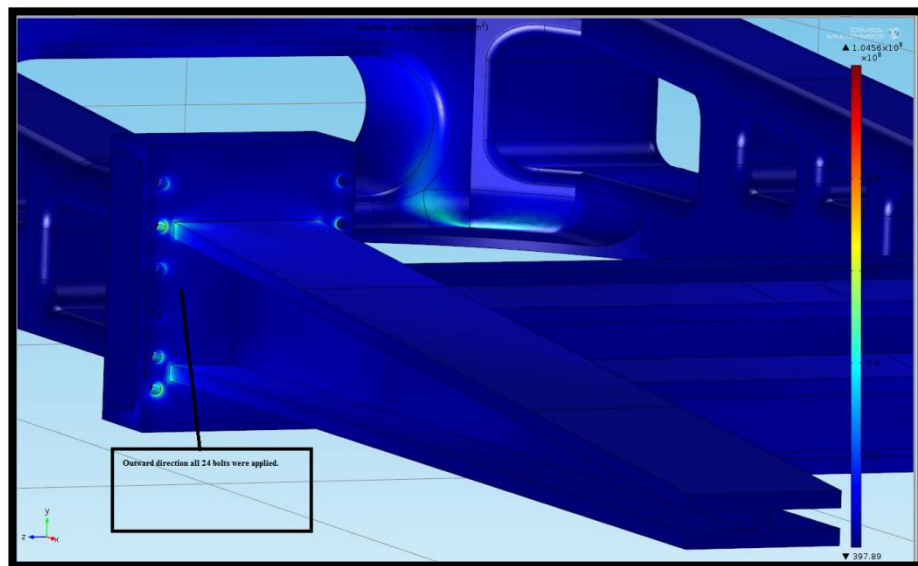


Figure 3. 22 : More detailed analysis using COMSOL including representative preloads.

CHAPTER 4

OPTIMIZATION STUDIES

4.1. TOPOLOGY OPTIMIZATION

Topology optimization is one of the well-known structural optimization methods that aims to find the best structure shape within a given design space and certain boundary conditions. Topology optimization method is nowadays highly used by engineers and it's a powerful technique to find the optimal shape which leads to cost reductions due to removal of unnecessary material. The method is quite effective in determining unnecessary regions of a structure that minimally carries any loads which can be removed from the system without much expense of increased stress levels. Topology optimization is a finite element based numerical method which identifies the optimal material distribution that will have the maximum stiffness for a given set of boundary conditions and design criteria. For structural analyses, design parameters can be both stress and deflection values for a body.

During the optimization process OPTISTRUCT module of HYPERMESH have been used for main topology optimization of the design, and ANSYS shape optimization modules have been used the refined optimization stage. Topology optimization for the cast part was necessary because of the stress values obtained from the COMSOL analysis indicted that there were some regions of the structure which did not carry any loads. Therefore, removal process for these regions was essential part of the project which led to weight reduction of the bedplate and the cost decrease on the casted part.

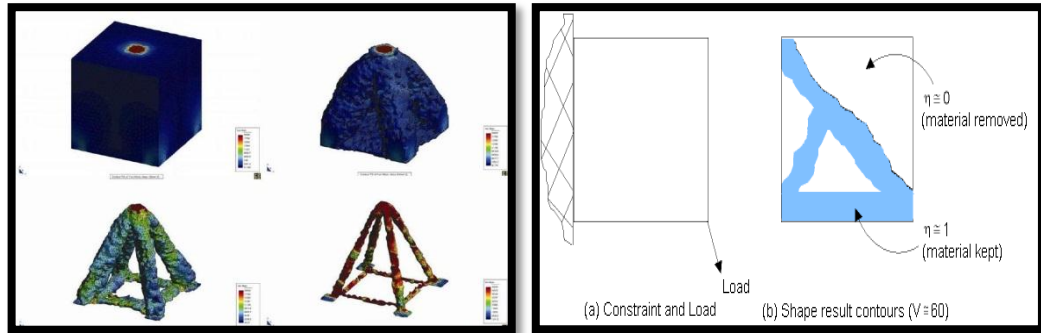


Figure 4.1: Topology optimization samples (17).

As shown in the Figure 4.1; the load bearing regions can be identified with the aid of the topology optimization. The structural removals in topology optimization can be made in either 2D or 3D.

4.1.1. SIMP Models

Solid isotropic material with penalization method is the fundamental theory behind the topology optimization which makes the material distribution via using density on a given design set with some boundary conditions. SIMP model has five different parameters which has to be solved. SIMP uses these parameters to solve the problem with a technique called minimum compliance or maximum stiffness for the design set with the material distributions.

First, an objective function should be introduced among the parameters, which has the form of $\int_{\Omega} \phi(\rho) * d\Omega$, where Ω represents the design set or a field to be optimized. This function is to be minimized using minimal compliance method for topology which aims to maximize the stiffness of the bodies.

Ω is the second important parameter for SIMP model which is design space or allowable volume to topology design. This parameter is significant and widely used in the OPTISTRUC analysis for the bedplate.

Third, the ρ_d value stated at the objective formula represents the discrete selection field which always takes values between 0 and 1 according to the selection or deselecting of the points. The optimization is a discrete one. An iterative approach is needed to get further results. This value is also called as zone which is discretely optimized.

Other significant parameters for minimum compliance model approach are that design constraints which are widely used in main optimization stage of the bedplate. These parameters can be stress values or deflections or mode frequencies. Iterative topology approach checks for the constraint value given by the designer. At the end of all iterations design constraints have to be met due to convergence issues.

Finally; the governing equations for the mathematical model are most important. Those equations are also known from FEM analysis, and they are the equation sets that solve the physics behind the problem.

As a consequence, the parameter ρ is used for only discrete optimization problem. Designers want to keep this continuous variable between 0 and 1 to get removable regions in the domain.

4.2. WEIGHT AND STRESS OPTIMIZATION (Main Optimization Stage)

The main reason for the use of topology optimization in this project is the need to reduce the weight of the bedplate which was around 7000 kg. This has been accomplished without any loss on the safety factor and stress carrying capabilities. The casted part was bulky and heavy without an optimization. This is evident in the analysis results of the bulk model. There were a lot of regions that did not bear any stress which made them unnecessary to keep. The stress plots indicated that the relaxed regions on the casted part could be removed as they do not carry almost any stress.

4.2.1. Pre-Design

First iteration for the topology optimization was to decide on the element of the bedplate which was obviously casted part. There were a lot of regions with very small stress levels. Those regions did only carry more than 5 MPa at most. Therefore, they were decided to be removed because of the weight and cost reasons.

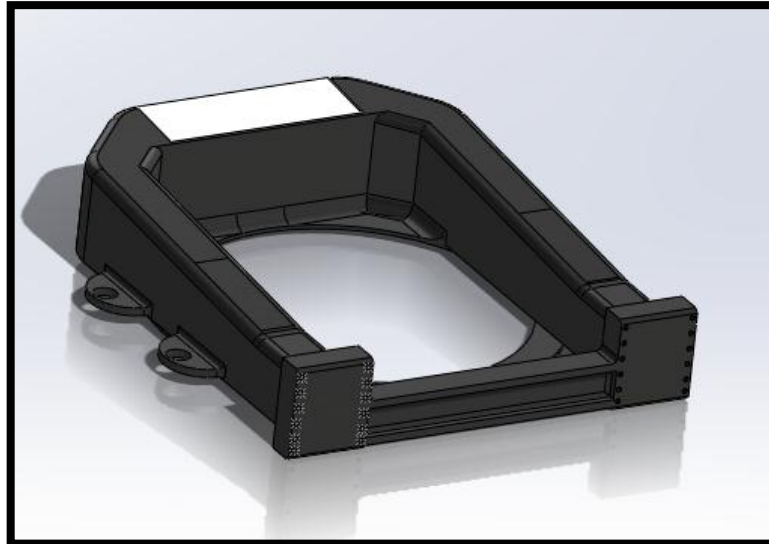


Figure 4.2 : The bulky model before the optimization applied.

As shown in the Figure 4.2, before the optimization process the structure did not have any holes. After some minor manual trims, the structure was still bulky and heavy at around 6500 kg. The assembled bedplate was around 7000 kg with the profile part and bolts integrated.

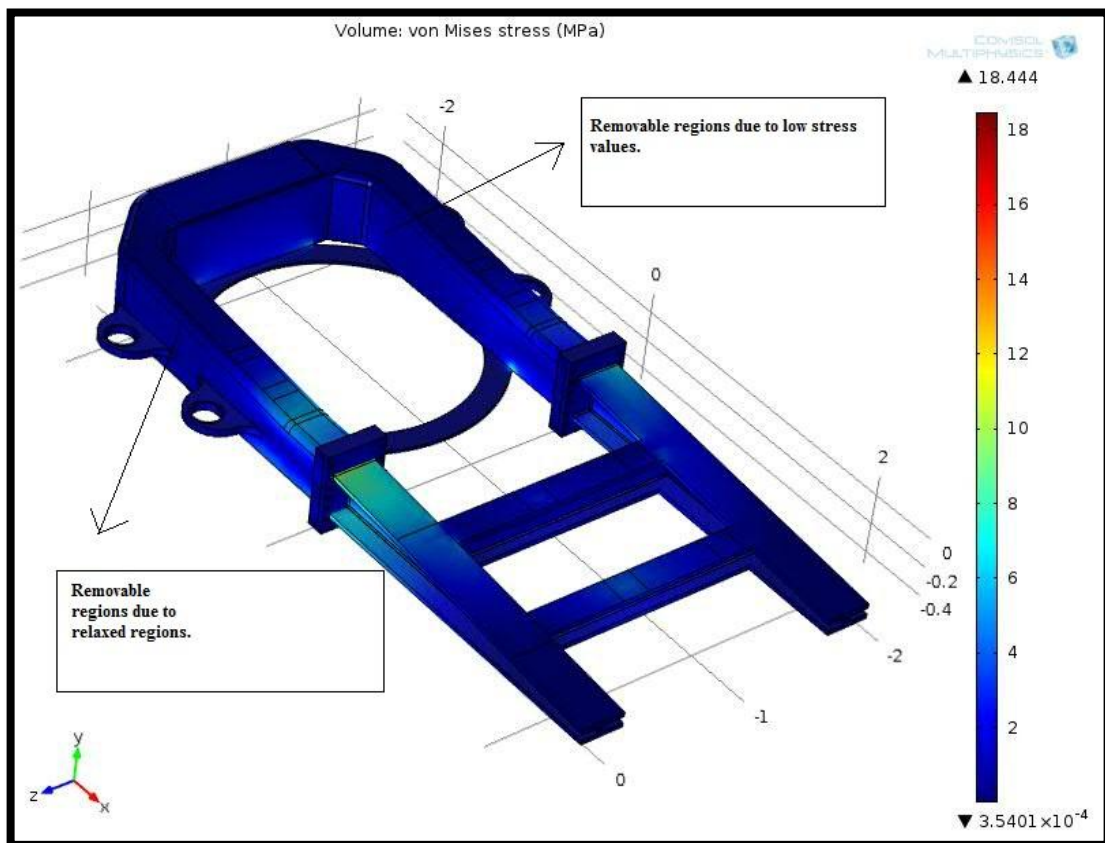


Figure 4.3 : Stress results before optimization applied.

As illustrated in the Figure 4.3, there were a lot of low stress regions in cast part. The locations of material removal are explained in the following parts of the chapter. Main stage of the optimization process has been performed with the aid of OPTISTRUCT code which is based on SIMP model mentioned above.

4.2.2. Design constraints

In order to complete the main stage of the optimizations, a finite element model has been formed in HYPERMESH environment to start with. OPTISTRUCT toolbox works with SIMP model while creating the optimization results. Only the cast part of the nacelle has been selected for topology optimization. Therefore, the boundary conditions have been applied on the cast part.

Objective function of the case has been selected to find the minimal volume of the design space that is the cast part in this design case. Therefore, the objective function is the minimization of the volume of the design space.

Design constraints can be both deflection based or stress based for the topology optimization. There is almost unlimited variety of design constraints in general. For instance; system mode frequencies, shear stresses or strain energy or thermal parameters can be included as design constraints. The optimization stage has been based on the full static loading of the bedplate which is described in Chapter 3. Design constraint was stress based that had to be lower than 30 MPa through the design space. Second design constraint was the removal fraction that is pertained to program. This fraction value should be given to define the maximum material removal rate for the necessary regions.

4.2.3. Post-Design

After completing the finite element model and definitions of the optimization constraints for topology, OPTISTRUCT solution has provided some guidance for the removal of the material for the casted part. After accomplishing the removal process the optimization or weight reduction holes have been formed under SOLIDWORKS. Then stress analyses have been repeated with weigh optimized model.

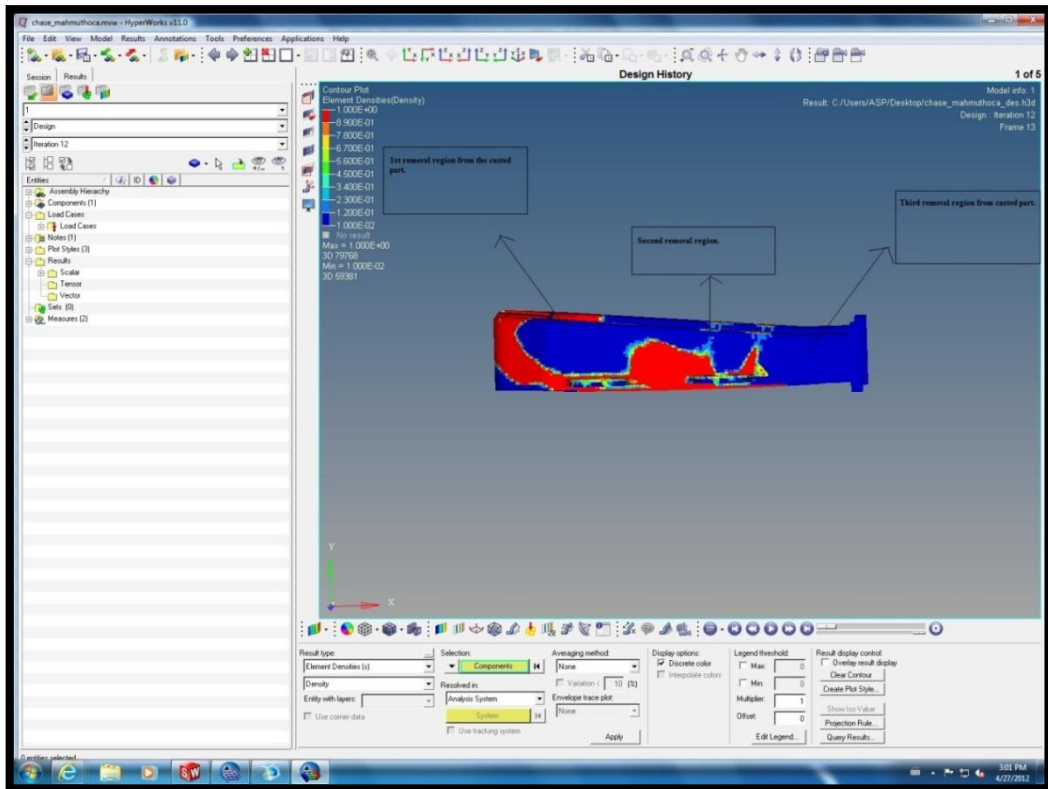


Figure 4.4: OPTISTRUCT solution providing guidance for optimization and material removal areas.

As shown in the Figure 4.4, the regions represented in blue are the relaxed areas that can be carefully removed. Especially, third region towards far right is highly relaxed. However, the second region should be carefully removed due to nearby high bending stresses from the reaction forces. There are some parts of this second region that is not removed due to this reason explained above.

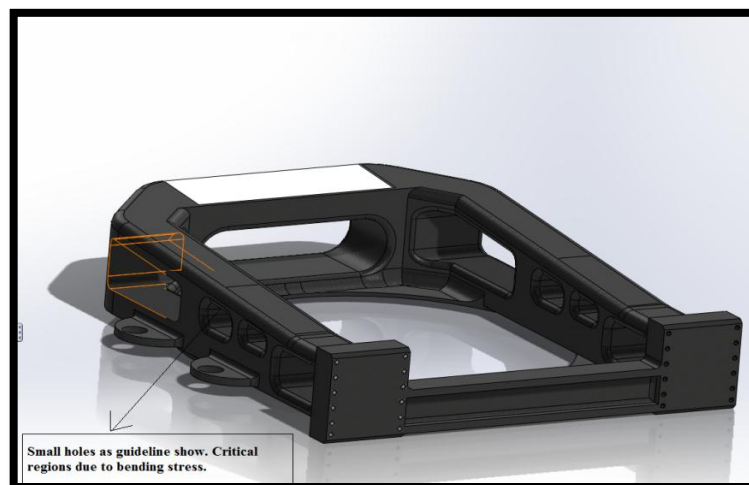


Figure 4.5: Cast part after main stage of optimization.

After the optimization holes are created, the design weight has been reduced to 4500 kg which is a reasonable value for main load frame design of middle power type wind turbines. As previously stated, second region is critical because this region is near areas that are under high bending stresses due to the reaction forces A and B illustrated in Figure 4.6. The forces are 270 kN and 60 kN respectively. Some small areas in this region have been removed with guidance provided by the OPTISTRUCT model. The design with small material removal holes, as illustrated in Figure 4.5, has been confirmed with a stress analysis that there is no critical regions or stress concentrations.

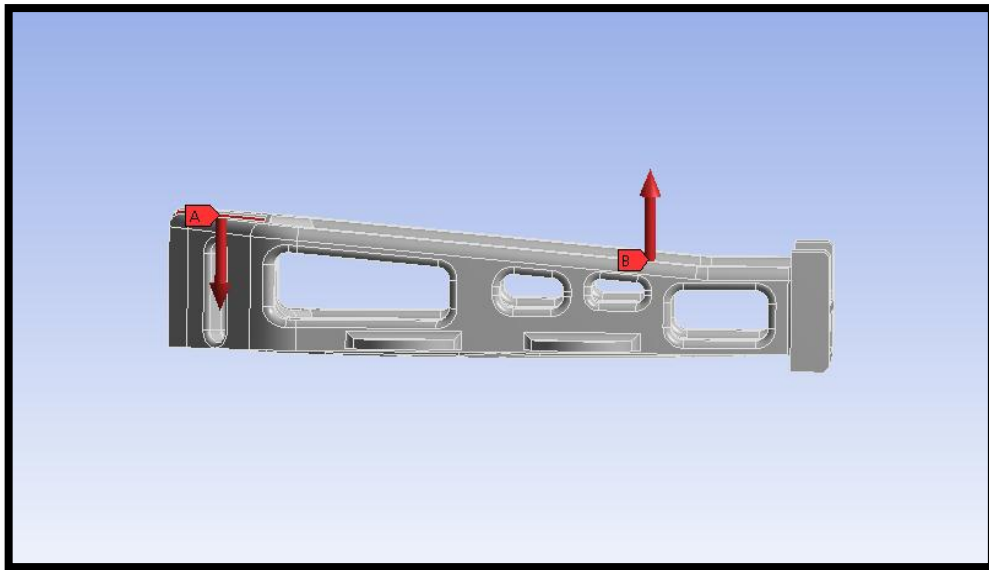


Figure 4.6: High bending stress region.

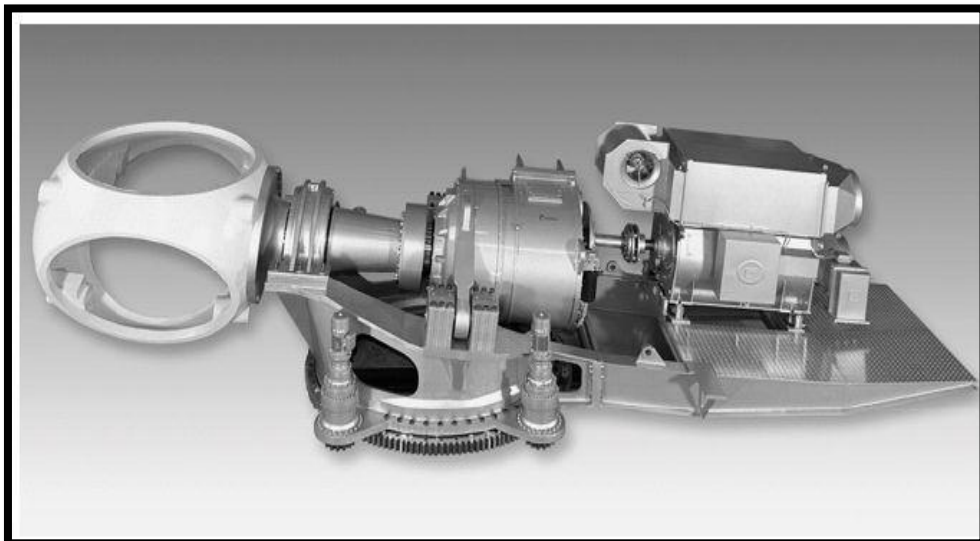


Figure 4.7: Secondary region without removal (4).

There are examples of bedplate designs that have no removal of material near the second region. Figure 4.7, illustrate one example where the second region is kept solid with no material removal due to the reasons explained above.

After topology optimization and introduction of material removal holes, stress analyses have been conducted again to validate the strength of the structure. The analyses did not show any critical regions under the full load conditions. Once the topology main iterations have been completed, the cast part weight has been reduced to around 5000 kg while the structure is kept strong enough to carry the full load combinations.

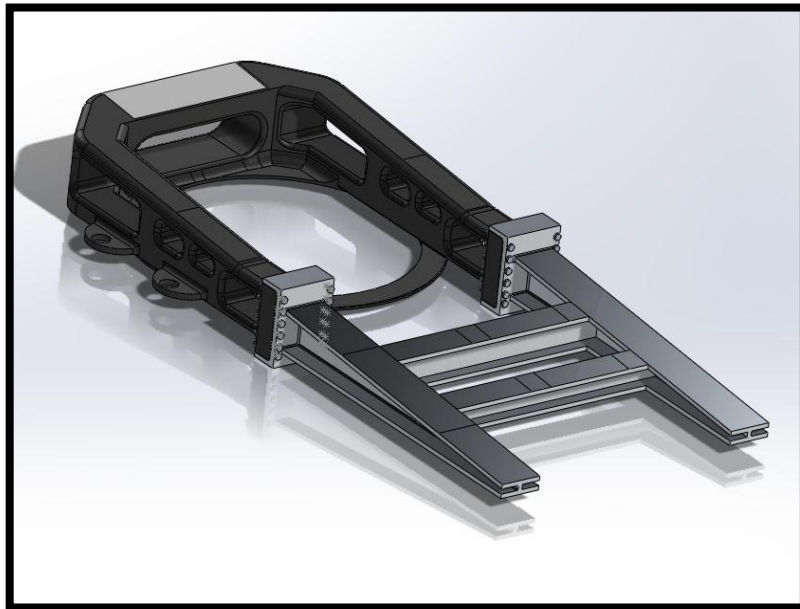


Figure 4.8: Final shape of the bedplate after topology optimization.

At the end of the main optimization stage, 0.28 m^3 of material has been removed while a % 40 removal fraction constraint has been applied to the structure. At the beginning of the optimization, the structure had a volume of 1.1 m^3 . Therefore, only 25.45 % of the material has been removed with a total weight reduction of around 2000 kg. This is a significant weight loss to be obtained. The results clearly show that the guidance by OPTISTRUC solution has been very beneficial.

4.3. SHAPE OPTIMIZATION (Refined Optimization Stage)

After completing the main optimization stage with the aid of the OPTISTRUC solver, supplementary changes have been conducted on the cast part in order to improve the modal behavior, and to increase the bending stiffness of the structure further. Once these additional changes had been completed, another topology optimization was needed. Refinement stage of the topology optimization has been performed using ANSYS software. Before the refinement stage has been applied, the weight of the structure was 5021 kg precisely.

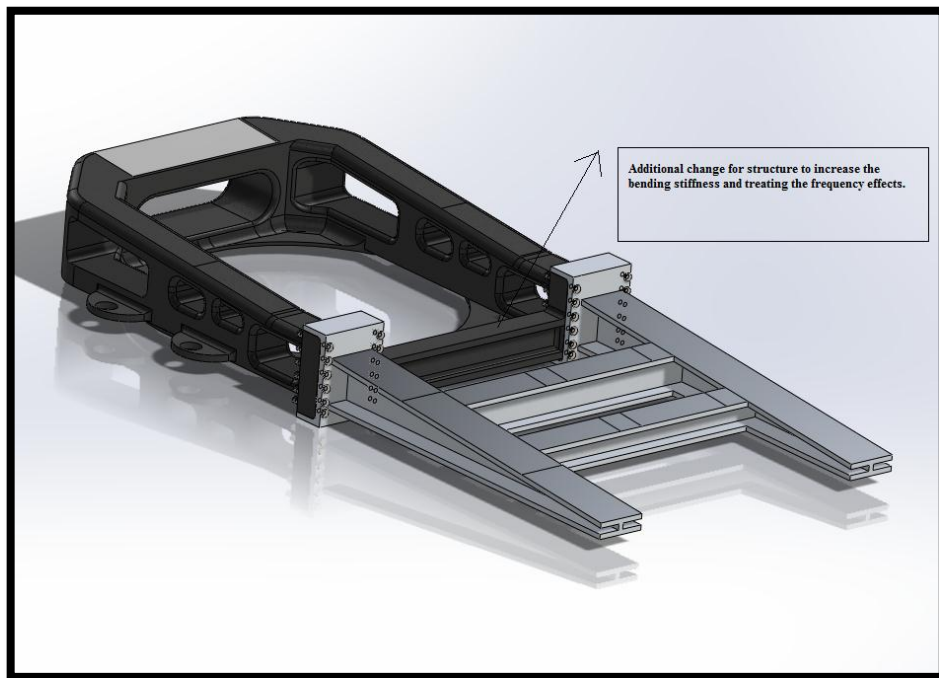


Figure 4.9: Additional material to the casted part.

4.3.1. The Casted Part with Final Shape

As explained above, the refinement stage optimization has been carried out under ANSYS environment. ANSYS has a shape optimization toolbox that is also based on SIMP model. The model has been created with the same load conditions as the OPTISTRUC model. The possible removal regions have been predicted at the locations of added material of the casted part which did not carry any significant stress.

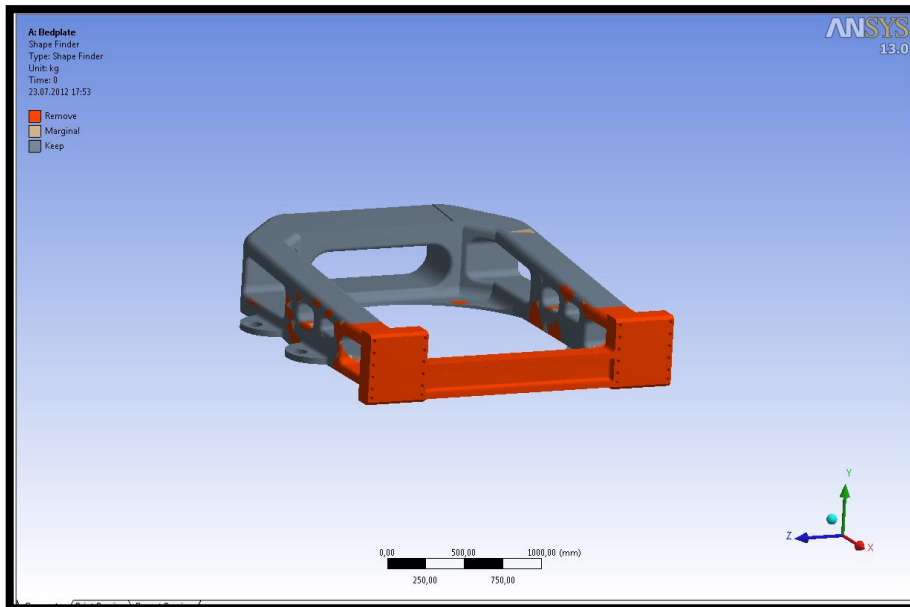


Figure 4.10: Removal suggestions by ANSYS optimization solution.

The ANSYS shape optimization results indicated that the material that has been added to the cast part after previous optimization stage should be completely removed. However, removal of this material is undesired for this design case. First, this area is needed for the assembly of some of the hydraulic and break mechanism. The modal effects should be considered as well. Therefore, instead of complete removal, some material has been removed as an optimization hole to reduce the weight further.

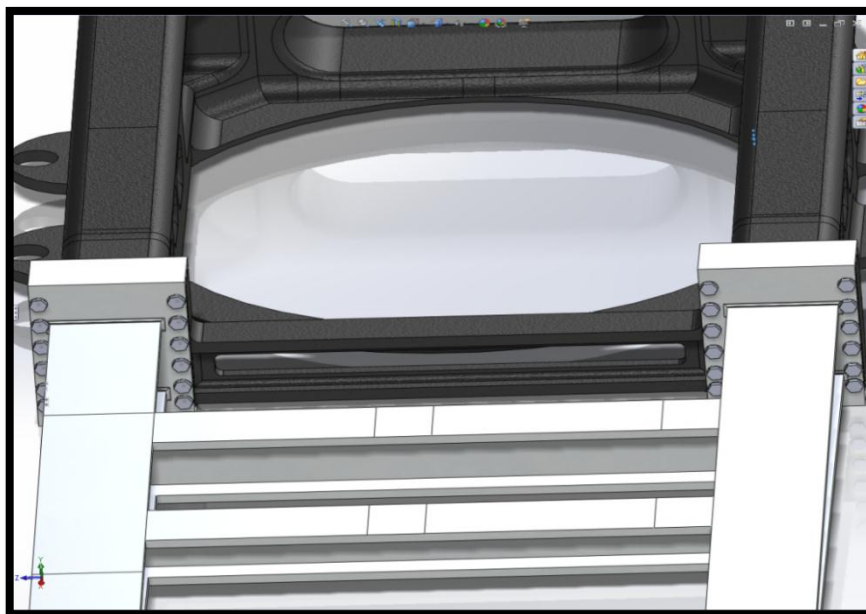


Figure 4.11: Final shape of the bedplate.

After the final shape has been obtained with the refined optimization stage, the total weight of the structure has been reduced to 4960 kg. After the all optimization stages have been completed, another stress analysis has been conducted to check the effects of the refinement optimization stage. As illustrated in Figure 4.12, analysis results have confirmed that stress values are in acceptable range.

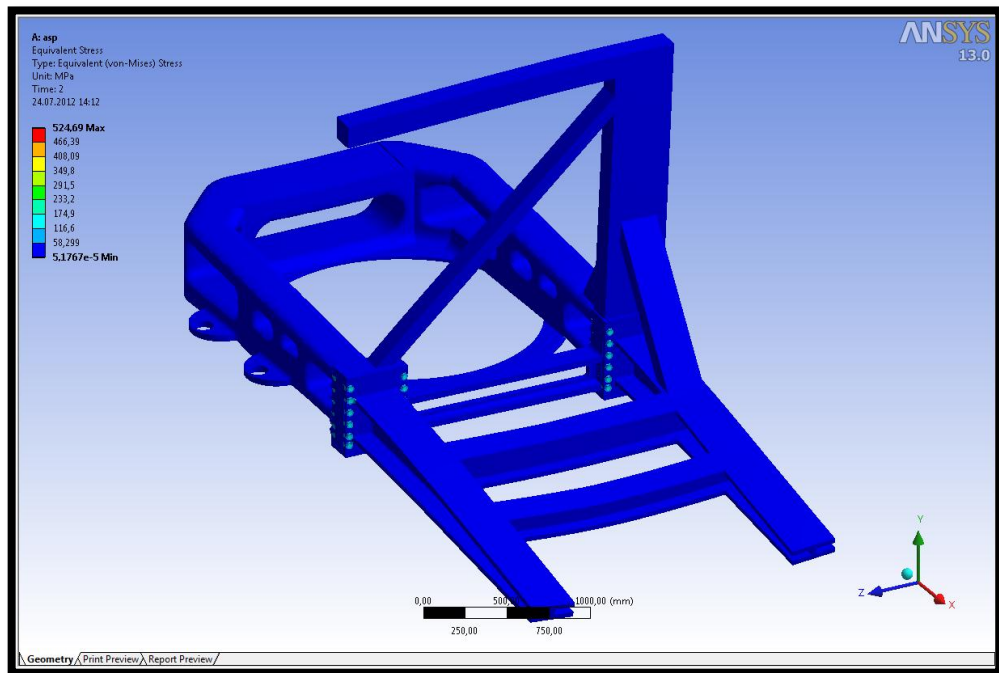


Figure 4.12: Analysis results after the refinement optimization stage.

CHAPTER 5

DETAILED DESIGN AND ANALYSIS OF MAIN LOAD FRAME

Detailed analysis stage of the thesis study is one of the most important parts of the project due to its significance. The design and analyses at this stage represent more realistic design and operational conditions for the bedplate. As mentioned before, unlike other designs, this work involves crane and maintenance loads and analyses. Detailed crane analyses for several working positions have been provided. Apart from the crane analysis, static and dynamic analyses of the bedplate have been supplied. In order to complete the stress analysis, modal analysis and joint analysis including analytical calculations and finite element results have been presented. ANSYS software has been used in order to accomplish the detailed analysis part of the thesis study, since it has more advanced mechanical tools than COMSOL.

5.1. STATIC ANALYSIS

The advanced static analysis portion of the work has been managed with ANSYS because of the strength of the code for nonlinear problems as compared to the other two codes mentioned before. ANSYS has a bolt pretension option that enables solutions for bolts and nuts with frictional contacts. ANSYS can also apply the external forces as a ramp input unlike the SOLIDWORKS simulations. With the aid of such advanced mechanical tools, safety factor calculations and even frictional stress calculations can be safely handled. The detailed model has two different load steps which represent real life conditions for the assembly stage of the bedplate. As in the real case, first the bolts are tightened, and turbine components are assembled while loading is applied proportional with time which resembles a ramp. With the aid of ramp input, convergence problems are also avoided in many run cases. Several contact groups has been formed during the ANSYS analyses. The code also has very functional fatigue tool. All analyses have been conducted with bolted joints with the preloads and external loads in ANSYS.

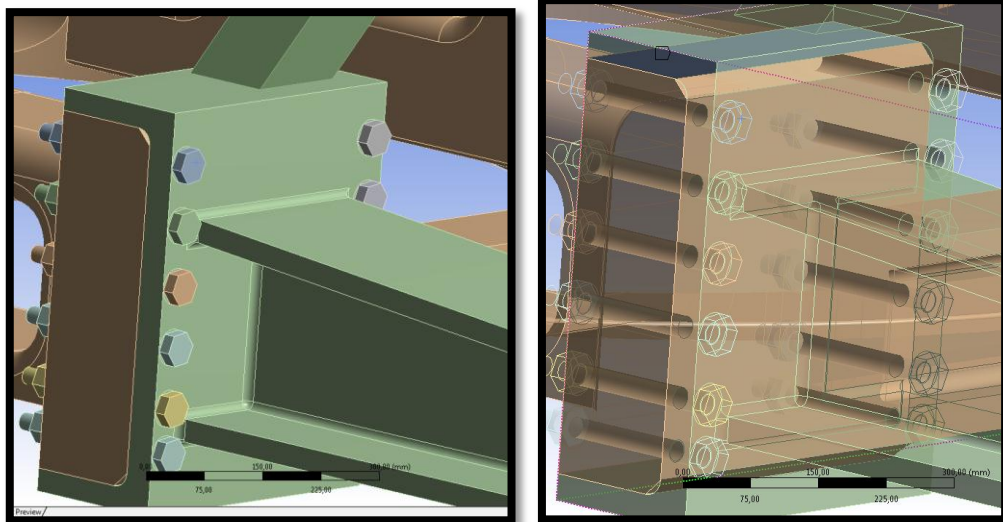


Figure 5. 1: Bolted joints and frictional contacts between the surfaces.

As illustrated in the Figure 5.1, nonlinear contacts have been successfully modeled with ANSYS. In the advanced analysis, 54 frictional contacts have been solved with a friction coefficient of $\mu=0.15$, including bolts heads and nuts and crane to profile joints and so on. Moreover, the model also has six bonded contacts for crane.

Advanced model has fine and smooth transitional 3D tetrahedral mesh including 2.908.496 elements and 645.199 degrees of freedom. System mesh quality is also fine for the analysis.

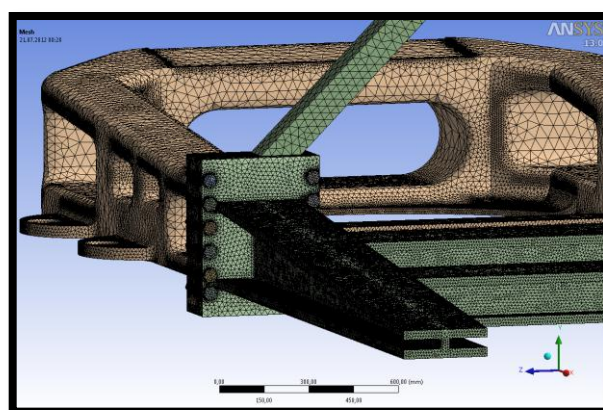


Figure 5. 2: Meshed model of the bedplate.

As previously stated above, ANSYS has an advanced loading option with several numbers of steps in that it is flexible for the users to choose load type and input type like step or ramp. The advanced model has 2 load steps in order to simulate the real life

case with preloads while no external loads are applied. The static loads come into system with ramp inputs just as in the real life assembly.

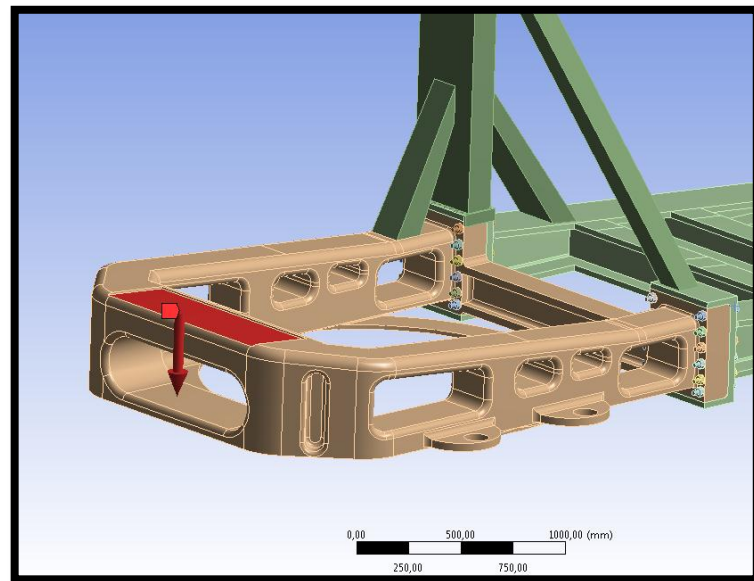


Figure 5. 3: Reaction 1 force illustration with 2 loads steps.

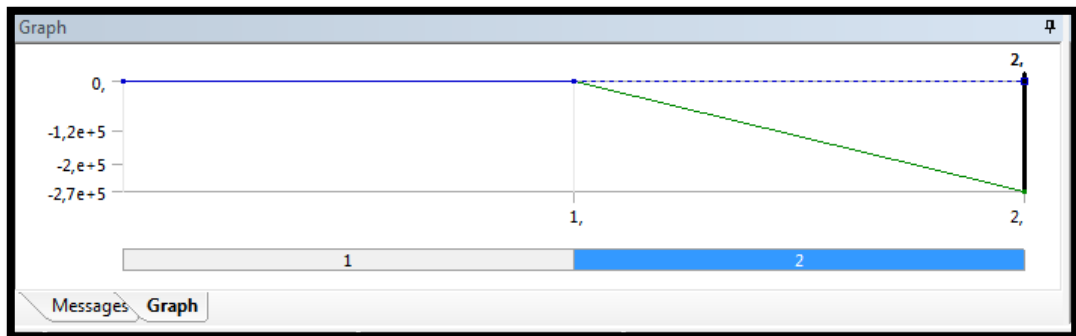


Figure 5. 4:Load steps application in ANSYS.

As can be seen from Figure 5.4, the reaction force 1 calculated previously and applied in 2 steps. Before the bolts are tightened (Step 1) reaction force starts with 0 N. When the preloads are applied, static reaction force starts with a ramp. As illustrated in Figure 5.5 the bolt pretension is applied as 2 opposite forces at the center of the body (bolt) which makes the simulation more realistic.

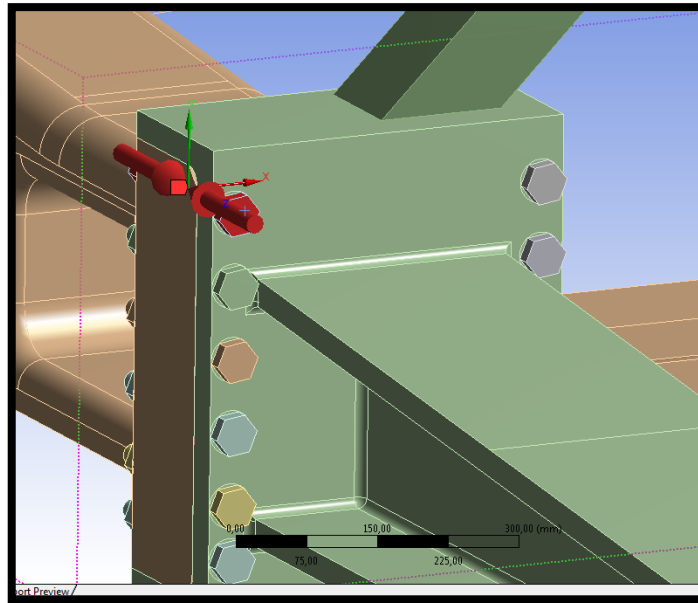


Figure 5. 5: Bolt pretension manifestation.

The code directly assigns a coordinate system at the center of mass for the body, and applies the preloads at the origin of the coordinate system which gives flexibility to the user to apply different load steps like lock or adjust. In this analysis second load step for bolts is locking just as the real life assembly.

Tabular Data				
	Steps	<input checked="" type="checkbox"/> Define By	<input checked="" type="checkbox"/> Preload [N]	<input checked="" type="checkbox"/> Adjustment [mm]
1	1,	Load	1,4805e+005	N/A
2	2,	Lock	N/A	N/A
*				

Figure 5. 6: Load steps for bolts with lock option.

The loads explained below are also applied under ANSYS environment with the pre loads of the bolts. Several iterations have been conducted under ANSYS with different preload calculations which are explained in joint analysis part in this chapter. The final stress, deflection and safety factor values have been calculated.

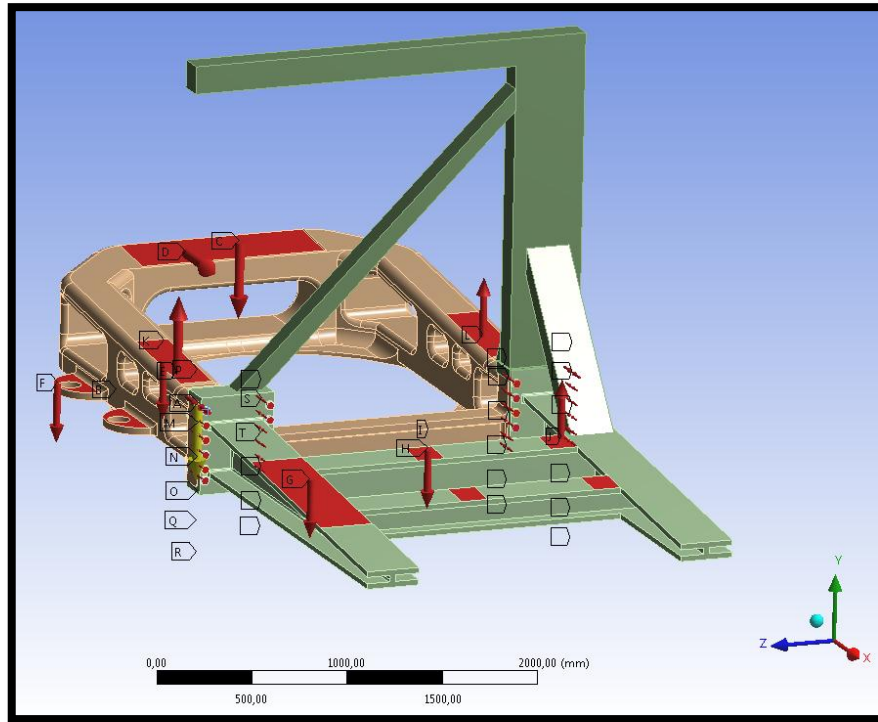


Figure 5. 7: Full static loading illustration under ANSYS.

5.1.1. Boundary conditions for detailed analysis

Boundary conditions for the detailed analysis are important to get reliable results. As defined in the earlier, boundary conditions have evolved with the stages of the design. In this chapter, applied boundary conditions final boundary conditions with the latest design have been discussed. Force values for static loads and crane analysis are the latest obtained in the project.

As explained in the Chapter 3, the load frame is fixed at the surface below the yaw bearing where it is attached to the tower. Some forces did change substantially during the progress of the project. As has been mentioned above, detailed analysis has frictional contacts and bolt preload details. The final system full load values are shown in Figure 5.7.

Table 5. 1: Boundary conditions for detailed analysis.

R1 (reaction at main bearing)	-260000N
R2 (reaction at gear supports)	60000N

Wind	110000N
Generator (Gravity Load)	50000N
Power Electronics	3000N
Yaw Motors	28000N(Total weight)
Crane	40000N
Load frame (Gravity Load)	50000N
Preload	148050N
Generator Torque	7296N
Gearbox Torque	13856N

As explained in the table 5.1, reaction forces are updated with the latest component forces. The calculation method is the same as previous as discussed in Chapter 3. The static analyses have been performed under full load conditions shown in the table. As will be explained in the coming dynamic analysis section, wind and generator torque forces are dependent loads and behave as cyclic forces which will be discussed in the following sections.

Some of the analyses have been conducted without the crane geometry that can be considered as preliminary analyses. Crane design task group has conveyed that weight of the winch will be at most 4000 kg. Therefore, the analyses have been performed with this value. The location of load application is also important. At the first design iteration, 4000 kg load has been placed at one location which is not correct with the three point crane support configuration. Therefore, a representative winch model and the full assembly has been analyzed again. A representative crane material has been selected for 4000 kg weight.

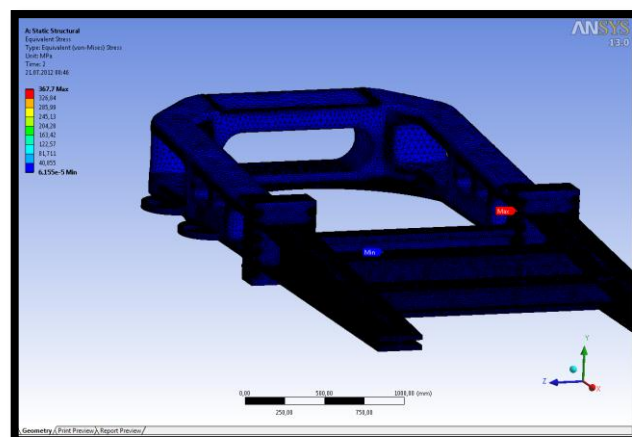


Figure 5. 8: First iteration without crane loads.

This iteration did not contain any crane load and the preloads were higher than the regular preloads. The bolt class was 12.9 here and 8.8 at the final analysis therefore preloads were different. The stress value after the analysis was around 367 MPa on the screw body where the material yield stress was 640 MPa thus the safety factor was around 1.9.

5.1.2. Static analysis results

The static analyses have been conducted with the latest boundary conditions under ANSYS workbench environment. The system has a representative three point supported crane mounted on the bedplate. The full load combination has been applied including wind and dependent working loads. The system has 8.8 class bolts and 70% preload tightening so the calculated force for bolt preload is 148050 N. The maximum stress always occurred on the bolts with high preloads.

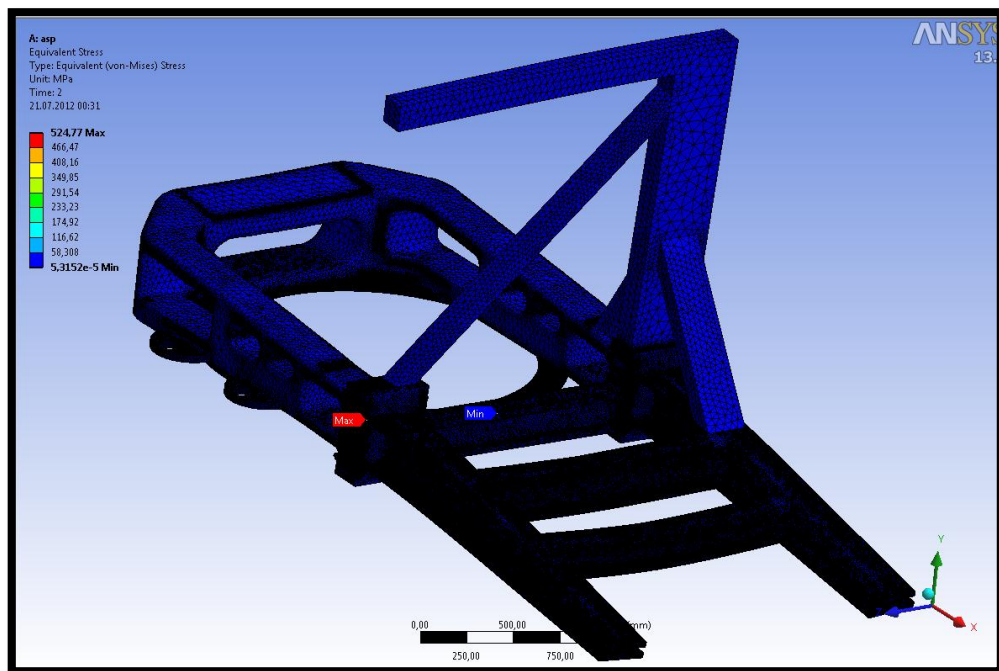


Figure 5. 9: Final design analysis results.

As shown in the Figure 5.9, stress values under realistic full load combination with the load step technique mentioned above is around 525 MPa on the bolts. The bolts are 8.8 class bolts. Under these conditions, static safety factor can be calculated with the formula given below.

$$n(\text{static}) = \frac{\sigma(\text{yield})}{\sigma(\text{max})} \quad (5.1)$$

Therefore the static safety factor for the bolts was around 1,221. Bolt material can be changed or preload can be reduced to increase safety factor on bolts.

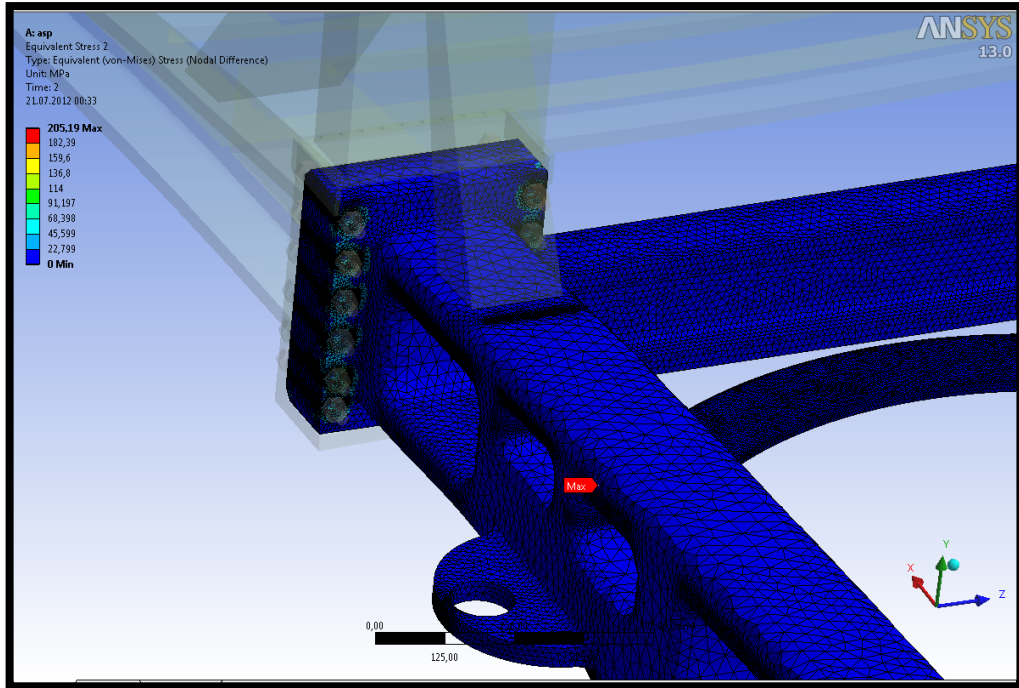


Figure 5. 10: Static stress values for casted part of the bedplate.

For the cast frame, the maximum stress value is around 205 MPa due to the finite element discontinuity problem which will be discussed at 5.4. Around the bolts nuts maximum stress under frictional contact was around 65 MPa. Even though the discontinuity occurred at one specific region, in the simulations the static safety factor is still sufficient for all related applications.

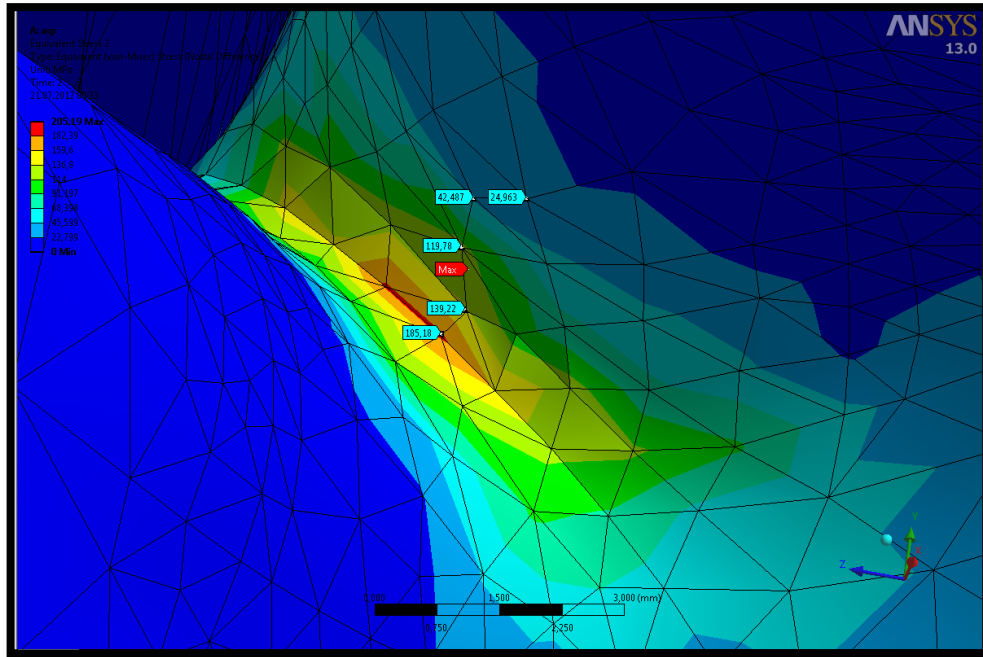


Figure 5. 11: Discontinuity region under the main frame.

Although a fine mesh has been applied, discontinuity problem has occurred where sharp edge of the yaw ring meets the frame base. Due to limitations of the software, fillet radius remained very sharp. However, in the actual cast operation, a more generous fillet radius and much less stress levels are expected. Part of this chapter explains the discontinuity problem in detailed. As shown in Figure 5.11, the maximum stress is 190 MPa at the sharp edge. However, just 3 nodes away stress drops to 42 MPa which clearly shows the discontinuity. In such cases, 2 nodes before the maximum value is generally considered as the actual. Therefore, 119 MPa is considered for a real value for the maximum stress. As also described in the formula given below, the static safety factor is around 2.1, which indicates that the design is safe even for the case that includes worst case crane loads.

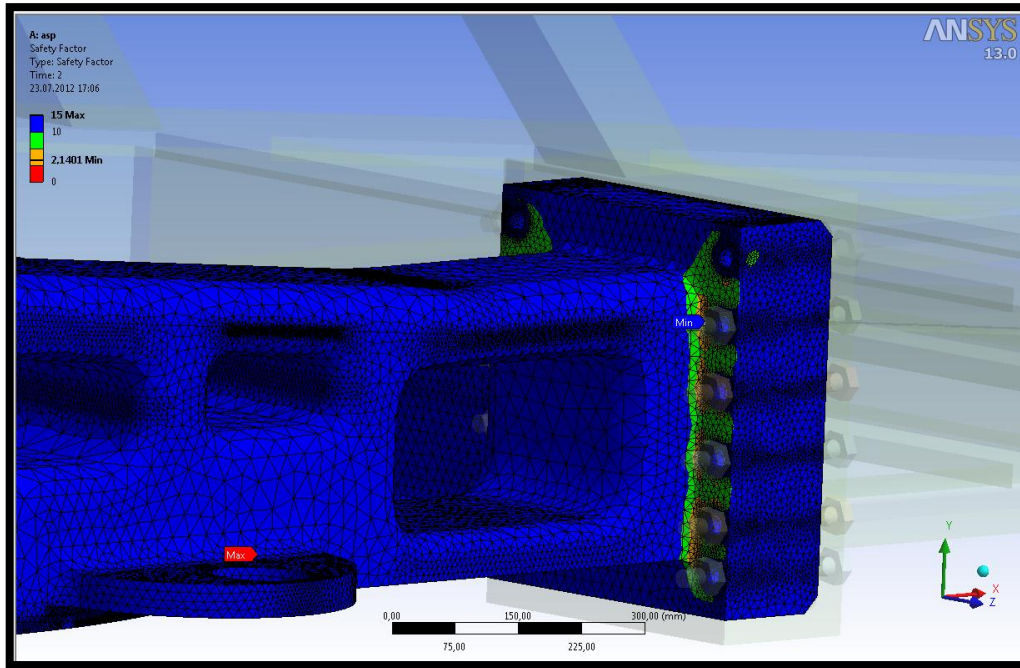


Figure 5. 12: Safety factor calculations with ANSYS.

As shown in Figure 5.12, the minimum safety factor on the casted part is 2.14, and over all structure safety factors are around 15 that mean the design is safe under all working conditions.

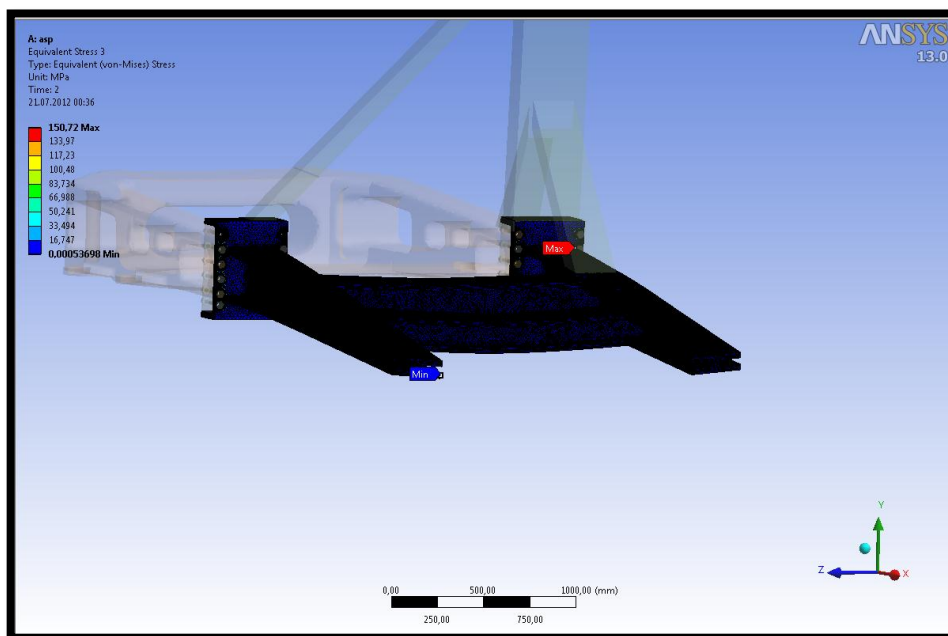


Figure 5. 13: Profile part stress values.

As part of the static analyses, stress values for the welded profile part that is also called generator support have been also calculated. Profile part has relatively high yield stress value and less amount of loading compared to cast part. The static stress level for

the profile part has been calculated as 150.72 MPa under the full load combination. The system is well designed and has a high safety factor around 2.12.

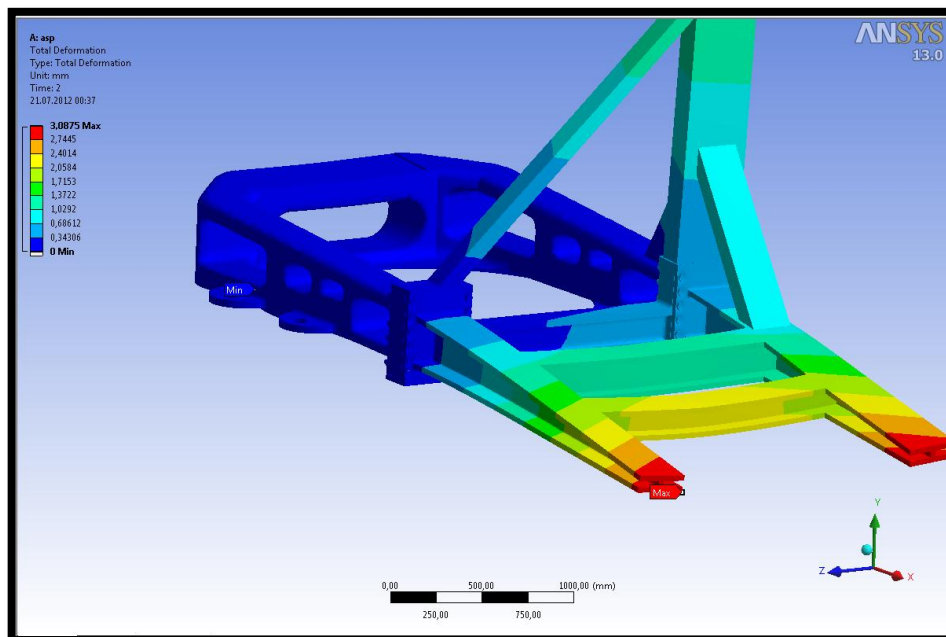


Figure 5. 14: Total deformation values under full static loading case.

As shown in the Figure 5.14, the deflection value under full static loading is around 3 mm. Even though, frictional contacts and nonlinear effects of materials like nonlinear elongations have been considered, system does not deflect much which is desired. Finally, frictional and shear stresses on the system have been studied to ensure the design safety.

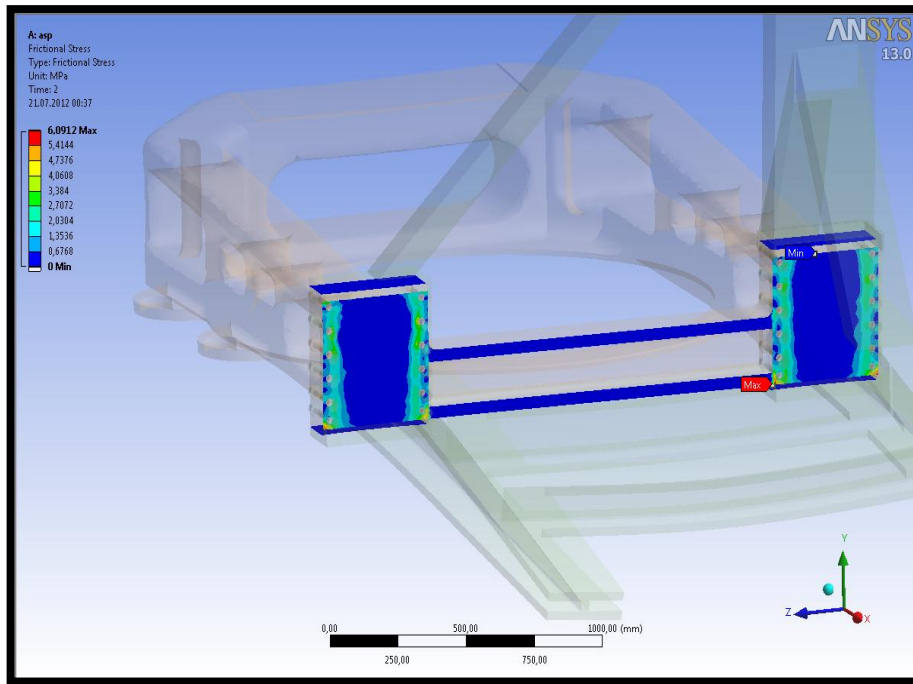


Figure 5. 15: Frictional stresses on the contact surfaces.

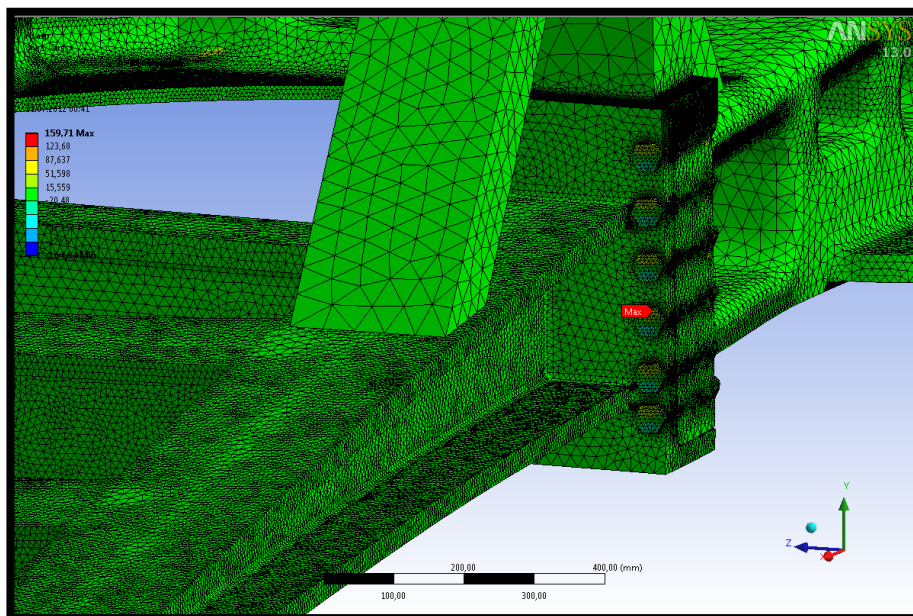


Figure 5. 16: Shear stress values for bolts safety.

As shown in Figures 5.15 and 5.16, contact frictional stresses and shear stresses on the system have been checked, and confirmed that they do not pose any risk for the system with the values around 6 and 150 MPa respectively.

Overall, ANSYS and COMSOL have been used frequently during the analyses through the design iterations. Direct sparse and MUMPS solver have been used throughout the process. The results indicate that the final design of the bedplate is strong and safe to carry the full load combination. The static safety factors for all bodies are high and acceptable for engineering purposes. Moreover, deflection values of the system are also acceptable.

5.1.3. Crane and maintenance loads analysis

Crane and maintenance loads analysis for the main load frame of 500kW wind turbine have been studied as part of this thesis study. Several iterations have been conducted to obtain the safety margins and stress values of the bedplate. Crane loads may increase the operational stress values on the bedplate, and analysis of the frame with the crane has to be completed. Positioning of the crane is significant in analysis. The possible worst case analysis should be considered for safety issues. Therefore, three point supported crane load analyses have been conducted using ANSYS for different maintenance load combinations. Boundary conditions are the same as those explained in Table 5.1 except the turbine working loads like wind and torque values. This is because while maintaining the turbine, no wind forces are assumed. Another difference is that, heaviest component on the turbine is applied to the far end of the crane arm. Therefore possible worst case conditions have been analyzed.

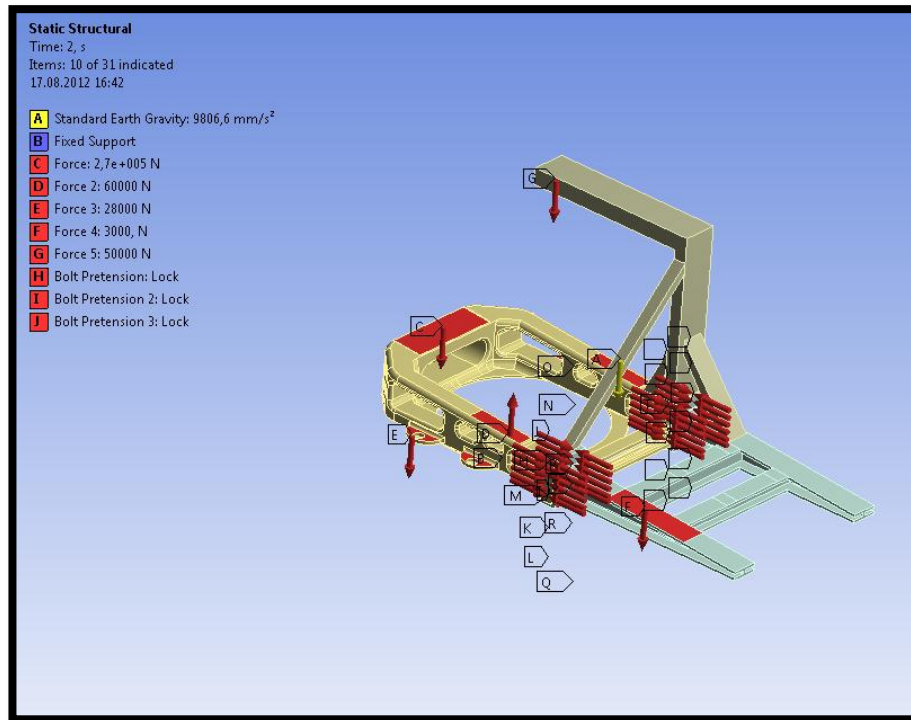


Figure 5. 17: Crane analysis load illustration.

As shown in the Figure 5.17, crane analysis load cases have been studied without wind and generator torque loads. It is also assumed that full weight of the generator is attached to the end of crane arm. This crane configuration is not yet finalized. Several analysis iterations have been performed with different configurations, however three point supported configuration has been decided for the project.

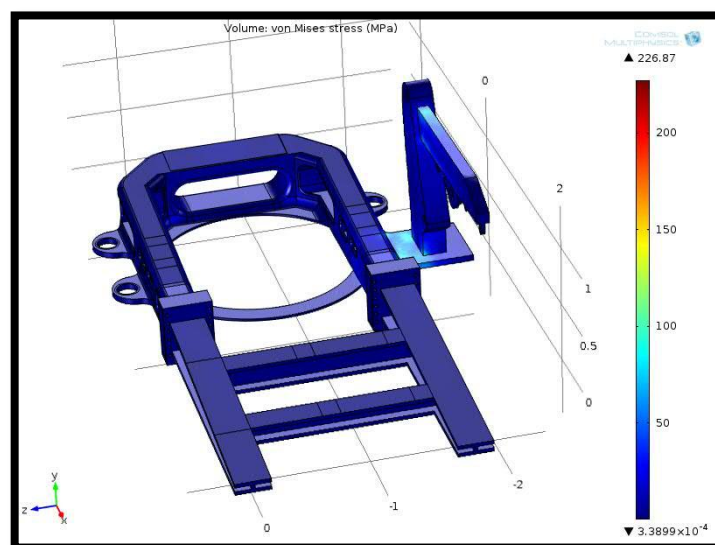


Figure 5. 18: A trial design for crane attachment to bedplate.

Figure 5.18 illustrates one of the configurations evaluated. This configuration has been discarded due to the very high stress around 227 MPa where the yield of the casted part is 250 MPa. Design constraints for crane support have altered after the analysis results. Three different support points for crane have been studied, and several iterations for the three point support configurations have been performed.

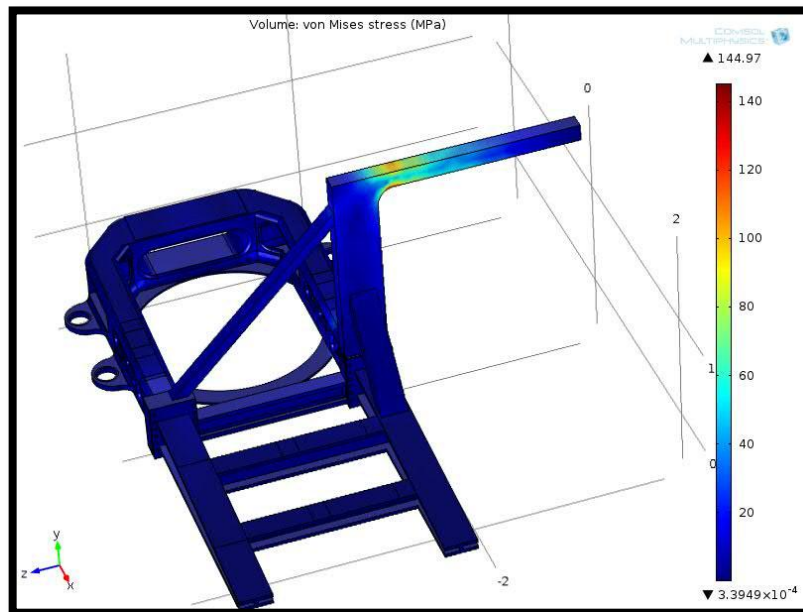


Figure 5. 19: Three point supported crane configuration (Orientation 1).

As illustrated in Figure 5.19, three point supported crane under maintenance loading proves better than the previous crane configuration in Figure 5.18. The maximum static stress value for the case was around 145 MPa. The safety factor for the case was 1.8. This orientation has been studied to see the effects on the support point located on the left side of the bedplate. In order to evaluate the worst possible stress combinations, several analyses for different orientations of the crane have been considered.

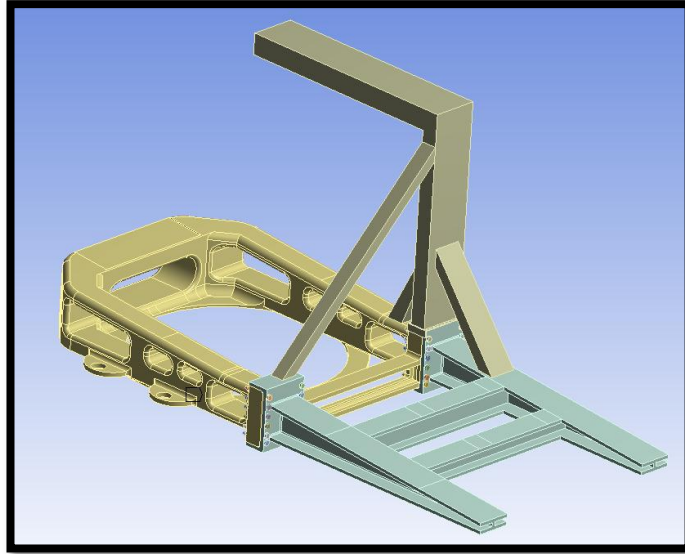


Figure 5. 20: Crane orientation 2.

As shown in the Figure 5.20, analysis for the orientation 2 is needed to examine the stress effects on the support points located on the right half of the bedplate. The stress concentration occurs on the crane arm because of the heaviest component is attached at the end of crane arm which creates large amount of bending moment.

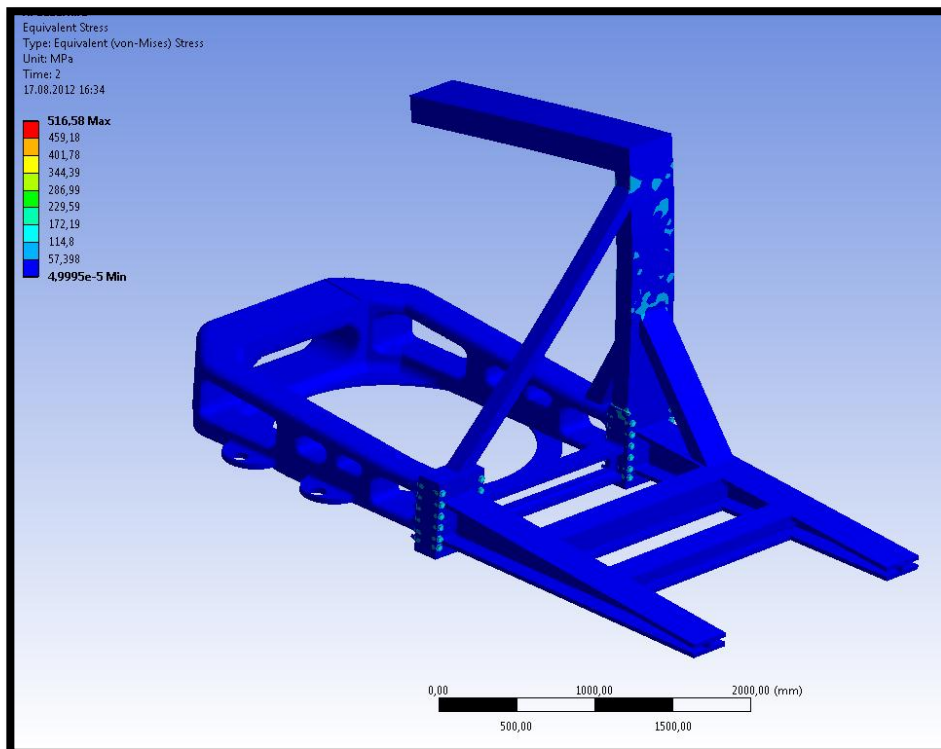


Figure 5. 21: Stress results for crane orientation 2.

As illustrated in figure 5.21, maximum stress values for the crane orientation 2 are concentrated on the simulated crane itself, and do not have sizable impact on the bedplate. Finally, crane orientation for the longest distance from the center of the yaw ring has been considered which could lead to excessive bending moments and stresses.

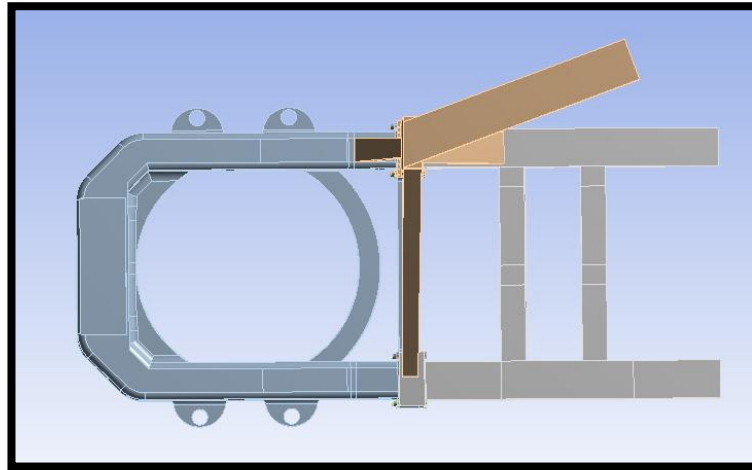


Figure 5. 22: Crane orientation 3.

In the configuration illustrated in Figure 5.22, load is applied at the longest distance effect from the center point of the yaw ring. In orientation 3, the heaviest load is applied as a boundary condition at the end of the crane arm to see the stress levels. As shown in the figure 5.23, analysis results indicated safe orientation of the crane arm under any maintenance load condition.

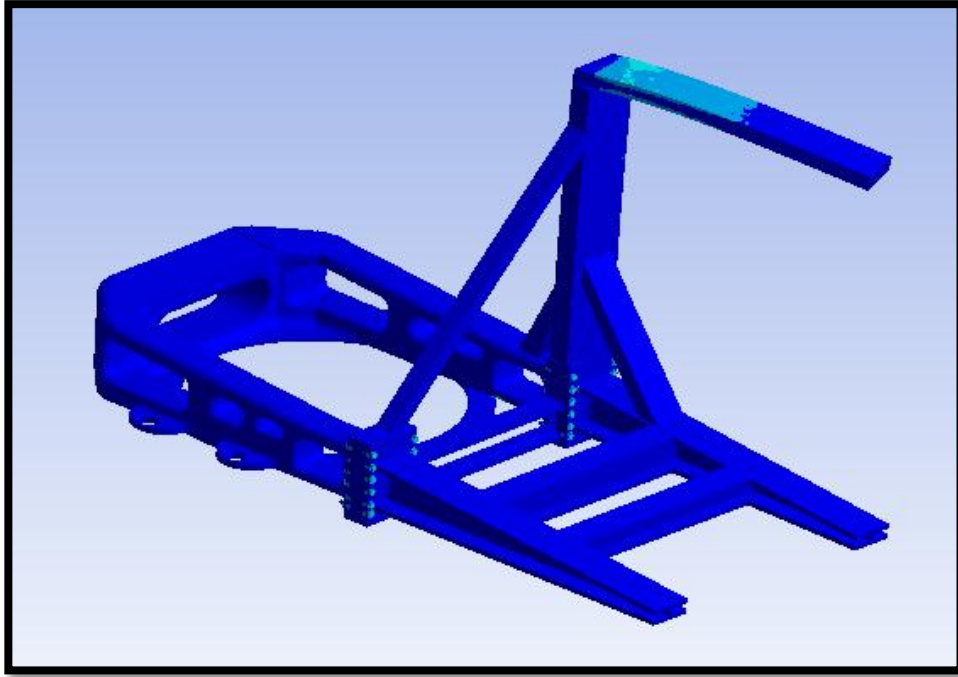


Figure 5. 23: Stress locations for crane orientation 3.

5.2. HIGH CYCLE FATIGUE ANALYSIS OF THE BEDPLATE

Completing the static analysis and ensuring adequate safety factors for the bedplate, dynamical analyses have been conducted for the components of the bedplate to ensure infinite fatigue life under dynamic loads. Turbine is exposed to dynamical loads due to wind loads. When the wind load increases, turbine starts operating and generator starts producing torque. Dynamic loads on the nacelle are transferred as generator force couple and gear box frictional torque which are dependent on the wind power profile.

The bedplate fatigue analysis has been based on high cycle fatigue theory. The bedplate has to have infinite cyclic life. It should have sufficient strength to carry the stress cycles due to wind power cycles and generator torques and so on. The bedplate should have relatively high dynamic safety factor and should be robust for stress concentrations.

There are three fatigue approaches and they are all used commonly. Stress–life, Strain-life and linear elastic fracture mechanics models are known for fatigue analyses.

Among the three models, Stress-life method has been used for fatigue analyses of the bedplate. In high-cycle fatigue (HCF) applications the component is expected to last for more than 10^3 cycles of stress. It works best when the load amplitudes are predictable and consistent over the life of the part. Stress-life method is a stress-based model, which seeks to determine fatigue strength, and endurance limit for the material so that the cyclic stresses can be kept below the endurance stress to achieve infinite number of cycles (14).

5.2.1. Strategy for the problem

Dynamical loads depend on the wind power, and should be modeled carefully. The nature of the wind turbine operation creates zero based cyclic stress, because it makes peaks starting from 0 to maximum wind force which causes maximum torque and force couples. There are fatigue analysis modules in most finite element codes. ANSYS and SOLIDWORKS Simulation toolbox have fatigue tools in which they treat all loads as dynamic. For the bedplate analysis purposes, most of the loads are static and gravity loads.

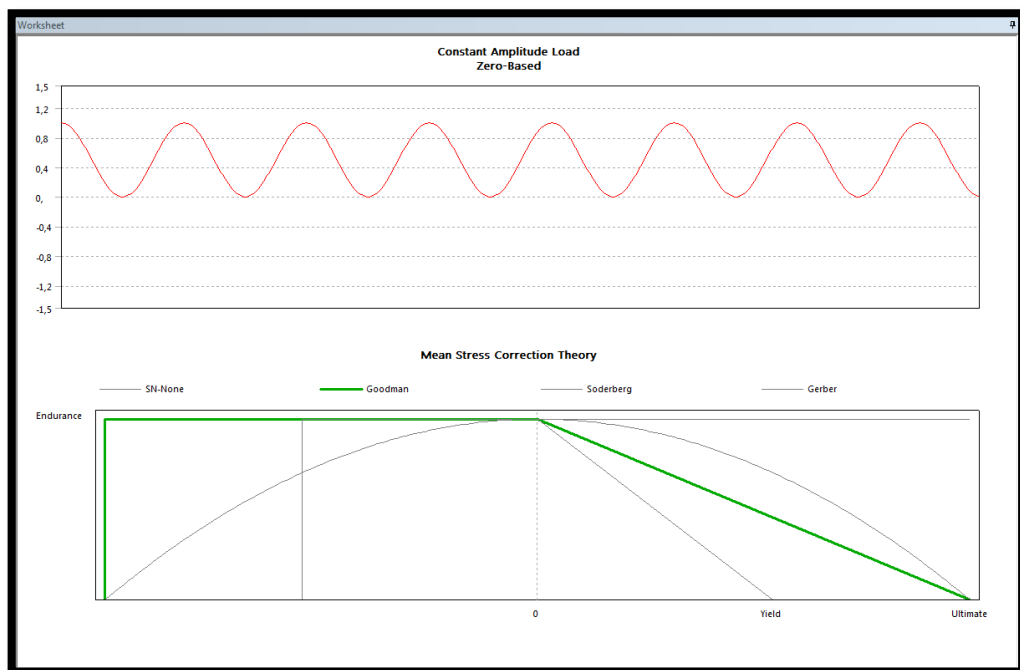


Figure 5. 24: ANSYS fatigue layout.

As shown in the Figure 5.24, fatigue model is satisfactory in which the code allows the selection of the stress ratio for the fatigue analysis, and the fatigue theory

which includes Goodman, Gerber and Sooderberg cycling theorems. The only drawback for these codes is that they assume all loads applied to the system as cyclic, which is not the case for the bedplate. In real life, the load from the component weights does not oscillate.

After applying full static loads including the axial wind load and generator force couple, at the first iteration ANSYS provided the high stress regions for both cast and profile parts. Another static analysis has been applied with only gravity loads on the turbine components to calculate the minimum stress values at highly loaded sections. After completing analyses, modified Goodman criteria formulation has been applied to conclude the fatigue life of the system. From the static cases, critical regions for the system were known which occurred on the cast part. However, fatigue analyses have been performed for both cast and profile parts.

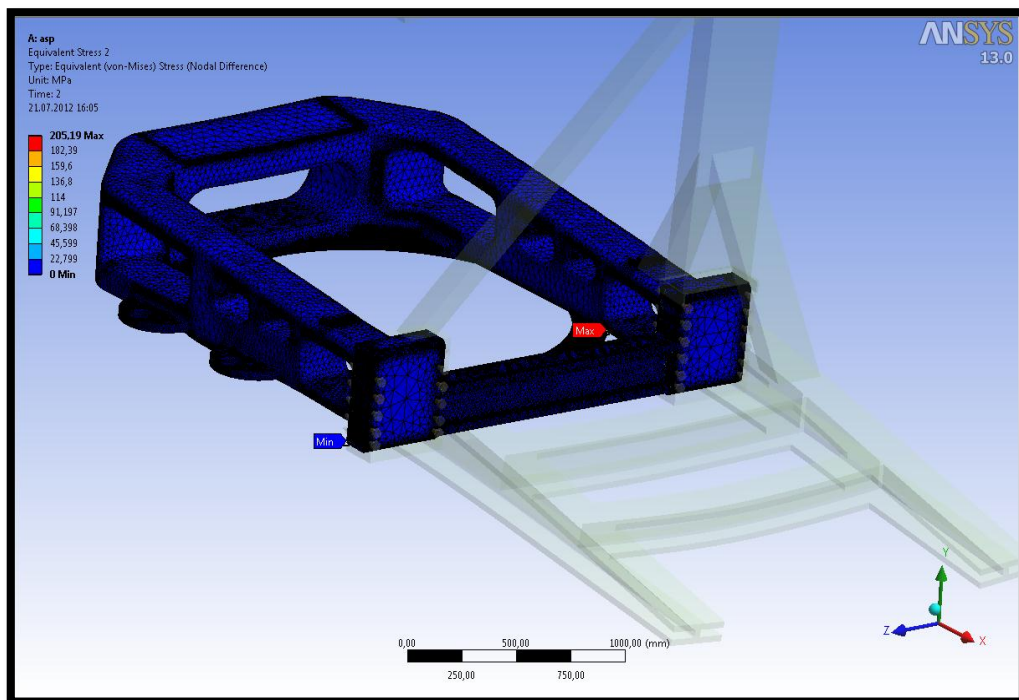


Figure 5. 25: Static results under full wind load.

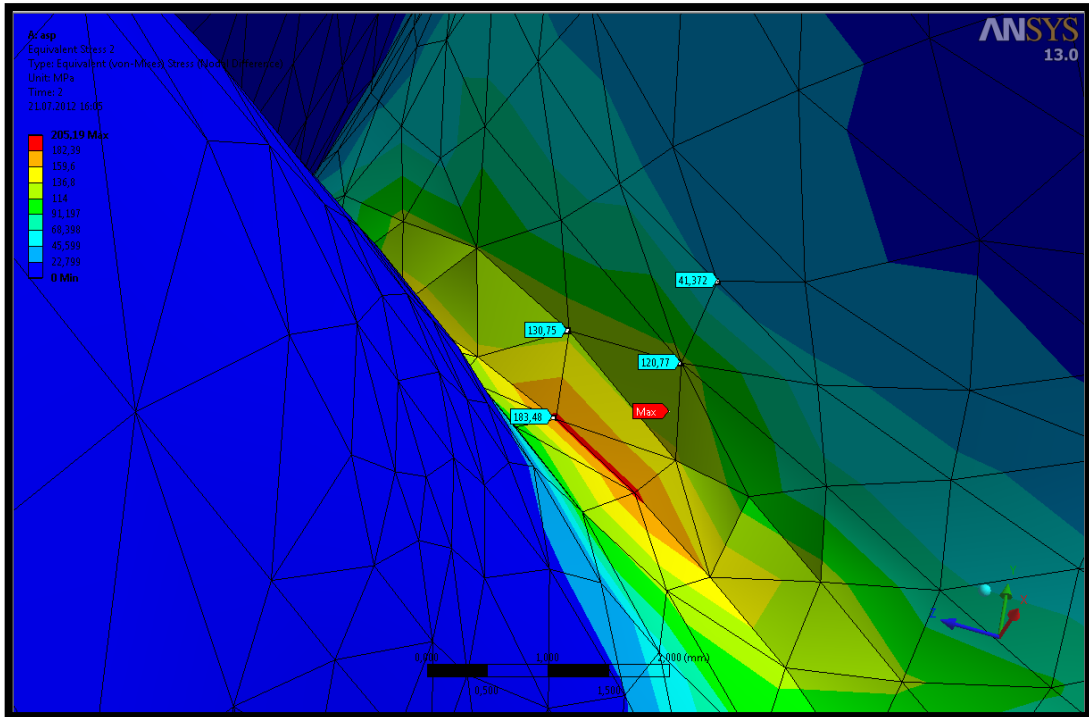


Figure 5. 26: High stress at discontinuity region.

As will be explained in the following chapters, the maximum stress values does not reflect the real results due to discontinuity. Therefore, the stress values at two nodes away have been considered. As shown in the Figure 5.26, the maximum stress value is 120, 77 MPa that is the minimum stress for the fatigue loading case.

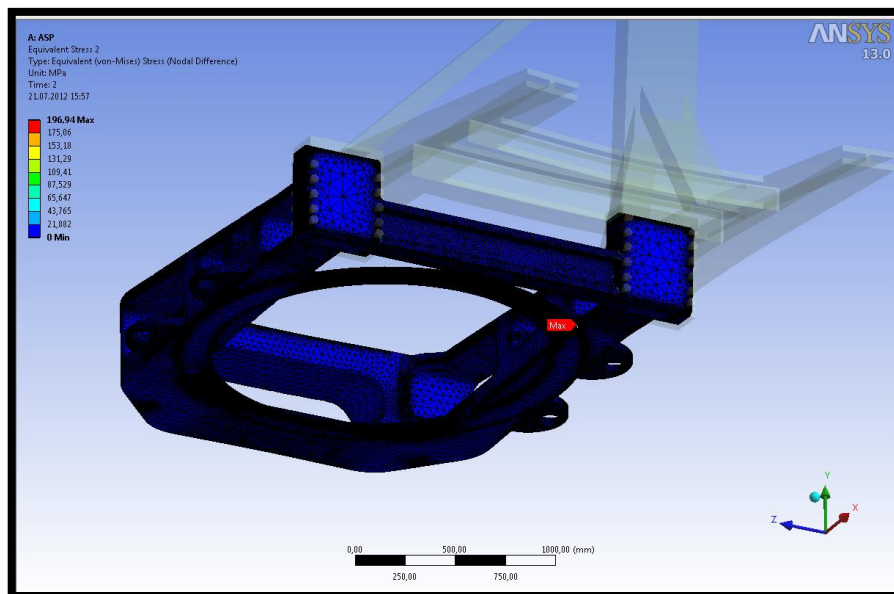


Figure 5. 27: Static value with only gravity loads.

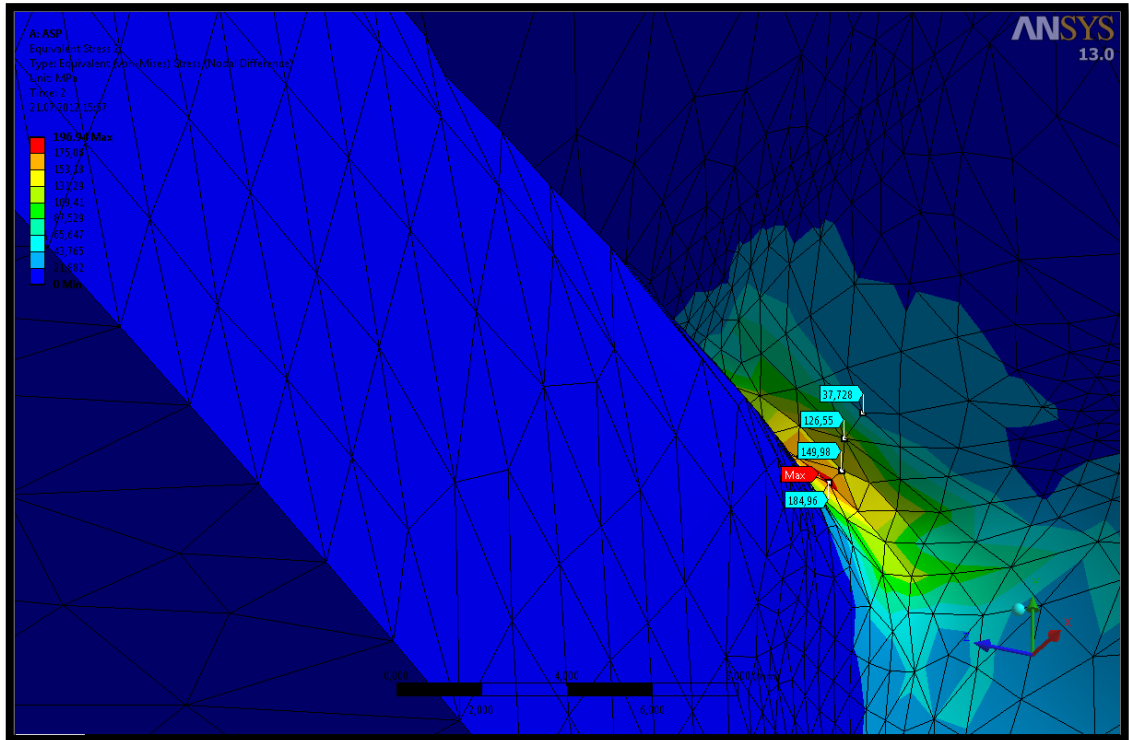


Figure 5. 28: Discontinuity region for fatigue analysis.

As shown in the Figure 5.28; maximum stress under gravity and operational load is 126,55 MPa. Therefore, this bedplate is exposed to stress cycles from 120.77 to 126.55 MPa. After the maximum and minimum cyclic stress values have been calculated, Modified Goodman method has been used to calculate the safety factors for the cast part. The following calculations are needed for modified Goodman formulation.

$$\Delta\sigma = \sigma_{max} - \sigma_{min} \quad (5.2)$$

$$\sigma_m = \frac{\sigma_{max} + \sigma_{min}}{2} \quad (5.3)$$

According to the stress range, alternating stress and mean stress values can be calculated for the modified Goodman criterion which allows calculation of dynamic safety factor. The stress range can be calculated with the aid of the Equation 5.2 as $126.55 - 120.77 = 5.78$ MPa. Alternating stress value can be calculated as 5.78 MPa. Finally, the mean stress value for this case have been calculated with Equation 5.3 as $126.55 + 120.77 / 2 = 123.66$ MPa.

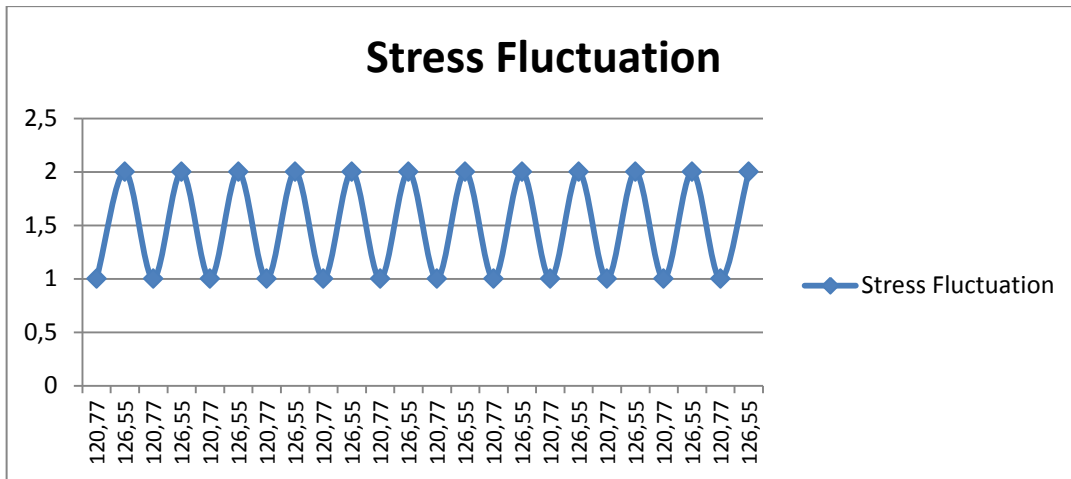


Figure 5. 29: Stress oscillation applied on the cast part.

In addition to the calculations shown above, some material coefficients for EN_GJS_400_18_LT and the cast part are needed to calculate the modified endurance limit for modified Goodman criteria.

$$Se = C_{load} * C_{size} * C_{surf} * C_{temp} * C_{rel} * Se' \quad (5.4)$$

Calculation of modified endurance strength for the cast part is illustrated in Equation 5.4. There are several factors to calculate the endurance of the material. Typically, Se' can be easily estimated as $0.5 * S_{ut}$ for steel based materials. The correction coefficients can be as:

- **Loading Effects:** The stress reduction load factor for the material is taken as $C_{load} = 0.7$ since the loadings are generally axial for the analysis (SHIGLEY & MISCHKE, 2001)
- **Size Effects:** “For length < 8 mm $C_{size} = 1$; For 8mm< length < 250 mm $C_{size} = 1.189 * length^{-0.097}$; For larger sizes than 250 mm. In this case is suitable for this parameter sizing factor is 0.6” (NORTHON, 2006, p. 327)
- **Surface Effects:** “Cast irons can be assigned as $C_{surf} = 1$ since their internal discontinuities dwarf the effects of a rough surface” (NORTHON, 2006, p. 328)
- **Temperature Effects:** “ $C_{temp} = 1$ for $T < 450^{\circ} C$ ” (NORTHON, 2006, p. 331). (THOMAS, 2010)
- **Reliability Effects:** “ $C_{rel} = 0.659$ for % 99.999 reliability” (NORTHON, 2006, p. 331).

Once the correction factors are identified, the modified endurance limit can be calculated with the aid of Equation 5.4. Se' is known from the previous information

given as $Se' = 0.5 S_{ut}$ which is 200 MPa. Therefore, the modified endurance limit of the EN-GJS-400-18 frame is calculated as 55.356 MPa.

$$\frac{\sigma_a}{S_e} + \frac{\sigma_m}{S_{ut}} = \frac{1}{n} \quad (5.5)$$

The formula of the modified Goodman criteria consists of alternating stress, mean stress, endurance limit of the material and ultimate strength of the material. By the aid of this formulation, dynamic safety factor for cast part can be calculated which is given as 'n' in the following formulation:

$$\frac{5.78}{55.336} + \frac{123.66}{400} = \frac{1}{n}$$

The dynamic safety factor has been calculated as 2.42 which is safe for a standard 500 kilowatt wind turbine.

Similar design approach has been applied to the profile part of the nacelle. This methodology is convenient for standard fatigue calculations.

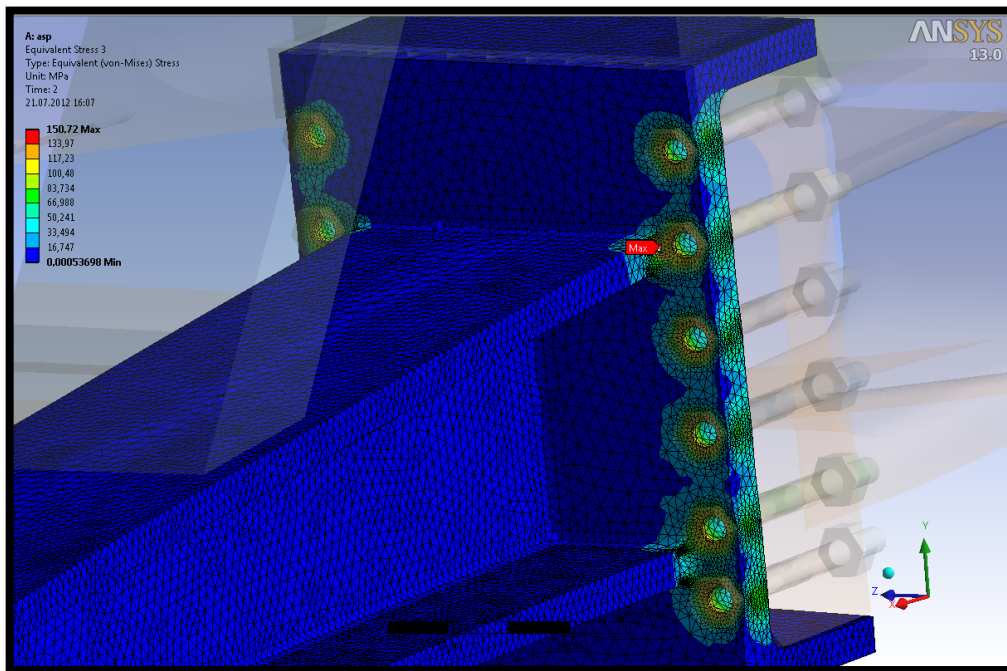


Figure 5. 30: Profile part under dynamic wind loads.

As illustrated in the Figure 5.30, analyses have indicated that the maximum stresses occurred around the frictional contact regions between the head of the bolt and the profile part surface. The maximum stress value is around 150.72 MPa.

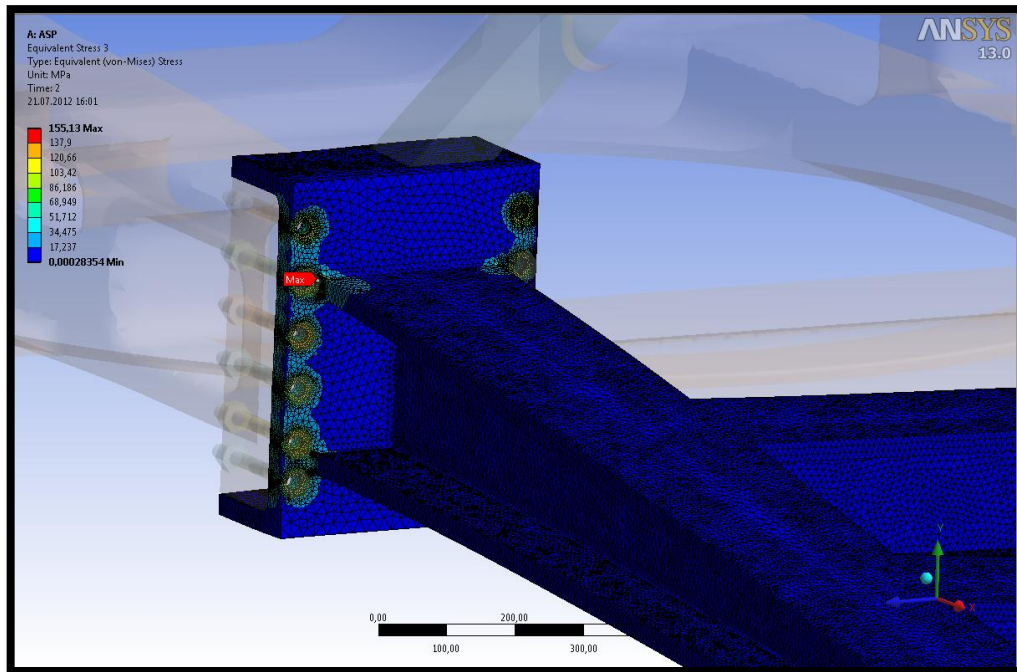


Figure 5. 31: Analysis results for the fatigue life calculations.

Similar approach has been applied to I shaped profile part of the bedplate. The maximum stress value has been calculated to be around 155.14 MPa. The stress fluctuates between 150.72 to 155.14 MPa for the profile part. The modified Goodman criteria can also be applied to this part. Oscillatory stress has been calculated as 4.42 MPa and the mean stress as 152.93 MPa.

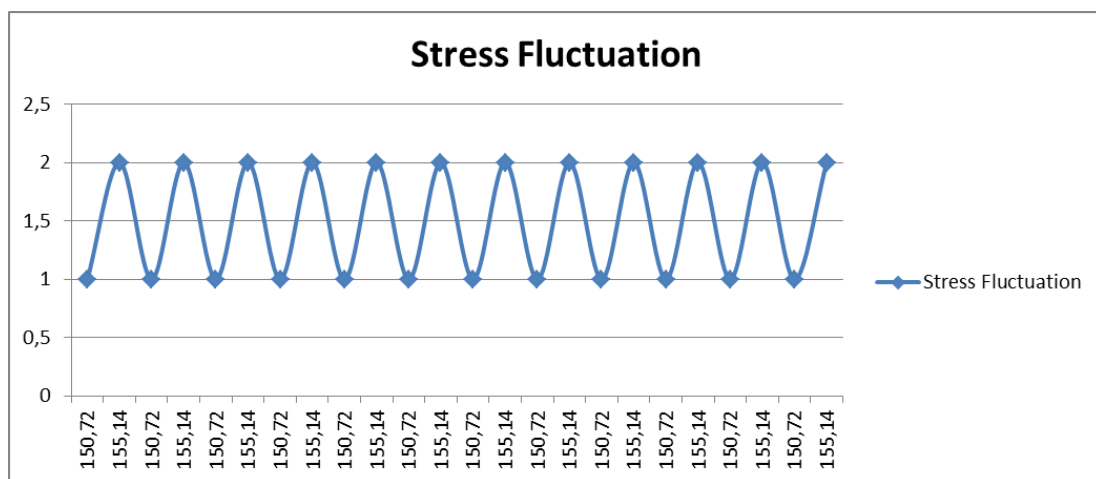


Figure 5. 32: Stress oscillations for the profile part.

The modified endurance strength for this part is different, even though the reduction factors are the same. The modified endurance strength for this part is 44.28

MPa while the endurance limit is 160 MPa. Therefore dynamic safety factor can be calculated with the modified Goodman criteria as follows:

$$\frac{4.42}{44.28} + \frac{152.93}{360} = \frac{1}{n}$$

The dynamic safety factor has been calculated from this equation as 1.9 which is also safe for a standard 500 kilowatt wind turbine with external crane loading.

5.2.2. S-N Curve and number of cycles

As has been mentioned above, dynamic safety factor values have been calculated using the modified Goodman criteria. Another important aspect for the fatigue analysis is the S-N curve of the material. There should be more than 10^6 cycles lives for both bodies for infinite life of the turbine. S-N curve for cast part is available as illustrated in Figure 5.33.

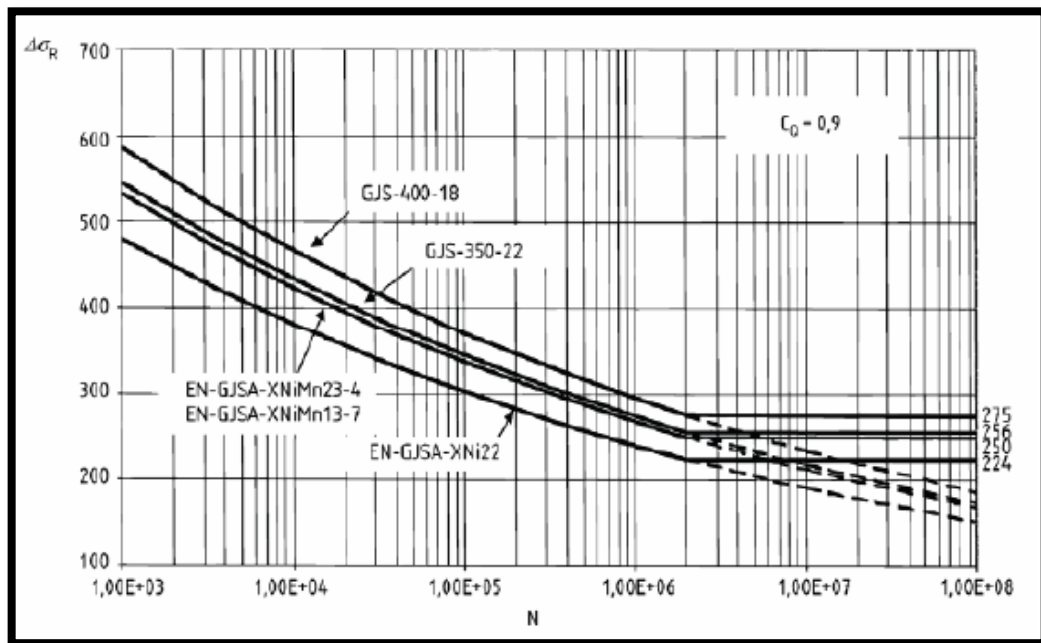


Figure 5. 33: S-N curve example for casted material (16).

For the loading case mentioned above, the alternating stress for the casted part has been calculated as 4.44 MPa which clearly shows that the material has infinite life.

5.3. Mesh Refinement and Convergence Issues

In numerical analysis methods, convergence is an important concept and has to be checked. Finite element method is a strong method for solution of complex physical problems using numerical solution methods like LU decomposition, central difference derivative and Newton-Raphson method. In finite element method, the mathematical model is based on meshed structure, and the differential equations are solved node by node. Therefore multi loaded complex 3D structures have to be solved numerically. Mesh refinement is important in order to see converged values of stress and deflection for a structure. Several iterations have been conducted using ANSYS to see the differences between incremental mesh adjustments, and convergence values have been obtained.

Initial mesh and DOF values were 48913 and 15230 respectively, and the stress value was 451 MPa which has considerable error when compared to actual value of 524.77 MPa for the bolt. Therefore, incremental mesh tuning is required to ensure analyses with the least numerical error.

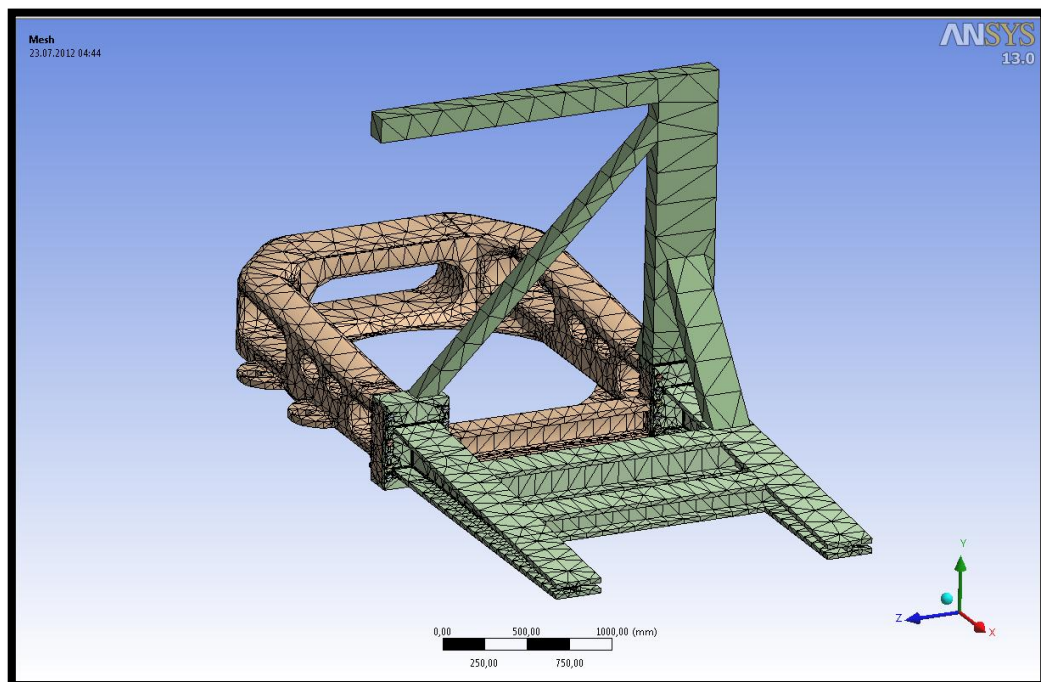


Figure 5. 34: Coarse meshed structural analysis.

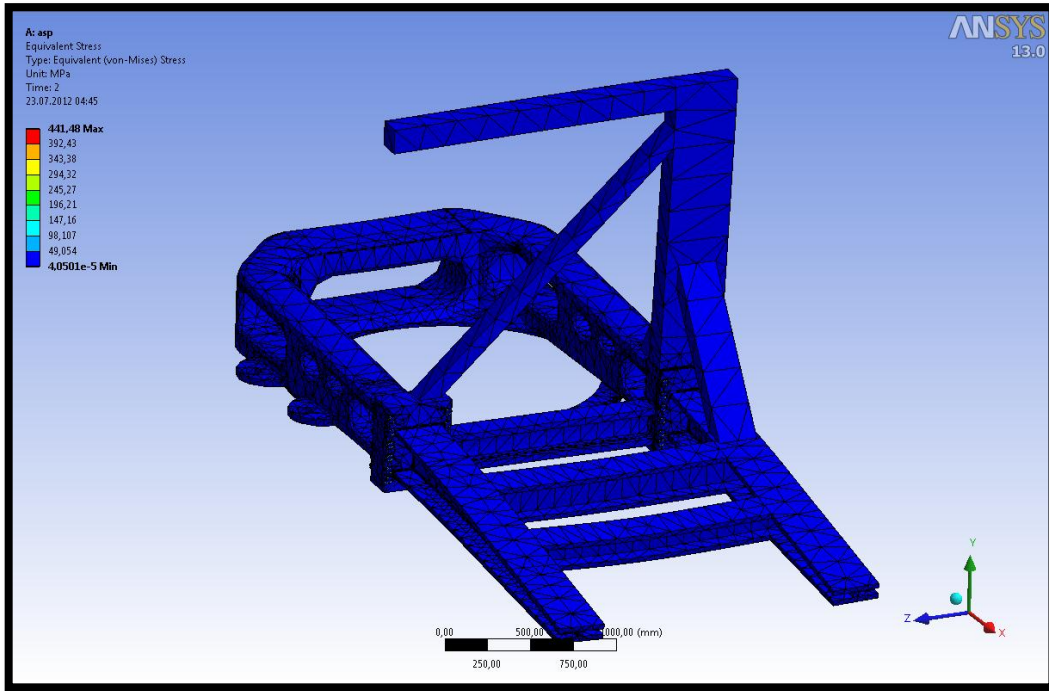


Figure 5. 35: Stress analysis with the coarse mesh.

The iterations have been performed to identify convergence of the mesh density which is shown in the Table 5.2.

Table 5. 2: Mesh refinement and converged stress values.

Mesh Number	DOF	Stress Value (MPa)
48913	15230	451
366256	96422	505.55
555681	155823	519
2455499	610927	523.81
2908253	645135	524.77
3211540	719658	No Data

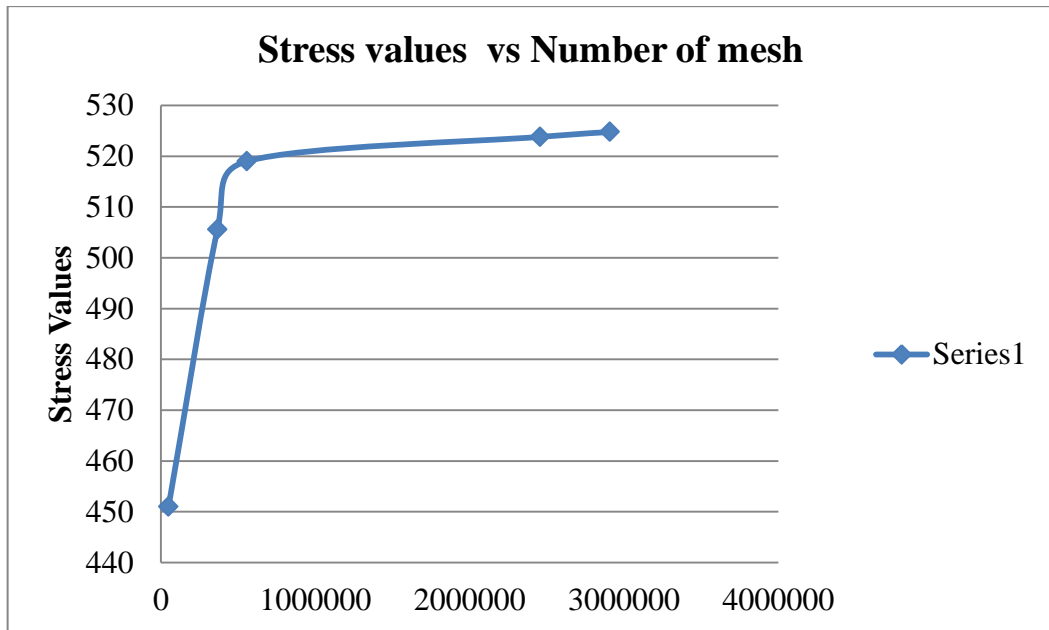


Figure 5. 36: Convergence of stress value around 524 MPa.

Finally the value of the 524 MPa has been assumed as converged with 3 mm total deflection which was also stated as a most realistic case at the static analysis part of this chapter.

5.4. FE DISCONTINUITY

At a specific point of the casted part, there was a sharp transition between the ring designed for main yaw bearing and bulk structure of the base frame. In the finite element analysis stage of the project, although the meshing of the model was fine enough, there was a discontinuous stress increase at this small region.

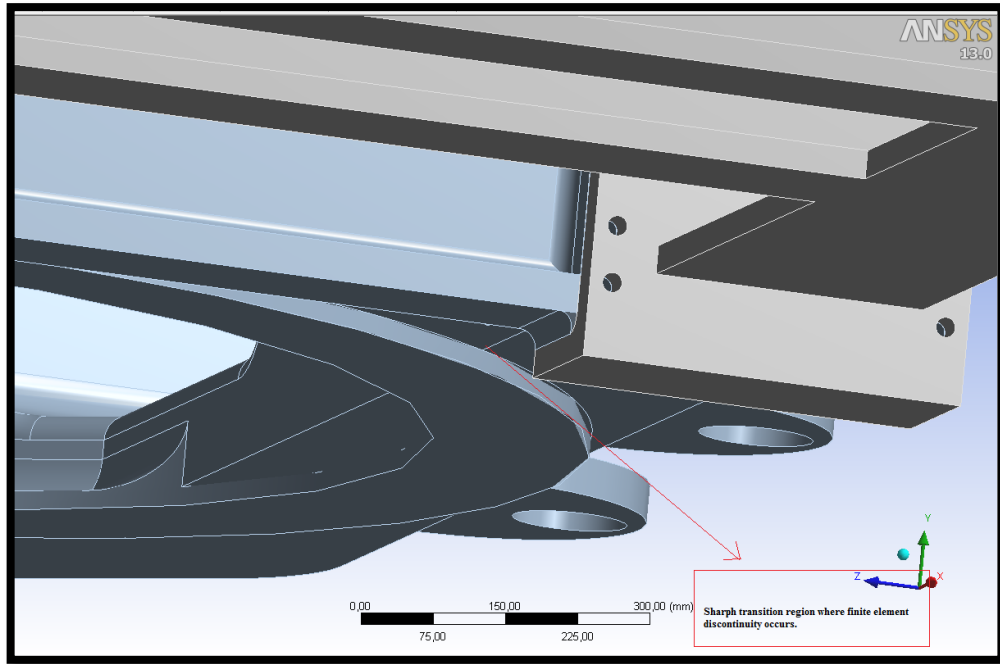


Figure 5. 37: Sharp transitional region.

The region shown in Figure 5.37 had problems during analyses because of the high stress concentration. However, although the model had sharp fillet due to code limitations as shown, it is evident that actual cast part will have more generous proper fillets for smooth transition which leads to continuous stress flow between the nodes of the mesh.

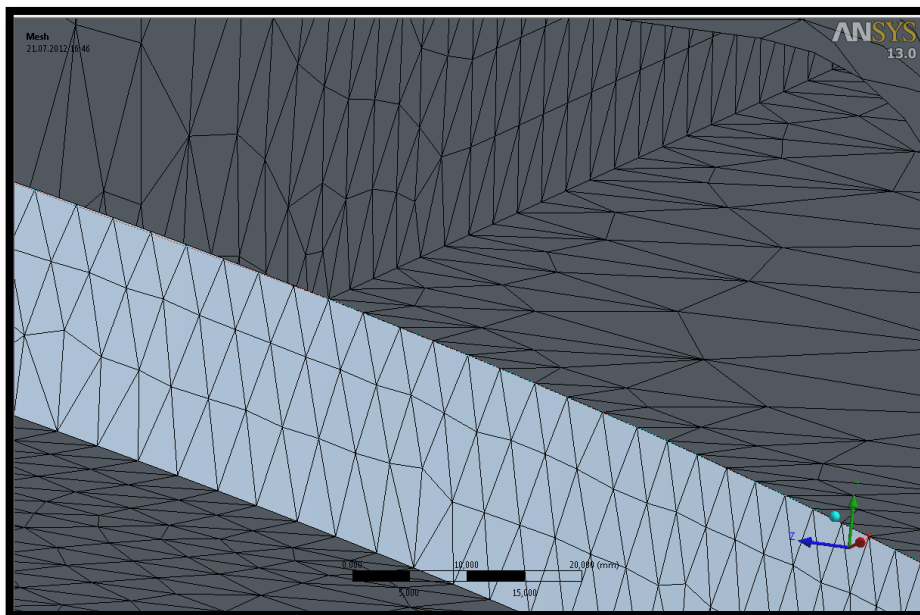


Figure 5. 38: 90 degrees sharp mesh nodes for the model.

As can be seen from the Figure 5.38, the intersection points have sharp perpendicular mesh transition which causes stress to go infinity. Several fillets for the region have been tried with SOLIDWORKS, and best combination of the possible variations was chosen for the sample bedplate design. The fillet is very complex including all faces at the region to get perfect sweep between the rings to bulk chase.

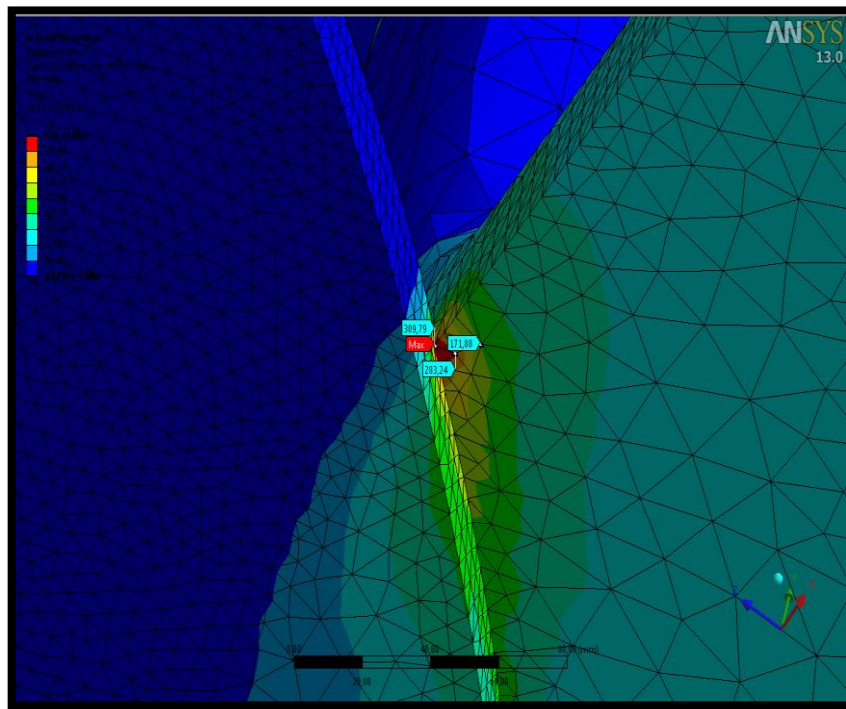


Figure 5. 39: Stress results for the chase without radius for the discontinuous region.

As can be seen from the Figure 5.39 the stress difference between the nodes of the element was around 120 MPa where the nodes carry 300 and 180 MPas respectively. This clearly shows that the region is discontinuous or singular point. The stress values would increase to infinity if mesh quality goes finer.

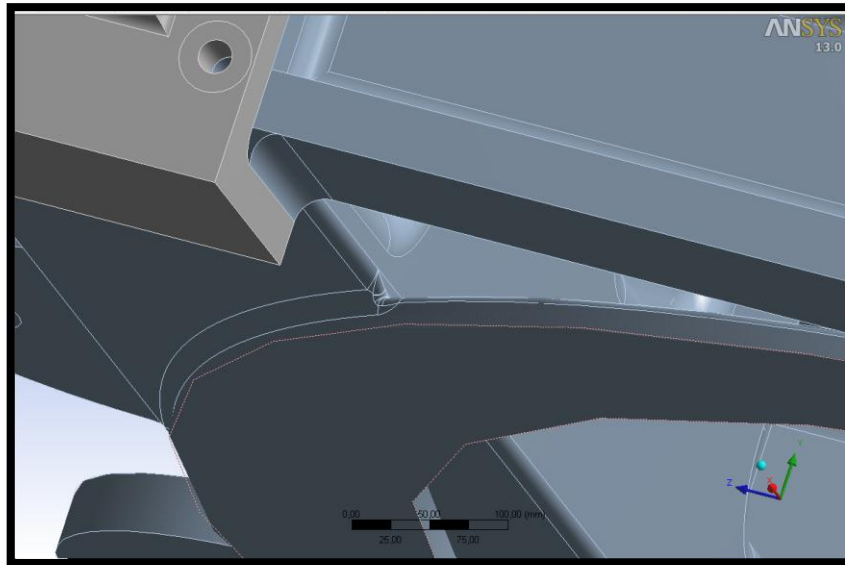


Figure 5. 40: Regional fillet for casted part.

As illustrated in Figure 5.40, sweep type of filleting has been applied between three problematic surfaces to get a smooth transitional region to avoid discontinuous region. This filleting was the best fillet that SOLIDWORKS was able to do.

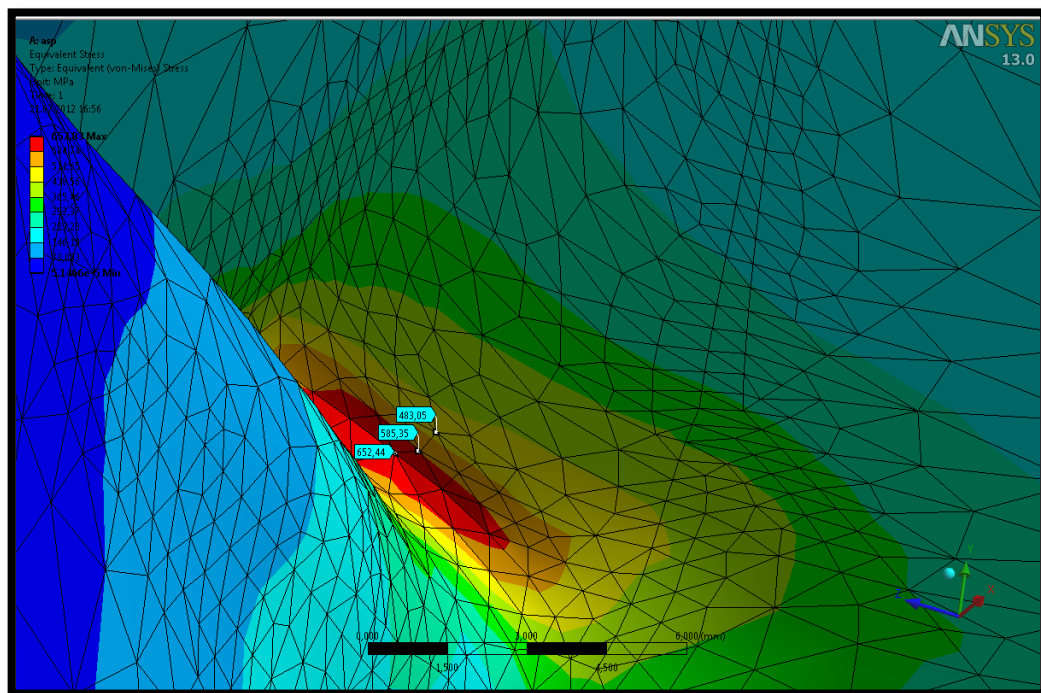


Figure 5. 41: Discontinuous region after filleting.

Unfortunately, the region was still a singular point after the best sweep type fillet has been applied. Stress increase increased from 420 to 580 and 670 MPa node by node. Over 100 MPa stress increment is quite irrational from one node to other. The stress

values did not reflect the real case because of the sharp fillet. The problem is based on the computational capability of the CAD software. Even though the casting process will handle the filleting and supply very smooth transitional locations, the regions safety must be checked. Therefore, new analyses have been conducted to evaluate more realistic stress values for the region and prove that the region does not carry such a high stress values.

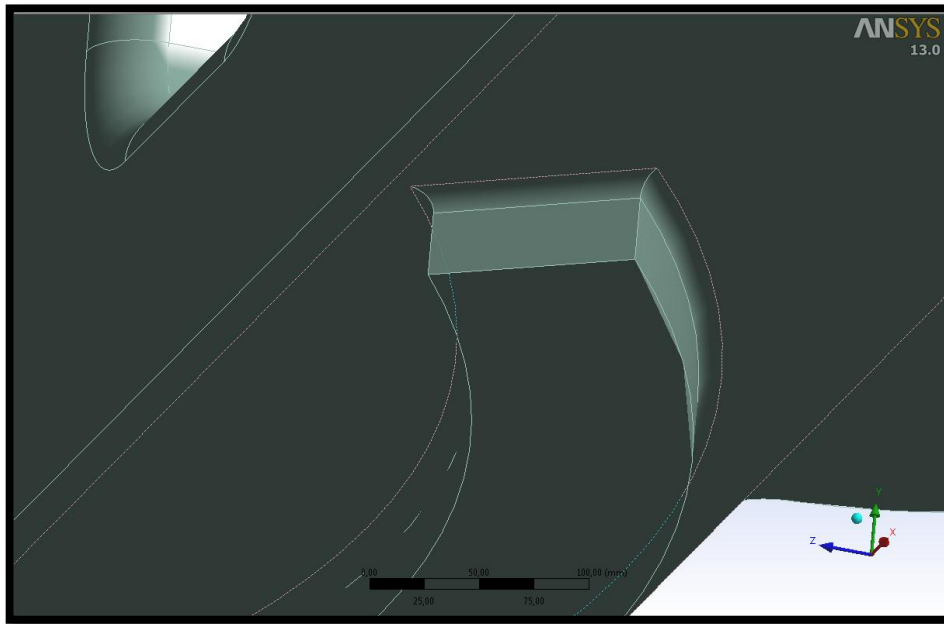


Figure 5. 42: New cad design for proof.

As illustrated in the Figure 5.42, transitional regions are removed to illustrate the incapability of the filleting due to CAD limitations. The stress values for this case indicated that the region is not critical; the high values are not real, and there is a finite element discontinuity.

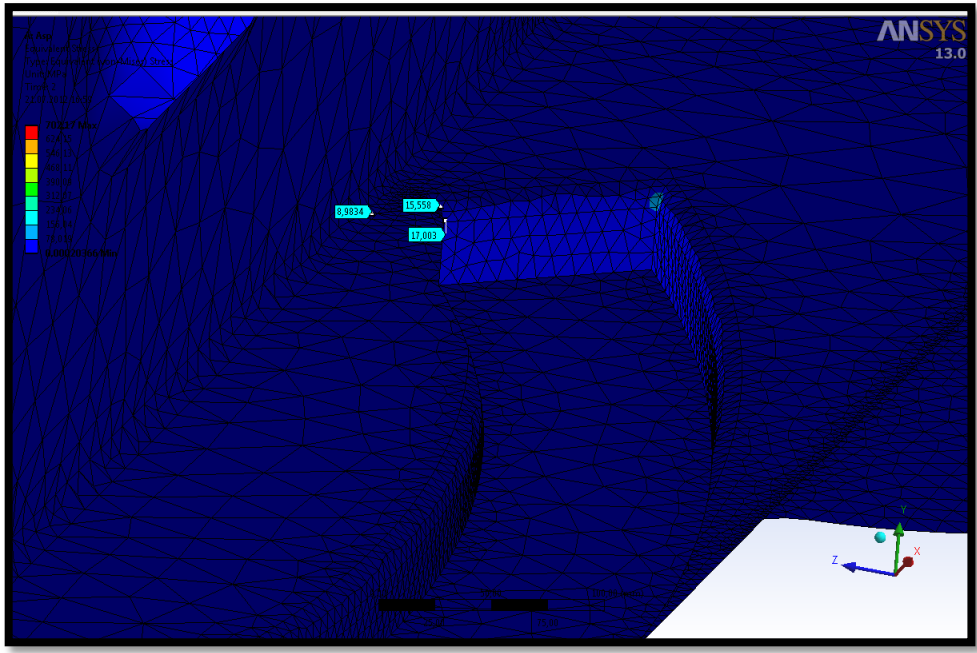


Figure 5. 43: 20 MPa for the critical regions.

Figure 5.43 shows that the region is not critical for stress values when there is no sharp intersection zone. In order to complete the analysis, the best filleted CAD model has been used to get the most realistic results with the discontinuity.

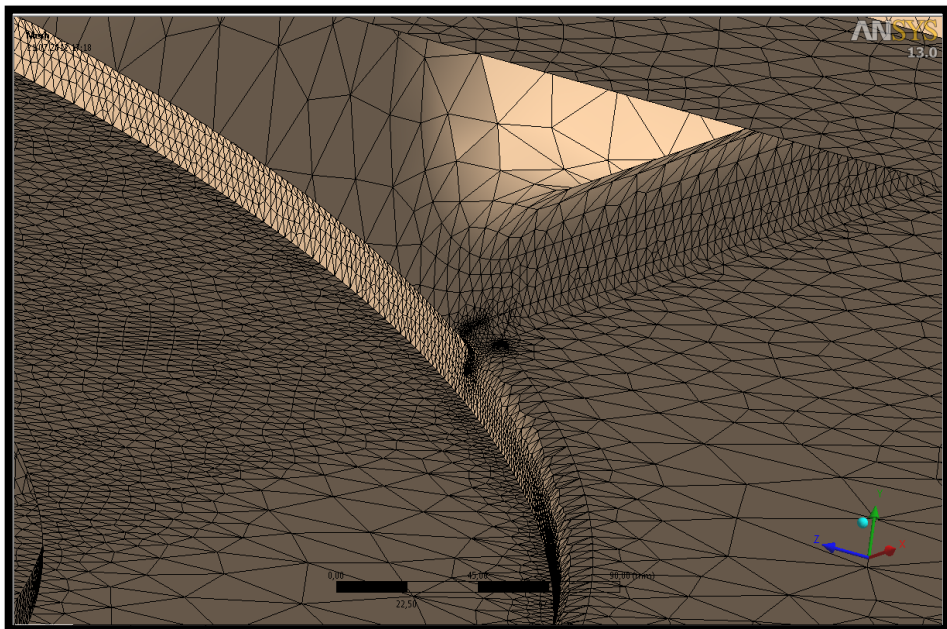


Figure 5. 44: Meshed model for discontinuous region.

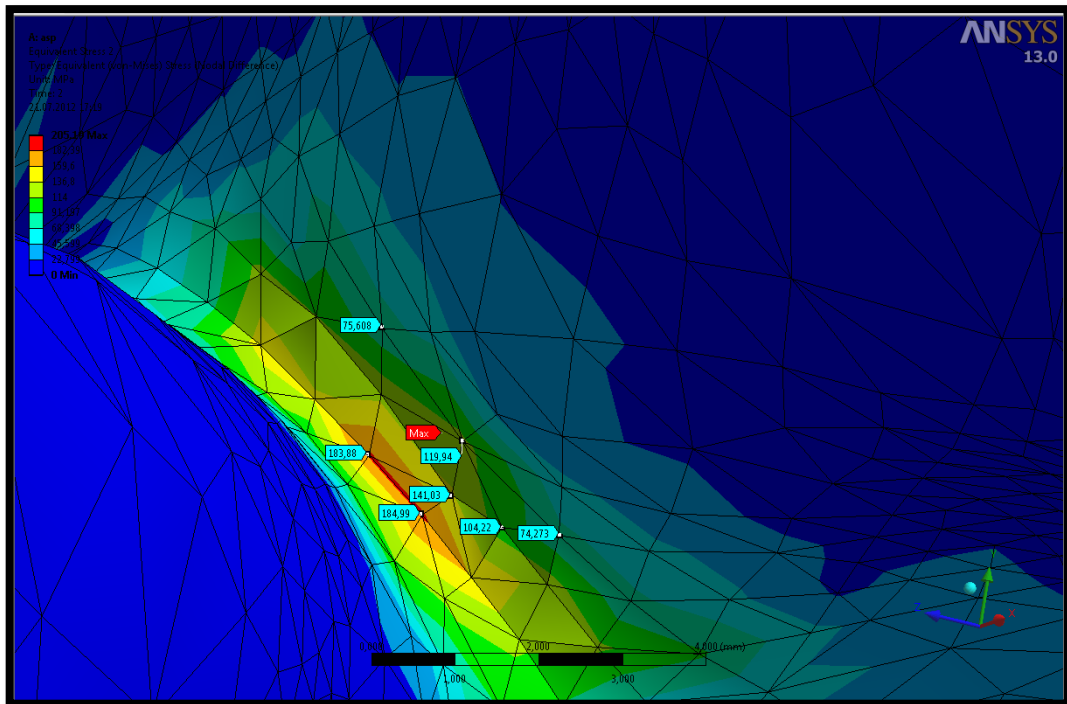


Figure 5. 45: The most corrected analysis results with smaller discontinuity.

This model shown in Figure 5.45 has the most realistic loadings including the representative crane on the models and all frictional contacts. This analysis also included the realistic bolt pretension values. The stress results for the case was 190 MPa maximum where there was a discontinuity as shown. Instead of the maximum at the singularity point, the value of stress at two nodes away from the discontinuity which is 120 MPa has been taken into consideration as the real value.

5.5. MODAL ANALYSIS

In structural engineering, modal analysis is one of the most important analyses types in order to see system's dynamic responses with the periodic frequencies called modes or natural frequency. Extensive modal analyses have been performed on nacelle bedplate to avoid the resonance probability. The bedplates' modal analyses have been performed with COMSOL and ANSYS codes to see the vibrational effects on the system under gravity load and full operational loads. In modal analysis with FEM, while the software tries to solve the stiffness matrix "K" iteratively, software finds the eigenvalues of the system in which refers to a mode frequency or a natural frequency in other words. System may have many modes, however, while solving the matrix the first three modes

are always dominant. Any dynamic force with some oscillation frequency that is near to one of the modes of the system can cause severe failure due to the excitation modes leading to resonance.

5.5.1. System working frequency definitions

The operational working load frequencies are very important for natural frequency analysis of the bedplate. The idea behind the modal analysis is to keep the system mode frequencies far away from the working frequencies of the plant. From this aspect, turbine working frequencies or the forces that may have any kind of oscillatory behavior have to be kept away from the bedplate frequencies. The oscillatory loads may come to the system from blades and rotational equipment (shafts and generator).

Table 5. 3: Operational frequencies.

Equipment	Frequencies
Low speed shaft	0.4 Hz
Blades (including all)	1.2 Hz
High Speed Shaft	13.66 Hz
Magnetic forces (from generator)	12.5 Hz

The frequency values are calculated as follows. For the low speed shaft frequency rotational speed for the shaft is 22.4 rpm. Therefore the corresponding frequency can be calculated as $22.4/60 = 0.4$. The blades are directly mounted on the low speed shaft. Therefore 0.4 Hz can be assumed for a single blade hence 1.2 Hz frequency was assumed for blades frequency. High speed shaft frequency value has been also calculated with the same method of the low speed shaft which is $820 / 60 = 13.66$ Hz.

Finally, the electromagnetic force that has an oscillatory effect has a 12.5 Hz frequency. The generator used in this turbine is doubly fed generator that will have 8 poles. 50 Hz AC signal is averagely produced by the generator magnets that has a 4 permanent ones. Therefore, the system would have one electromagnetic force that may have an oscillatory effect at 12.5 Hz.

5.5.2. FE results and system loads

After completing the definitions of the operational oscillatory loads from the wind turbine, the modal analyses have to be conducted. First six system modes have been considered and results are quite safe.

5.5.2.1. FE results for operational loads

As mentioned previously, first six modes have been considered. The results indicate that all modal frequencies are away from the systems operational frequencies.

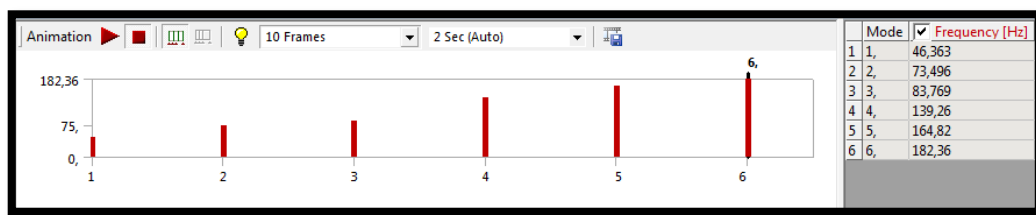


Figure 5. 46: First six frequencies of the bedplate.

As shown in the Figure, first six modes under full loads have been examined and proved that systems working frequencies are avoided and system is safe from modal aspects. First three frequencies are 46, 73 and 83Hz respectively. The natural frequencies are bending and torsional based and are shown below.

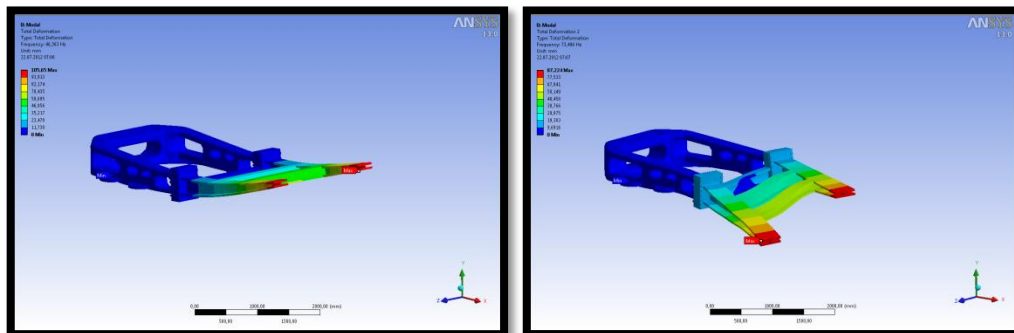


Figure 5. 47: First and second modes respectively.

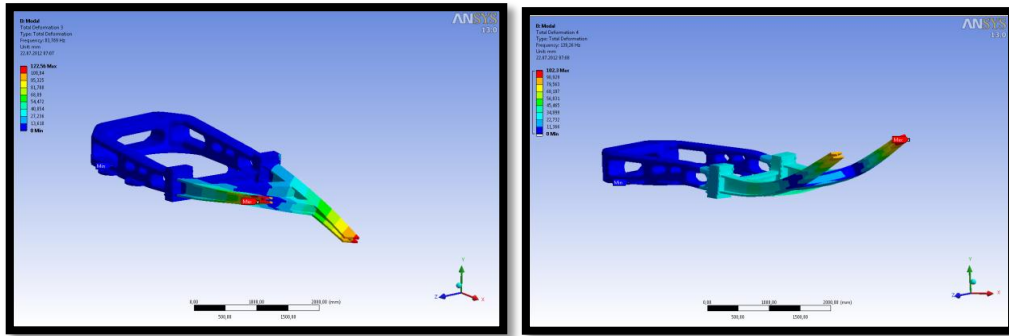


Figure 5. 48: Third and fourth mode shapes respectively.

5.5.2.2. FE results under gravity load

The bedplates gravitational load has been also calculated with the COMSOL. Both finite element programs gave very similar results. The gravity loaded modal analysis is important to show the vibrational effect of the bedplate. The system has a natural frequency around 40.7 Hz. Therefore, all modes are totally avoided from the operational frequencies of the turbine.

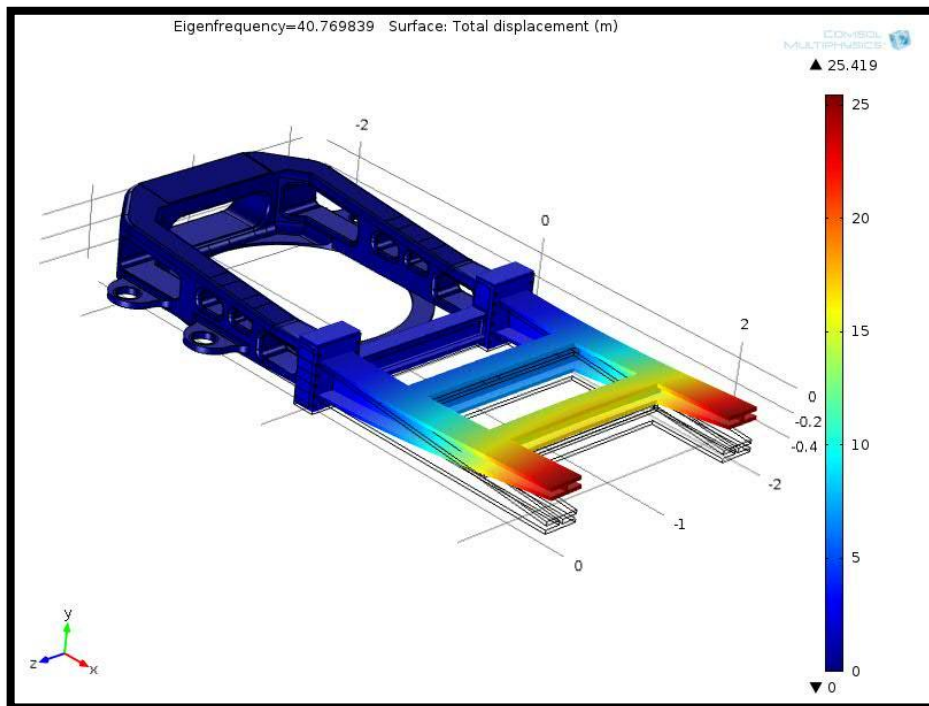


Figure 5. 49: Bedplate under gravity load.

5.6. BOLTED JOINT DESIGN AND ITERATIONS

The casted parts are generally bonded with the sheet metal parts with bolts in hybrid designs. In this bedplate, the joint was also designed with screws and nuts. The two joints have 24 M24 bolts and 48 nuts. The system is consistent with the literature examples. It is evidently safer than the literature samples of bedplates because in this design the bolts are not exposed to direct shear forces. The design strategy for the joint is to calculate the friction force vertically between the contact faces of cast and profile part. The friction force must be higher than the equivalent forces of the profile part including the generator torque and profile gravity load. The material of the bolts is AISI 4135 as explained in the material section earlier. The bolt quality will be either 8.8 or 12.9 which is not determined. However, both analytical and numerical calculations were done for either bolt quality.

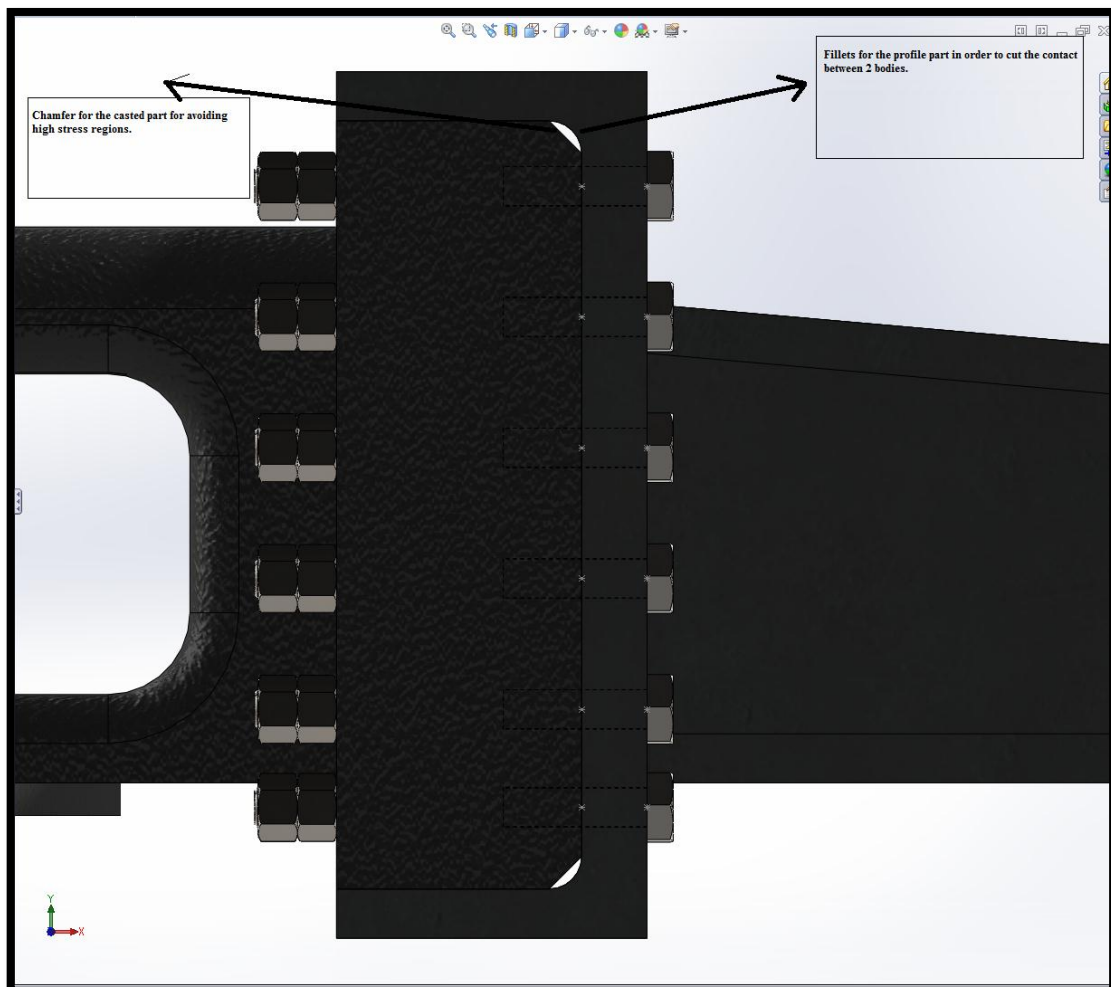


Figure 5. 50: Joint design with fillet and chamfer.

The frontal view of the joint as shown in the Figure 5.50 has chamfer and fillet to avoid sharp contact region which may lead to stress concentrations or notch effect. The system has 2 nuts for each bolt in order to prevent nuts getting loose under vibrational effects.

5.6.1. Joint force calculations

The joint force calculation strategy was previously explained that is based on carrying the gravitational loads on the profile parts with the friction force between the contact surfaces of the cast and the profile part. The loads from the profile part are due to gravity acting on crane, generator, electronic converters, and profile parts. The joint should also carry the generator torque which is applied as force couple. Therefore, joints total forces are different for the left and right joints. In order to calculate the friction force between surfaces, the normal load should be calculated first, than the friction force will be the force that has a positive vertical axis orientation.

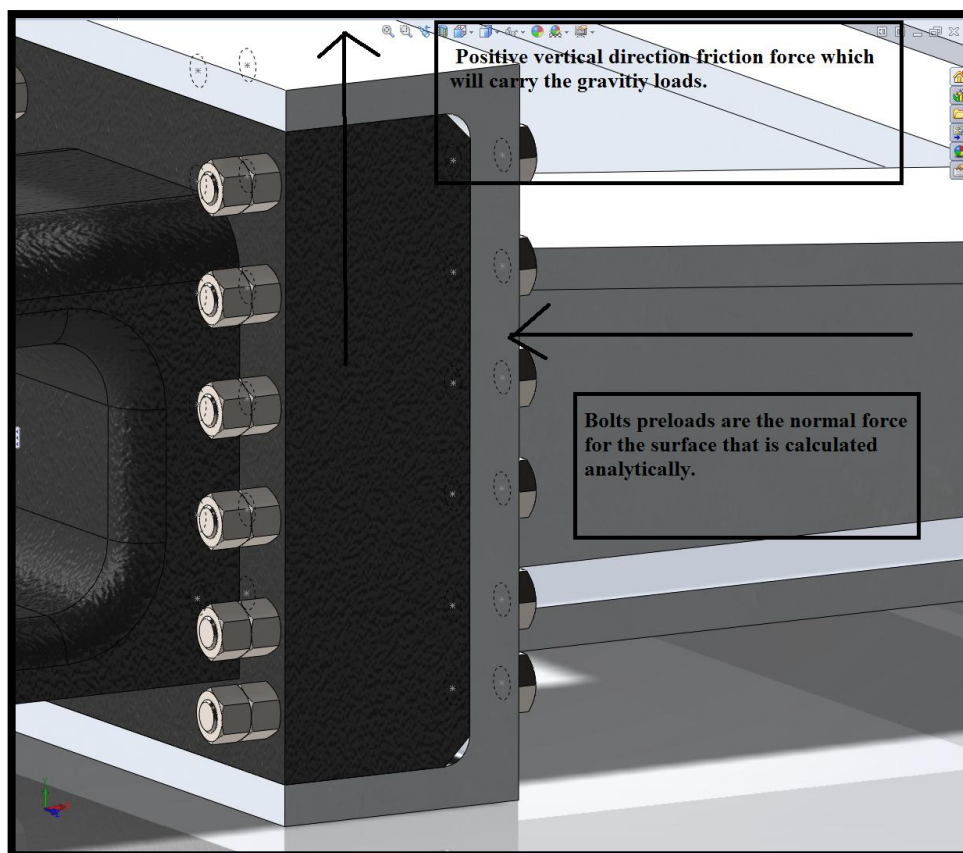


Figure 5. 51: Friction force illustration.

Total force that is to be carried by the left joint is 57 KN that consists of generator, profile part, electronics equipment, and generator force couple which has previously calculated 8 KN contribution downwards for the left joint. 12 bolts should be strong enough to carry the load with the continuous friction force on the left joint which is calculated with the aid of the formula shown:

$$F_f = \mu * F_{bolt} \quad (5.6)$$

F_{bolt} is the bolt preload which is calculated with formula given by (13):

$$F_i = 0.7 * S_p * A_t \quad (5.7)$$

where F_i is the preload for the bolt and S_p is the proof strength of the material which is classified with respect to bolt class as 8.8 or 12.9. In this case, proof stress also means that the stress at the bolt begins to take a permanent set which is not the same as yield. Coefficient of 0.7 is the initial preload margin. This value is dependent on the design engineer selection of safety factors for the joint. Moreover, formula represents the tensile area of the bolts which is tabulated with respect to the diameter of the bolts. In this case bolts will be M24 and calculations are done with respect to both 0.9 and 0.7 preload coefficients which will be shown respectively. Therefore, initial load for the M24 can be calculated as;

$$F_i = 0.7 * 600 * 352.5 = 148050 \text{ N}$$

where 600 was the proof strength with the 8.8 quality bolts and 352.5 mm^2 is the tensile stress area that is also calculated as;

$$A_t = \frac{\pi}{4} * d_0^2 ; \quad d_0 = (d_2 + d_3)/2 \quad (5.8)$$

where d_3 and d_2 are tabulated with respect to the diameters of the bolts also known as a root and pitch diameters of the bolt. The other parameters like d_3 and d_2 are 20.319 and 22.051 mm for M24. Therefore, by doing the calculations A_t would be 352.48 mm^2 after finding the tensile area of the bolt, initial load of the M24 bolts can be calculated. The total preload of 12 bolts is $1.776.600 \text{ N}$ and the total friction force is $F_f = 0.3 * 1776600 = 532980 \text{ N}$. Therefore, total friction force for left joint is 533 KN and the total load to be carried was 57 KN which looks safe for the left joint. Same calculations can be done for the right joint in which the friction force is the same and the load to be carried was 41KN. Therefore, both joints are safe enough for the initial design. Real design will be based on FEM. Similarly, the bolts may be tightened with the reduction of 0.9 that will result in 190350 N for initial loads of the bolts which looks also safer but it results in

operational stress close to yield of the material. The preload coefficient is dependent on safety factors for bolts that will be decided by the engineer. Therefore, 8.8 bolt class M24 bolts with 0.7 reduction coefficient are preferable for this joint and looked suitable.

Similarly, 12.9 class of bolts are also analyzed with both analytically and numerically the preload for the 12.9 class bolts with 0.7 reduction coefficient is 239348 N the proof strength for the 12.9 quality bolt is 970 MPa and the other parameters were the same. In addition to M24 bolts, M27, M30 and M 20 bolts were also calculated for these joints and they were all safe. Both class 8.8 and 12.9 bolts can be found easily from local resources all calculations were confirmed with the FEM simulations and safety factors were calculated. Absolute decision about 8.8 and 12.9 class bolts will be based on the costs of the bedplate and the safety factor.

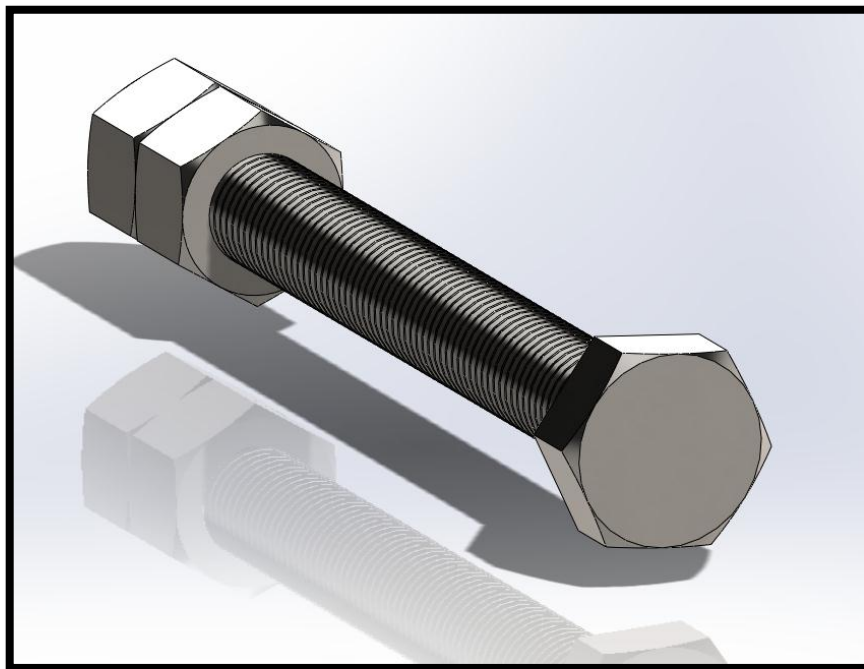


Figure 5. 52: M24 bolt with 2 nuts supported.

5.6.2. Joint calculations using FEM

As stated previously, analytical calculations were verified with FEM stress results to calculate the maximum stresses on the bolts and safety factors for both classes of the bolts. ANSYS software has been used to calculate the bolt stresses with the aid of bolt pretension function. Preload calculations have been performed on all bolts and the stress values have been evaluated under full load conditions. The numerical results will be shown for class 8.8 and 12.9 respectively.

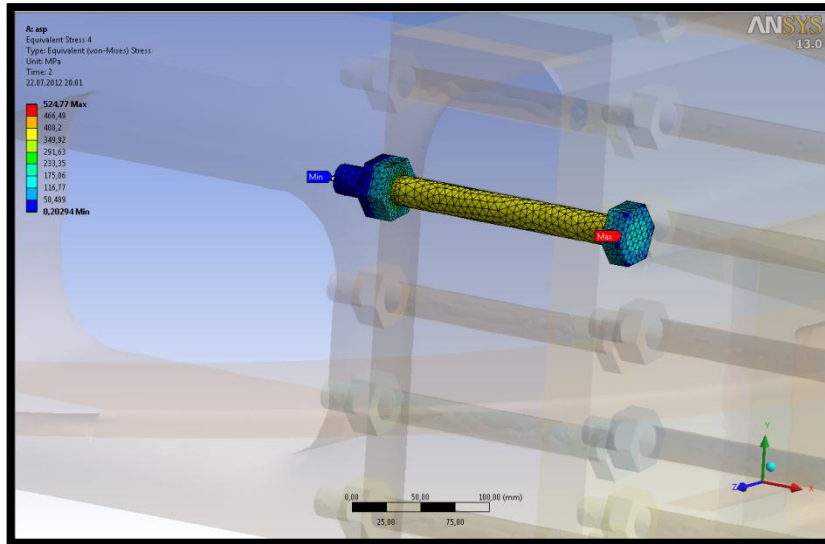


Figure 5. 53: Class 8.8 bolt results.

As illustrated in the Figure 5.53, the maximum stress on the class 8.8 bolts is around 525 MPa where the yield stress of the material is 640 MPa. Hence, the safety factor under % 70 preload ratio is 1.22 which is low but reasonable for such a joint. The preload has been applied at the center of mass of the bolt as 148050 N.

The results for 8.8 bolts under % 90 preload ratio is as follows. The maximum stress occurs at the same bolt, and the stress value is around 620 MPa.

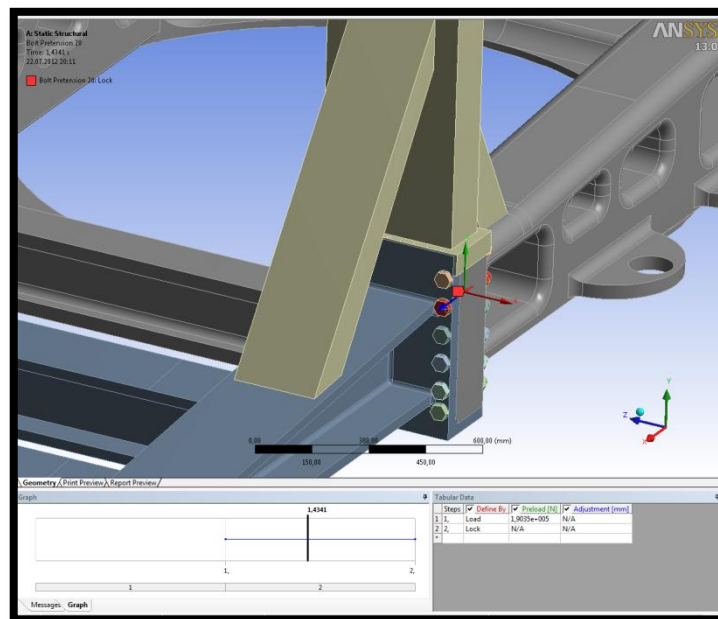


Figure 5. 54: 90% reduction ratio bolt analysis.

The preload applied to the bolt is 190350 N and the stress value reaches to critical levels. For this case 90% preload ratio for pre tightening should not be applied.

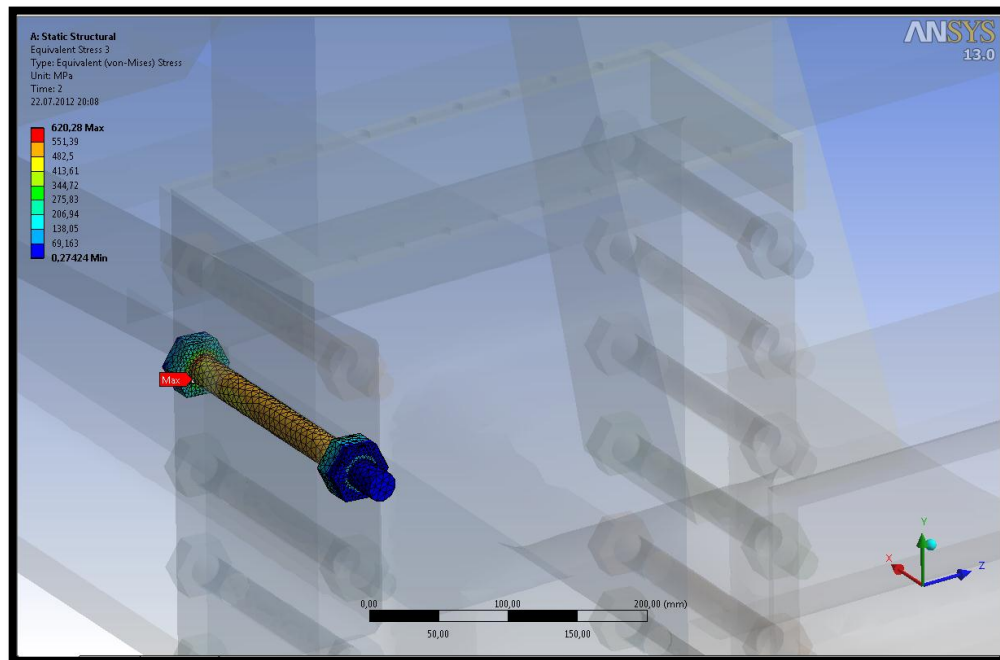


Figure 5. 55: Stress value for 90% preload ratio.

As shown in the Figure 5.55 maximum stress for this bolt is around 620 MPa where the yield of the material was around 640 MPa. Therefore, the safety factor for this bolt is 1.03 which is critically low.

Finally 12.9 class bolt analysis results are shown. The stress value for this bolt is around 865 MPa. Fine pitch 12.9 class bolts should be used for this joint with the pre tightening coefficient of 70%.

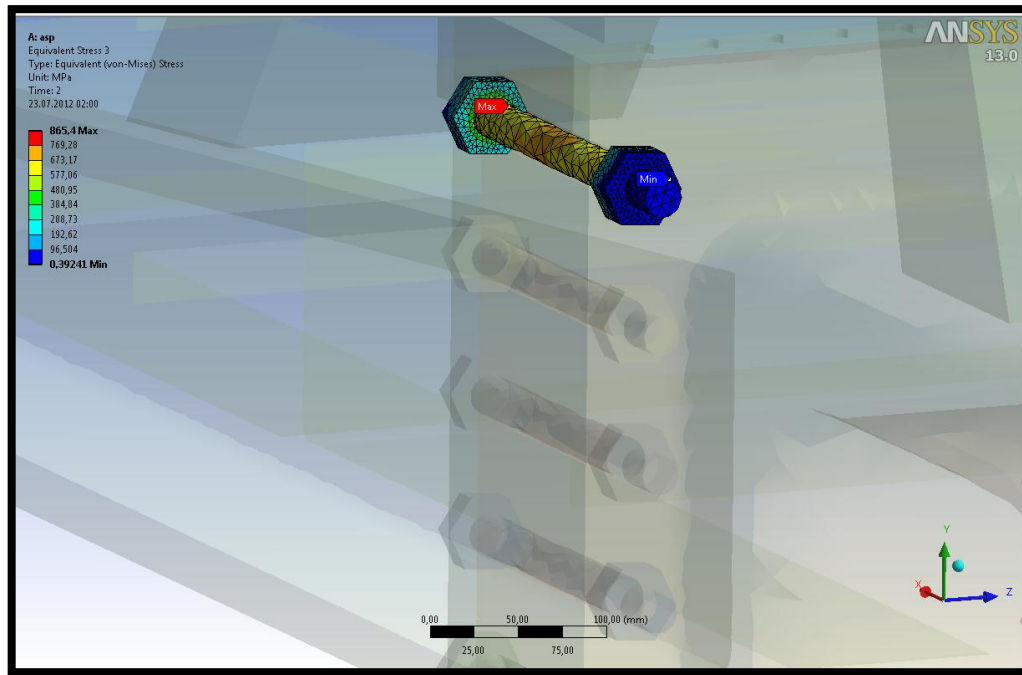


Figure 5. 56: Bolt analysis for 12.9 class.

As shown in the Figure 5.56, the stress value is around 865 MPa where the yield stress is 1080 MPa . Therefore, the safety factor is around 1.25 which is slightly higher than the 8.8 bolt. As a consequence, 12.9 class bolts is suggested for this joint with a 0.6 or 0.7 tightening coefficient.

CHAPTER 6

CONCLUSION

This thesis work involves design and analysis of nacelle bedplate structure for a 500 kW horizontal axis wind turbine as part of national wind energy project. A hybrid nacelle structure has been developed that included a cast main frame and a welded profile extension. Design has been evolved iteratively, as boundary conditions and loads became available from other teams responsible for designing the other subsystems in the project. Both static and dynamic load cases have been analyzed. Fatigue life of the structure has been estimated. Once some basic design maturity was achieved, a topology optimization study has been performed.

The optimization work successfully reduced nacelle bedplate weight nearly by 30%. Once an optimum design is reached, a group of modal analyses have been performed to obtain and manage system natural frequencies. The results indicated that all of the natural frequencies are well beyond system excitation frequency ranges.

Unlike common wind turbines, this nacelle has been designed with a heavy duty crane capable of lifting the heaviest component in the nacelle. This aims ability to self-maintain the turbine without any need for expensive external crane help. Separate group of analyses have been conducted to ensure structural safety under extreme crane loads.

Changes in design philosophy like shift from 2 point suspension shaft design to 3 point suspension system as well as the dependency to other groups for some needed loading information caused some delays and extra iterations in the work. Overall, a good nacelle design has been achieved with less than 5 tons weight and with maximum stresses less than half the yield strength of the material.

As future work of this thesis study, technical drawing of the nacelle bedplate will be drawn and sent to manufacturers. After the completion of the cast part and profile part, bedplate will be assembled.

REFERENCES

1. Turbo Squid. [Online] [Cited: March 1, 2012.] <http://www.turbosquid.com/3d-models/wind-turbine-direct-drive-3ds/474771>.
2. **CLARKE, S. OMAFRA.** [Online] September 2003. [Cited: August 1, 2011.] <http://www.omafra.gov.on.ca/english/engineer/facts/03-047.htm>.
3. **BURTON, Tony, et al., et al.** *Wind Energy Handbook*. West Sussex : Wiley, 2001.
4. **HOLIERHOEK, Jessica.** ECN. [Online] [Cited: September 29, 2011.] <http://www.ecn.nl/nl/nieuws/newsletter-en/2010/december-2010/start-of-integral-design-wind-turbines/>.
5. International Symposium on Fatigue Design & Material Defects. [Online] [Cited: April 6, 2012.] <http://www.ntnu.no/videre/konferanse/FatigueDefects2011/gallery.html>.
6. VAWT. [Online] [Cited: May 5, 2012.] <http://turbinesint.com/wind-turbine-power-generation/>.
7. MWPS. [Online] [Cited: March 3, 2012.] <http://www.mywindpowersystem.com/2010/01/10/wind-turbines-glossary/>.
8. **PENG, Tian, et al., et al.** *Research on Static and Dynamic Characteristics for Nacelle Bedplate of HAWTs Based on Finite Element Method*. s.l. : China Resources Wind Power Development Co. Ltd.; Institute of Energy Science of Shantou University.
9. *Ductile Iron for Heavy Section Wind Mill Castings: A European Experience.* **ROEDTER, H. and GAGNE, M.** Montreal : s.n., 2003. Keith Millis Symposium on Ductile Iron.
10. **Vonroll-Casting.** [Online] [Cited: June 8, 2012.] www.vonroll-casting.ch.
11. alu. [Online] [Cited: March 31, 2012.] http://aluminium.matter.org.uk/aluselect/03_physical_browse.asp.
12. MatWeb. *AlSi 5120*. [Online] [Cited: July 11, 2012.] <http://matweb.com/search/DataSheet.aspx?MatGUID=9e8bb9860fcd4d94a5bd1bdea72e1c6d&ckck=1>.
13. OPTENG. [Çevrimiçi] [Alıntı Tarihi: 12 May 2012.] <http://www.opteng.com.tr/opt-optimization-en.html>.
14. **SHIGLEY, Joseph E. and MISCHE, Charles R.** *Mechanical Engineering Design*. New York : McGraw Hill, 2001.
15. **NORTHON, Robert L.** *Machine Design An Integrated Approach*. New Jersey : Pearson, 2006.
16. **THOMAS, Michael R.** *Shape and Topology Optimizaiton of Brackets using the Level Set Method*. Boston : Rensselaer Polytechnic Institute, 2010.
17. *Topology Optimization of Structures under Dynamic Responce Constraints.* **RONG, J. H., et al., et al.** 2000, Journal of Sound and Vibration, pp. 177-189.

18. *Topology Optimization of Structures: A Minimum Weight Approach with Stress Constraints*. **NAVARRINA, F., et al., et al.** 2005, *Advance in Engineering Software*, pp. 599-606.
19. **BYWATERS, Garrett, et al., et al.** *US 7,109,600 B1* United States, 2006.
20. *Load History Effects in Ductile Cast Iron for Wind Turbine Components*. **HUBNER, P., et al., et al.** 2007, *International Journal of Fatigue*, pp. 1788-1796.
21. *Fatigue Life Distribution and Size Effect in Ductile Cast Iron for Wind*. **SHIRANI, M. and HARKEGARD, G.** 2011, *Engineering Failure Analysis*, pp. 12-24.
22. ANSYS. [Online] [Cited: May 6, 2012.]
<http://www.ansys.com/Products/Simulation+Technology/Structural+Mechanics/ANSYS+Structural>.
23. ANSYS Solver. [Online] [Cited: April 19, 2012.]
http://www.kxcad.net/ansys/ANSYS/ansyshelp/Hlp_G_BAS3_4.html.
24. MatWeb. *AI SI 5135*. [Online] [Cited: July 11, 2012.]
<http://matweb.com/search/DataSheet.aspx?MatGUID=02e484d291b14d0d848a9e5fd167f5a3>.
25. SolidWorks Help. [Online] [Cited: April 1, 2012.]
http://help.solidworks.com/2011/English/SolidWorks/cworks/LegacyHelp/Simulation/Fundamentals/Running_Analysis.htm.
26. **BENDSOE, M. P. and SIGMUND, O.** *Topology Optimization*. Berlin : Springer, 2003.
27. **BYWATERS, Garrett, et al., et al.** *US 7,075,192 B2* United States, 2006.
28. **HAU, ERICH.** *Wind Turbines*. Berlin : Springer-Verlag, 2005.
29. **PAPALAMBROS, Panos Y. and WILDE, Douglass J.** *Principles of Optimal Design*. Cambridge : Cambridge University Press, 2000.
30. **COMSOL.** *Solving the Linear System Matrix: Direct and Iterative Solvers*. s.l. : COMSOL.
31. **ROQUET-COORDINADOR.** *Life Design*. s.l. : ROQUET-COORDINADOR.
32. **ANSYS.** *Structural Analysis Guide*. [Çevrimiçi] April 2009. [Alıntı Tarihi: 17 May 2012.]
<http://www.ansys.com>.
33. *İskele Kalıp Dünyası*. [Çevrimiçi] [Alıntı Tarihi: 20 April 2012.]
<http://www.iskelekalipdunyasi.com/teknik.bilgi/68/Kule.Vinc.Nedir?.Kule.Vinc.Ozellikleri.Nelerdir?>.
34. *Reel Makina*. [Çevrimiçi] [Alıntı Tarihi: 15 May 2012.] <http://reelmakina.com/>.
35. *Han Makina*. [Çevrimiçi] [Alıntı Tarihi: 18 March 2012.] <http://www.hanmakina.com>.

36. *Advancing Analysis Capabilities in ANSYS Through Solver*. **POOLE, Gene, LIU, Yong-Cheng** **ve MANDEL, Jan**. 2003, *Electronic Transactions on Numerical Analysis*, s. 106-121.

37. MatWeb. *AISI 4135*. [Online] [Cited: July 11, 2012.]

<http://matweb.com/search/DataSheet.aspx?MatGUID=58c8ecbfbbb74e208ef745ab062e47a2&ckck=1>.

38. *Economic and technical issues affecting the development of the wind-power industry in Poland*. **Drwiega, Andrzej**. Pszczynska : Applied Energy, 2003.

APPENDIX A

AUXILLARY DESIGN AND CAD INTEGRATION

In the scope of the thesis study, main purpose was to design the bedplate and complete analyses of the bedplate. However, as the project progresses some other requirements were occurred related to bedplate. Therefore, beside the bedplate analyses, system cad integration, calculations of yaw motors and yaw bearing design were also done in the content of thesis study.

1.1. YAW BEARING FORCE CALCULATIONS AND BEARING SELECTIONS

Firstly, yaw bearing for the turbine was designed and selected as an auxiliary design. The yaw bearing is a significant component for modern wind turbines that orients the turbine according to wind direction automatically via this main bearing and gear system. The system is also known as main turning tables that are very commonly used in several industrial equipment and constructions like cranes, cement pumps, construction machines and electronic radars and satellites. The design is important because the complete loadings flows from nacelle to tower through this bearing in other words the bearing supports the loads from nacelle.



Figure 0. 1: Example places for turntables.

After completing required research on the yaw bearings for wind turbines applications, triple rowed roller bearing with an external gear is decided to be used. Just like the other components in the project, the yaw bearing should be domestically accessible.

Material for such bearing is 42CrMo4 in ISO standards which corresponds to AISI 4140 steel. Moreover, roller material is 100cr6 steel which is AISI 5210. These materials are generally known and used by domestic industry and have quite strong mechanical properties.

Table 0. 1: Mechanical Properties for materials (12).

	Elasticity(Pa)	Density(kg/m ³)	Poisson Ratio	Yield (Mpa)
AISI 4140	2,05e11	7850	0.29	485
AISI 5120	2,1e11	7810	0.3	635

The required force calculations are based on the full static loadings and demanded radial and axial force components of the bearing was found. In addition bending moment for the bearing was also calculated. The bearing selection was done after completing the required safety factor multiplications according to both calculations and design dimensions.

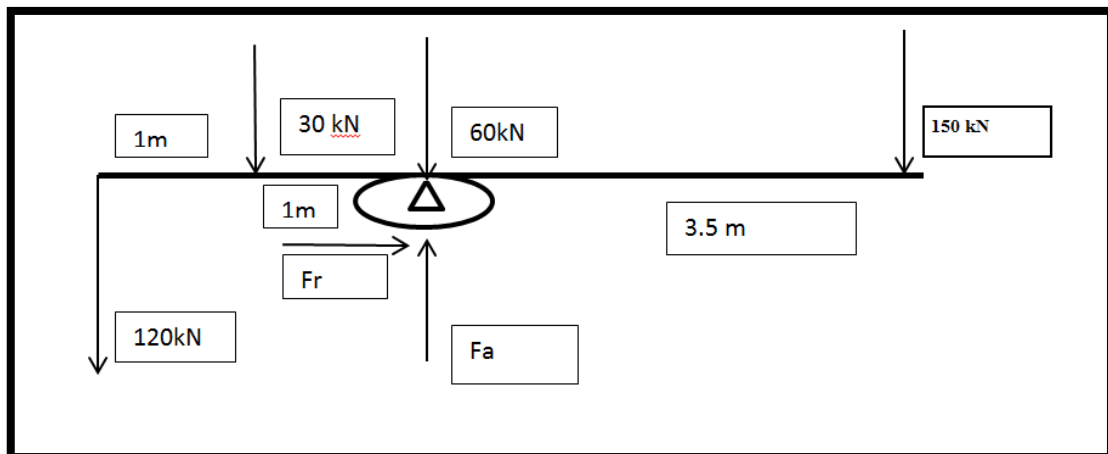


Figure 0. 2: Static loading condition for the main bearing.

The axial force calculation was done according to formula that:

$$\sum F = 0 \quad (0.1)$$

Sum of the downwards forces are equal to the axial force for the bearing which is 360kN. The safety factors for the wind turbine applications of the bearing should be 2 therefore, the axial force should be 720kN at least (Reel Makine, n.d.).

The radial force is given from TUSAS as 110kN and the bending moment is calculated with the formula:

$$\sum M = 0 \quad (0.2)$$

Therefore; $M_{bending}$ can be calculated as $M_{bending} = 150 * 3.5 - 30 * 1 - 120 * 2 = 255 \text{ kNm}$. This moment value should also be multiplied with the safety factor of 2 therefore the moment 510 kNm opposite way bending moment is needed from the bearing at least.

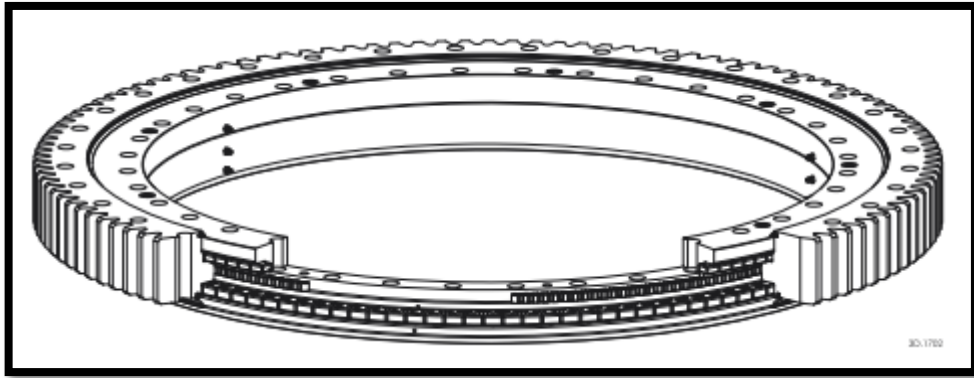


Figure 0. 3:Illustration of the main bearing that is chosen for the project (18).

After completing the required calculations, the bearing selection process was done. Domestic suppliers were found for the yaw bearing design. As mentioned above the system should also have a rack and pinion geared system which is external to the bearing. The CAD design and assembly of the turbine was completed.

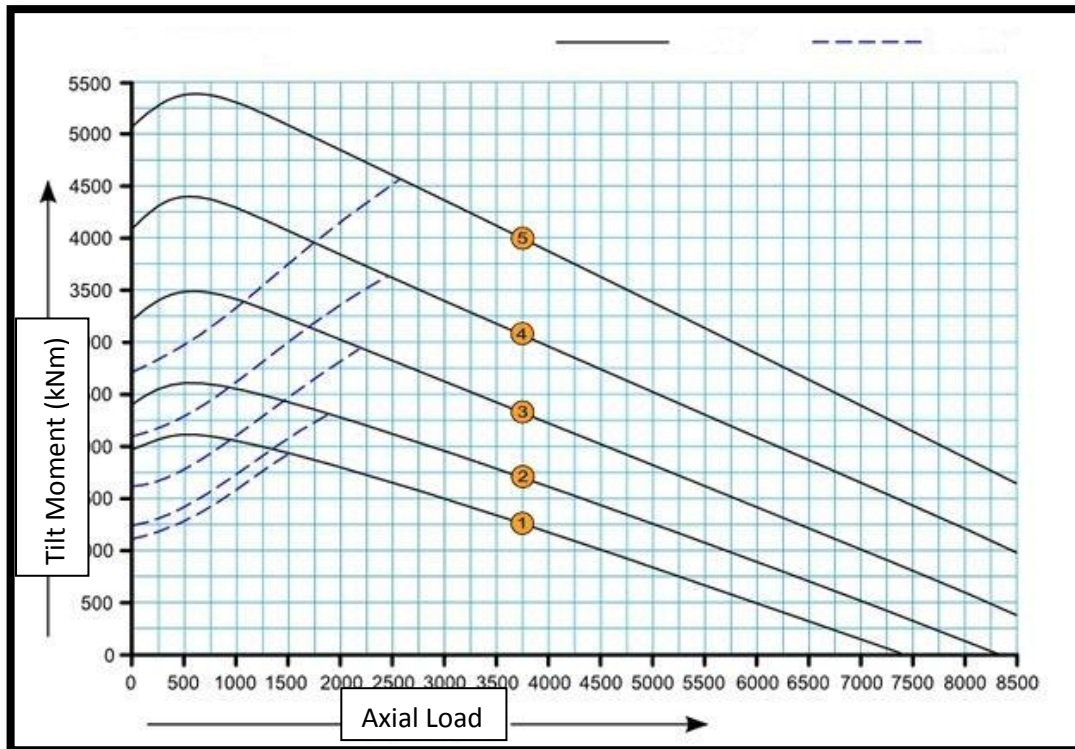


Figure 0. 6: Static loading curve for the yaw bearing (17).

After completing the required calculations, static load coefficients were checked and class 2 bearing was found as suitable for the case but the dimensioning of the turbine was more important. Class 1 and 2 type bearings do not reach to pinions teeth because of the small dimensions. Bedplate's width should at least be 2.2 meters. Therefore class 5 type of bearing was selected for the application which has a wider variety of dimensions and suitable strength for the case.

APPENDIX B

1.2. CAD INTEGRATION AND FINAL ASSEMBLY

In order to see the physical constraints of the wind turbine design, system CAD assembly was an absolute requirement. System parameters like complete mass, inertia matrix and dimensions of the components were predictable values before the final assembly was accomplished. After the CAD model was done, total mass and the system inertia matrix around a certain coordinate system became feasible to calculate. Moreover, ergonomics of the human entrance to the turbine was checked thanks to

CAD assembly. In this part of the chapter several renders of first national wind turbine design will be illustrated.

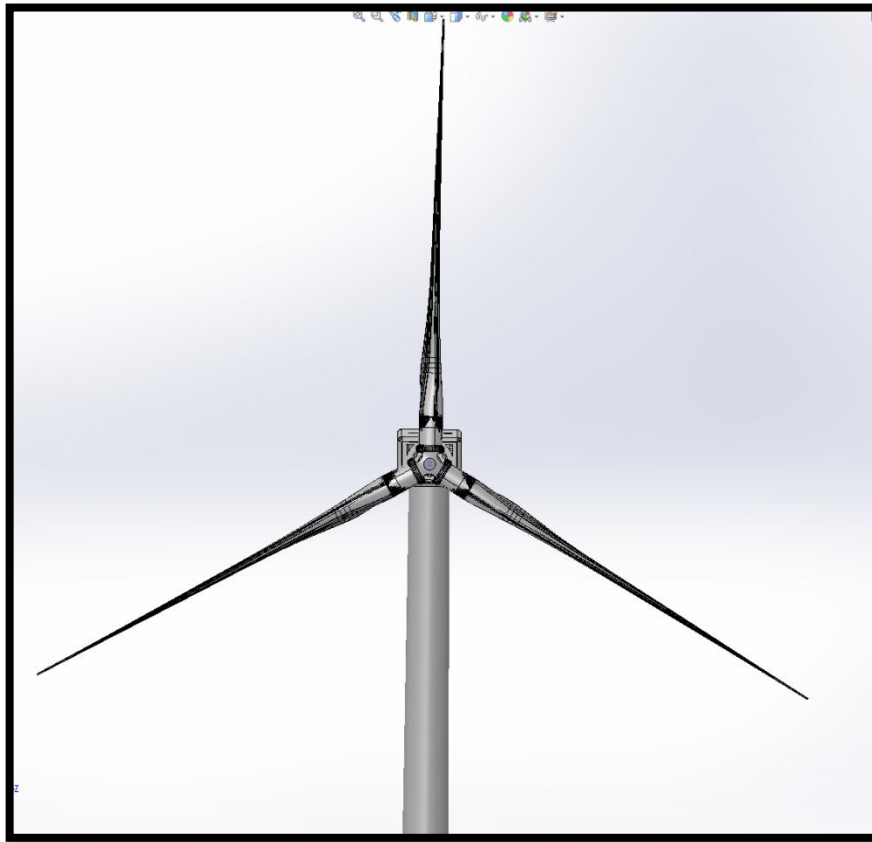


Figure 0. 7:Frontal view of the wind turbine.

Alternatively, isometric view of the first domestic 500 kW wind turbine can be seen in the Figure shown below.

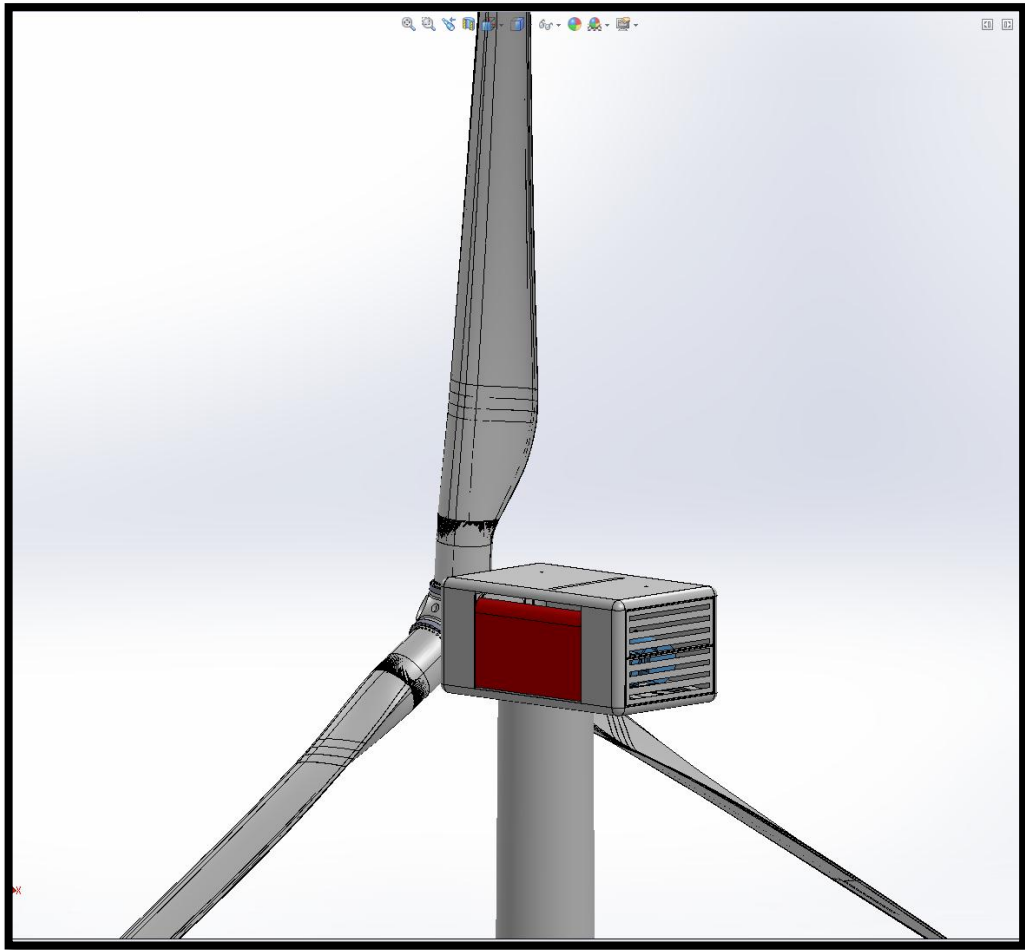


Figure 0. 8: Isometric view of the complete wind turbine.

The system has 24 m radius of blade swept area and 5.3 meters Nacelle length and 3.2 meters width. Total mass of the system excluding tower is around 41000kg and volume of the system is around 65 m³. Finally, internal isometric view of the system will be provided below.

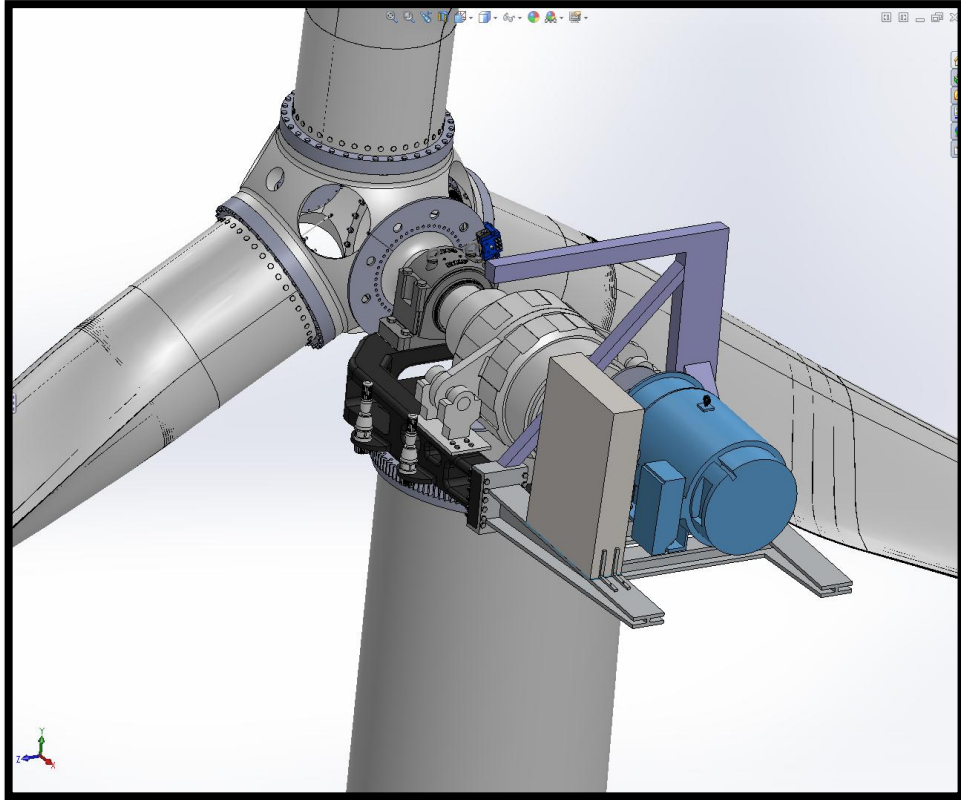


Figure 0. 9:Internal view of the national wind turbine.

1.3. YAW MOTOR TORQUE AND POWER CALCULATIONS

After completing the system cad integration and the yaw bearing design, yaw motors torque requirement became an issue to be solved. In order to achieve the mass-inertia matrix of the full system, cad model of the turbine had to be accomplished. In order to calculate the yaw motors total torque requirement, an inertial matrix around the towers' coordinate system was needed and required coordinate system was formed under SOLIDWORKS environment. General wind turbines have four yaw motors to start up the system rotate with the orientation of the wind speed.

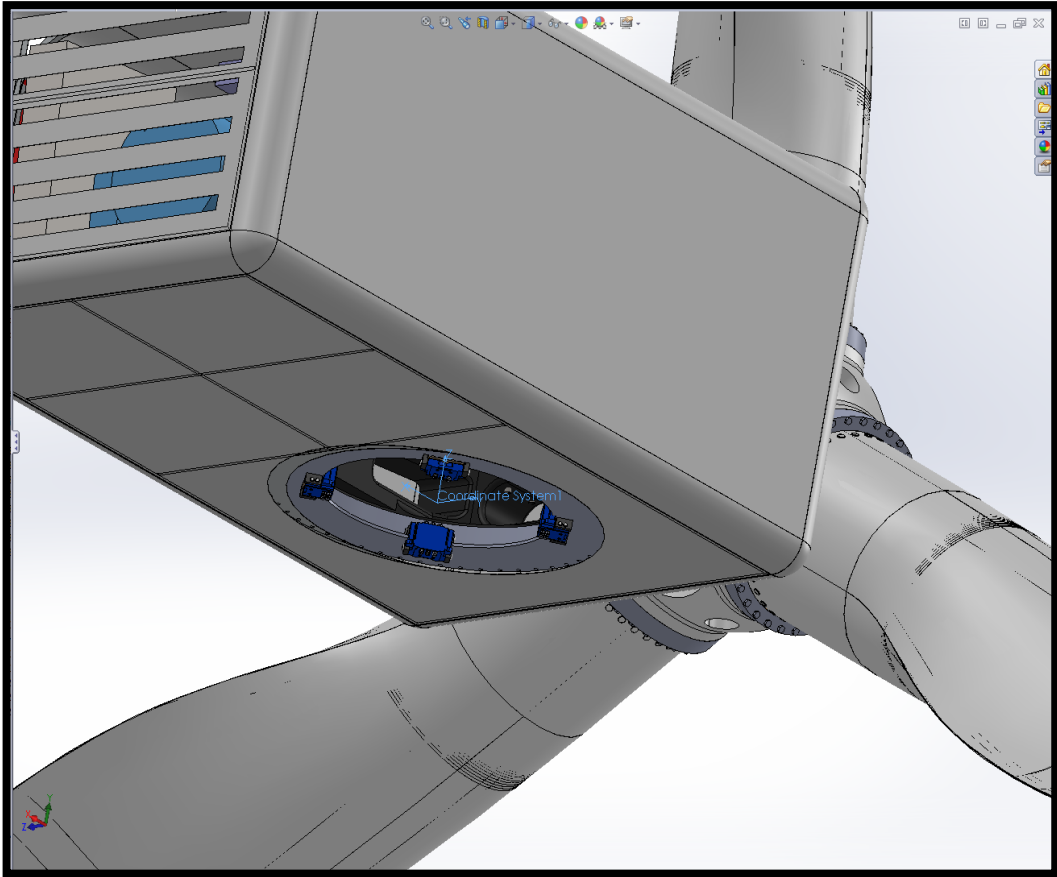


Figure 0. 10: Complete system with a convenient coordinate system.

As illustrated in the Figure 5.10, system has a suitable coordinate system. Before calculating the inertia matrix of the system around the coordinate system, proper material information was applied to the components of the wind turbines. SOLIDWORKS did give the proper inertia matrix around the coordinate system, thus the required torque became calculable.

Moments of inertia: (kilograms * square meters)		
Taken at the output coordinate system.		
Ixx = 478292.73	Ixy = 4315.01	Ixz = 16524.31
Iyx = 4315.01	Iyy = 368497.53	Iyz = 1034.56
Izx = 16524.31	Izy = 1034.56	Izz = 346728.53

Figure 0. 11:Mass - Inertia matrix of the system.

As shown in the Figure 0.10, moment of inertia around the z axis was calculated which is 346729 kg*m². Therefore the torque value can be found from the formula:

$$T = I * \alpha \quad (0.3)$$

α is assumed as 0.5 rad/s^2 which is also consistent with the SAMCEF for wind turbines software. Resultantly total required torque value to start up the system is $T = 346729(\text{kgm}^2) * 0.5 \left(\frac{\text{rad}}{\text{s}^2}\right) = 173364,5 \text{ Nm}$ calculated. This value does not include the initial dry friction torque between the gear and pinion which is calculated as;

$$F_n = \mu * F_a \quad (0.4)$$

Here, F_a is the axial force for the bearing which was calculated as 41kN and μ is 0.3 assumed which is general used in metal to metal contact. Therefore friction force is 12300N calculated at the outer diameter of the bearing. The torque value here is 12.3 kNm because the distance from center the force is around 1m. Therefore the total torque needed to start up the system rotation is around 186 kNm.

Even though the system will have a four yaw drives, three of them will be designed to be enough for beginning of the rotation around the tower. Therefore, the torque requirement from each motor is $186 / 3 = 62 \text{ kNm}$. Therefore, yaw motors that will be able to produce at least 62 kNm torque will be ordered to rotate the system. In addition, the power requirements from the motors were also calculated as $62\text{kNm} * \pi/60 \text{ rad/s} = 1.03 \text{ kW}$ motors will be provided. The system should not rotate fast in order to have smaller motors and prevent the possible gyroscopic force effect for the main bearing.

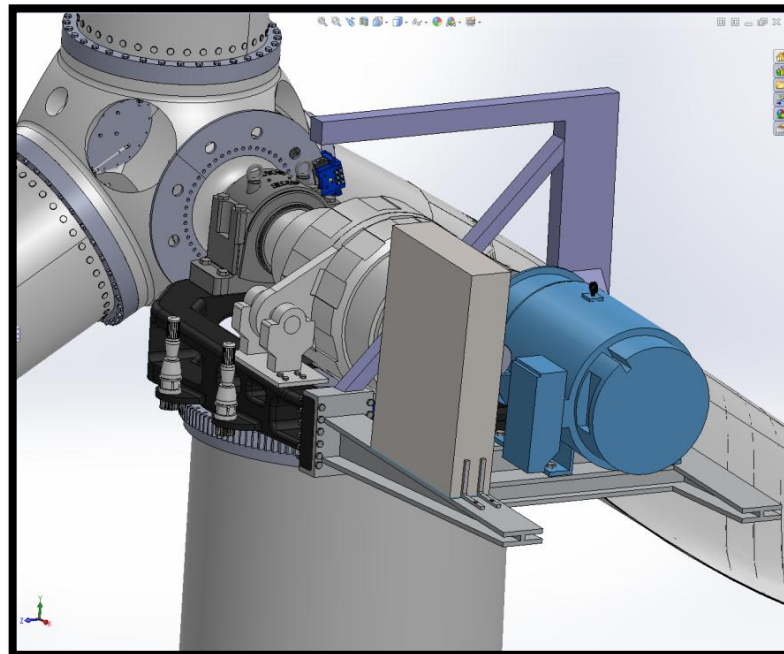


Figure 0. 12:Yaw motors integrated to the system.